3-6-2008

Constellation Design of Geosynchronous Navigation Satellites Which Maximizes Availability and Accuracy Over a Specified Region of the Earth

Halil Ibrahim Ozdemir

CONSTELLATION DESIGN OF GEOSYNCHRONOUS NAVIGATION SATELLITES WHICH MAXIMIZES AVAILABILITY AND ACCURACY OVER A SPECIFIED REGION OF THE EARTH

THESIS

Halil İbrahim ÖZDEMİR, Captain, TUAF

AFIT/GSS/ENG/08-01

DEPARTMENT OF THE AIR FORCE

AIR UNIVERSITY

AIR FORCE INSTITUTE OF TECHNOLOGY

Wright-Patterson Air Force Base, Ohio

AFIT/GSS/ENG/08-01

CONSTELLATION DESIGN OF GEOSYNCHRONOUS NAVIGATION SATELLITES WHICH MAXIMIZES AVAILABILITY AND ACCURACY OVER A SPECIFIED REGION OF THE EARTH

THESIS

Presented to the Faculty

Department of Electrical and Computer Engineering

Graduate School of Engineering and Management

Air Force Institute of Technology

Air University

Air Education and Training Command

In Partial Fulfillment of the Requirements for the

Degree of Master of Science in Space Systems

Halil İbrahim ÖZDEMİR, B.S.E.E.

Captain, TUAF

March 2008

AFIT/GSS/ENG/08-01

CONSTELLATION DESIGN OF GEOSYNCHRONOUS NAVIGATION SATELLITES WHICH MAXIMIZES AVAILABILITY AND ACCURACY OVER A SPECIFIED REGION OF THE EARTH

Halil İbrahim ÖZDEMİR, B.S.E.E.

Captain, TUAF

Approved:

/signed/	06 March 2008
Dr.John Raquet (Chairman)	Date
/signed/	06 March 2008
Dr.Gary Lamont (Member)	Date
/signed/	06 March 2008
Lt.Col.Nathan Titus, PhD (Member)	Date

Abstract

Currently, there are four Global Navigation Satellite Systems (GNSS) either being developed or in existence-GPS, GLONASS, Compass, and Galileo. Additionally, there are several Regional Navigation Satellite Systems (RNSS) planned or in existence, as well as numerous augmentation systems (which require a GNSS for operation). It can be anticipated that there will be interest in developing additional independent regional navigation satellite systems to cover areas of interest to particular countries or regions, who want to have their own system.

In this paper, a genetic algorithm is used in an effort to determine near-optimal RNSS constellations. First, a cost function is setup, which involves a weighted combination of dilution of precision (DOP) values and percentage availability for any number of receiver locations on the ground (which themselves can be weighted). Effectively, using this approach it is easy to quantify the quality of coverage, in terms of measurement geometry, over a specific region of the earth. Next, a genetic algorithm is used in order to attempt to converge to the lowest-cost constellation possible.

Due to the extremely large size of the search space, there appears to be benefit to constraining the search space, using reasonable knowledge of the problem. One example is to constrain the constellation to include two geostationary satellites. This approach was taken, and slightly better costs were obtained over the unconstrained

case. What is interesting to note, however, is that the genetic algorithm tended to result in generating three geostationary satellites (when only two were specified), strongly suggesting that three geostationary satellites is the correct approach for the region that was evaluated. This paper shows the solutions generated by genetic algorithm, and conclusions are drawn about what appear to be the best constellations for the specified region. Overall, the genetic algorithm approach appears to be a useful tool for constellation optimization for RNSS systems.

Acknowledgements

First and foremost, I would like to thank my family for supporting me in all cases. I would also like to express my appreciation to Dr. John Raquet for his ideas and teachings. He not only taught some knowledge but also showed the proper way of using that knowledge. His advices about the research lead us for this valuable study.

I also would like to thank Lt.Col Nathan Titus for providing an outstanding teaching about the spaceflight dynamics.. Finally, I would like to express my appreciation to Dr. Gary Lamont for his excellent guidance in Genetic Algorithms.

Halil İbrahim ÖZDEMİR

Table of Contents

List of Figures

List of Tables

List of Symbols

Symbol		Page
i	Inclination	40
ω	Argument of perigee	40
ν	True anomaly	40
Ω	Right Ascension of Ascending Node	40
Ω_{LAN}	Longitude of Ascending Node	42
Ω_{shift}	RAAN Correction	42
n	Mean Motion	43
$\dot{\Omega}_e$	Earth's Rotation Rate	43
θ_{GMST}	Greenwich Mean Sidereal Time	43
μ	Gravitational Constant	43
t_{sim}	Simulation Time Period	44
t_{step}	Simulation Time Step	44
p	Semiparameter	45
$\mathbf{r}_{PQW}$	Position Vector in Perifocal Coordinate System	45
$\mathbf{v}_{PQW}$	Velocity Vector in Perifocal Coordinate System	45
θ	Earth's Rotation Angle	47
$\mathbf{T}_{ECItoECEF}$	Rotation Matrix from ECI to ECEF Frame	47
$\mathbf{r}_{ECEF}$	Position Vector in ECEF Frame	47
a_I	J_2 Acceleration in I axis	48
a_J	J_2 Acceleration in J axis	48
a_K	J_2 Acceleration in K axis	48
$R_\oplus$	Earth's Radius	49
El	Elevation Angle	49
El_{mask}	Mask Angle	49
$GDOP_T$	GDOP Threshold Value	50
C_f	Cost Function	51
W_{GDOP}	GDOP Weight	51
n_r	Number of Receiver Points	51

Symbol		Page
W_i	Weight of i^{th} Receiver Point	51
$\overline{GDOP}$	Average GDOP	51
W_α	Availability Weight	51
α	Availability	51

List of Abbreviations

Abbreviation		Page
HDOP	Horizontal Dilution of Precision	25
VDOP	Vertical Dilution of Precision	25
TDOP	Time Dilution of Precision	25
NaN	not-a-number	35
RAAN	Right Ascension of Ascending Node	40
LAN	Longitude of Ascending Node	42
WGS84	World Geodetic System 1984	49
LOS	Line-of-Sight	49

CONSTELLATION DESIGN OF GEOSYNCHRONOUS NAVIGATION SATELLITES WHICH MAXIMIZES AVAILABILITY AND ACCURACY OVER A SPECIFIED REGION OF THE EARTH

I. Introduction

1.1 Satellite Navigation Background

The space age began with the launch of first artificial satellite, *Sputnik I* by the Soviet Union in 1957. The launch of *Sputnik I* triggered the desire to discover the details of the satellite orbit. It was possible to determine the position of the Sputnik by the radio signals transmitted by itself. It was recognized that this technique could be inverted: if the satellite's orbit was already known, a radio receiver's unknown position could be determined accurately by using the same type of measurements. Satellites could be designed specifically for the purpose of providing location . This idea was realized in the *Transit* Navigation Satellite System by the U.S. Navy. Two virtually identical systems were developed by the Soviet Union: *Parus* for the Soviet Navy and *Tsikada* for merchant ships [23].

The success of Transit motivated the U.S. Navy and the Air Force for follow-on programs for space-based navigation systems which resulted in the Global Positioning System (GPS). The Soviet Union undertook to develop a similar system called GLObal NAvigation Satellite System (GLONASS). The GPS is fully operational and has var-

ious application areas today. After the dissolution of the Soviet Union, the Russian Federation who has assumed the responsibility for GLONASS was not able keep the GLONASS fully functional due to economical problems. The GLONASS needs more satellites to compete with the GPS. Therefore, being provided the required budget, GLONASS is planned to have global coverage at the end of 2009 [24, 28].

Another project in development is the European system, Galileo, which has launched its first satellite in 2005. The full constellation was planned to be operational by 2009. However, it is unlikely that full operational capability will be available until 2012-2013 [27].

There are also Satellite Based Augmentation Systems (SBASs) which are essentially extra satellites transmitting signals intended to address shortcomings of GNSS for enhanced accuracy, availability, and integrity for civil aviation users. The GPS augmentation system, Wide Area Augmentation System (WAAS), performs well in the US and it is widely used. The European augmentation system, European Geostationary Navigation Overlay System (EGNOS) (also includes corrections for GLONASS), is becoming mature and will be ready for certification for Safety of Life operations in mid 2008 over Europe. Japan prepares for operations with the augmentation system MTSAT (Multi-Functional Transport SATellite) based Satellite Augmentation System (MSAS), interoperable with EGNOS and WAAS. Japan is proceeding with the regional GPS augmentation, Quasi-Zenith Satellite System (QZSS), which will have the first satellite launched in 2009. India is proceeding with its re-

gional augmentation system which is called GPS and GEO Augmented Navigation (GAGAN) [28].

Regional Navigation Satellite Systems (RNSSs) are intended to provide navigation service over a nation or region. Their satellite constellations are much smaller than GNSSs, perhaps only 5-7 satellites (depending on the specific orbit configuration). They may be considered as first steps to GNSSs [27].

Japan has intentions to build a regional system, Japanese Regional Navigation Satellite System (JRANS), which will consist of 3 QZSS satellites, the MTSAT satellite and three additional satellites in high earth orbit [27].

China has developed an RNSS which is called *BeiDou-1* and it is reported to have an accuracy of dozens of meters [24]. China participates in the Galileo program and is developing a global satellite navigation system *BeiDou-2* (or *COMPASS*) as a follow up of the regional *BeiDou-1* [28].

The Indian government has started a project of an independent regional navigation satellite system which is planned to be completed by 2011. The Indian Regional Navigation Satellite System (IRNSS) will have a seven satellite constellation [15].

There are also plans for completely commercial satellite navigation systems. Some companies, like Lockheed Martin in cooperation with NEC of Japan and Alcatel of France and Boeing, have plans for their own augmentation systems. It is appealing to own a satellite based navigation system due to the political and economic benefits.

Just as satellite based communications was commercialized, governments, companies and multinational conglomerates may be competing to exploit those benefits [18].

Global Navigation Satellite System (GNSS) is the generic name for the class of systems of which GPS is currently the only working system. The technology has advanced significantly and the world political order has shifted since GPS was designed in the 1970s. The U.S. wants to maintain leadership among GNNSs and has plans to develop GPS III which is a more capable system. The GLONASS is planned to be revived, and the Galileo has the momentum and the funds to be operational. The GNSS world is going towards more competition and cooperation. It is advantageous to have more satellites and better signal quality of multiple systems for users. Major components are the USs modernized GPS and planned GPS-III, the revitalized GLONASS, and Europes planned GALILEO system. In addition, the SBASs and RNSSs will provide extra satellites and signals to the GNSS "mix". The user community will benefit more from modernized GPS, GLONASS, Galileo, SBASs and RNSSs [24, 27].

The future of GNSS/RNSS is promising. More satellites and more signals will be welcome by many users. Better performance can be achieved by integrating all these satellite systems into one Global Navigation Satellite System of Systems. The benefits of satellite-based positioning, navigation and timing offered by compatibility and interoperability of all GNSSs, SBASs and RNSSs are far greater than what any individual system can provide.

1.2 Problem Statement

As stated in Section 1.1, having a satellite navigation system is politically and economically beneficial. On the other hand, building and maintaining a satellite navigation system is extraordinarily expensive depending on the size of the satellite constellation. In order to minimize the cost and maximize the benefit of such a system, the requirements for the coverage area and the expected performance of the system should be determined. Based on those requirements, an optimized satellite constellation that meets the requirements can be designed. There has been some studies to provide solutions for both regional and global coverage requirements.

The previous research on regional and global navigation satellite systems has proposed solutions which are exploiting the combinations of common orbits, like Low Earth Orbits (LEO), Geostationary Orbits (GEO), Geosynchronous Orbits (GSO), and Medium Earth Orbits (MEO), as solutions [7, 8, 17, 20, 26].

The previous research on the satellite constellation design using Genetic Algorithms (GA) has showed the power of the GA in satellite constellation optimization [8, 10–12, 30–32]. Previous research used GA to optimize combinations of the above mentioned orbits considering the distribution of the orbital planes on the equator and the distribution of the satellites on those orbits. While much work has been done on constellation optimization, very little has been done to design a constellation for navigation purposes to serve within a specified region of the world. The goal of this research is to design a constellation of geosynchronous navigation satellites which

maximizes availability and accuracy over a specified region of the earth by using the GA for optimization. In order to accomplish this goal; a simulation tool is developed to evaluate the navigation performance of satellite constellations in which the satellites have GEO period as a constant and the other orbital parameters as variables, a genetic algorithm is designed to find an optimal or a near-optimal solution to the problem. The objective is to find a solution which provides 100% availability with the best available accuracy.

1.3 Scope and Assumptions

Simplifying assumptions are needed to focus the research in a direction so that conclusions can be reached without making the simulations overly complex. Several assumptions were made to limit the scope of the research:

- The simulation of the satellite orbits for optimization is based on two-body equations of motion. For the analysis of the final candidate solutions, J2 perturbation is included to make it more realistic.
- The performance of the simulated navigation system constellations will be evaluated considering the accuracy of the position estimate and availability of a given level of accuracy .
- The measurement accuracy assumed to be consistent for a given system (a reasonable assumption commonly made with satellite navigation systems). Therefore, the accuracy of the position estimate is assumed to depend only on the geometric quality of the constellation.

- The candidate region for the navigation service is as depicted in Figure 1.1.

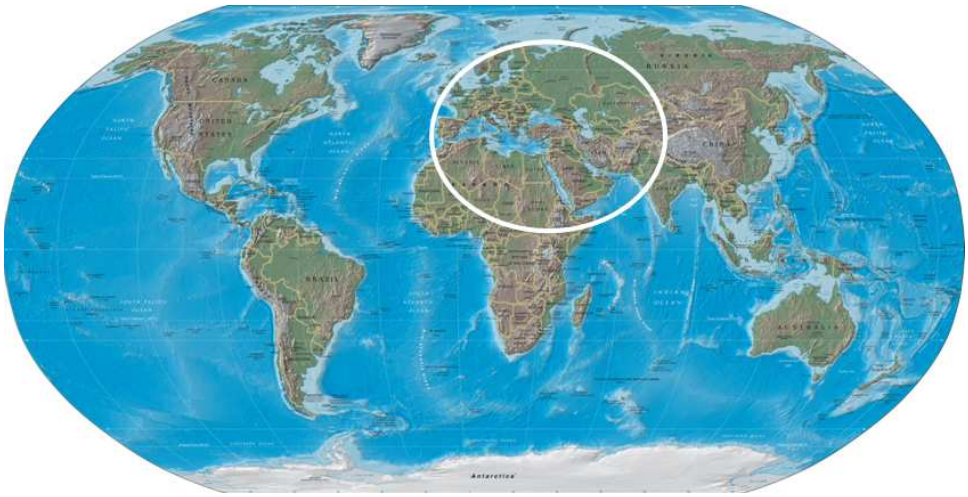

Figure 1.1: The candidate region for the navigation service

1.4 Related Research

Romay-Merino, Cobo, and Herraiz-Monseco studied the design of high performance and cost efficient constellations for future global navigation systems. They analyzed three types of constellations: GSO/GEO constellations, GPS like constellations, and hybrid constellations (GPS/GSO/GEO). They used an adaptive random search method to optimize these constellations in order to minimize the worst performance values even in case of satellite failures. They used a geographical distribution of weighting function to have the constellation provide better performance over highly populated areas. The constraints on satellite constellations that they applied include all satellites at geosynchronous altitude, all satellites in inclined planes have the same

inclination, fixed number of inclined planes, several satellites in the same ground track and fixed number of GEO and GSO orbits.

The results of optimization of GSO/GEO constellation indicated that at least 35 satellites are required to accomplish the requirements. They also reported that failure of a satellite in this kind of a constellation would significantly deteriorate the performance of navigation service over the area covered by the failed satellite. They also performed an optimization of a regional GSO/GEO constellation to provide better performance over Europe. They found that at least 22 satellites are required to satisfy the requirements over Europe. They made another optimization for GPS-like constellations and concluded that at least 45 satellites are required to satisfy the requirements and the performance is about the level of performance provided by the 35 satellite GSO/GEO constellation [8]. Finally, they optimized the hybrid (GPS/GSO/GEO) constellations and concluded that at least 42 satellites are required. The overall conclusions for their study as follows [8]:

- The use of an optimization tool allows to design cost efficient and high performance navigation satellite constellations.
- GSO/GEO constellations can be designed to provide better performance over desired regions by using geographically distributed weighting functions.
- A regional satellite navigation constellation using GSO/GEO can easily be transformed into a global constellation easily.

Renault discussed the properties of regional navigation constellations which are combinations of GEO and GSO orbits. He stressed that synchronous orbits are the best suited orbits for a regional service, since their visibility over a regional area is maximum. Therefore he suggested that a regional constellation should be composed of both GSO and GEO satellites. He analyzed the performance of both GEO and GSO based constellations. He noted that GEO based constellations had better vertical performance and GSO based constellations had better horizontal performance. He concluded that three GEOs and three GSOs on three planes define a minimal navigation constellation for a mid-latitude region [26].

Micheau and Thiebolt studied the satellite constellation design for navigation needs. They specifically studied LEO constellations with complementary GEO satellites. The low cost properties of LEO satellites made them appear to be a sensible choice. They emphasized maximizing the position accuracy over Europe. They used both analytical methods and genetic algorithms to find an optimal constellation solution to meet the civil aviation specifications over Europe. The comparison of the results obtained by different methods showed that the the results of Genetic algorithms were the only one that met all requirements [20].

Carnebianca studied regional to global satellite based navigation systems. He suggested to create a constellation with two GEO satellites and two or three satellites on inclined orbit of 12 or 24 hour period for a regional navigation service. The three major trade-off elements considered in his study are number of GEO satellites, their location and equatorial spacing and the properties of inclined satellites such as number

of inclined satellites, their apogee loop location and their phasing relationship. He analyzed different combinations of GEO, Highly Elliptical Orbit (HEO)[1] and Tundra[2] orbits to create a global navigation constellation. He emphasized the advantage of GEO satellites for serving a region of the earth. He stated that the use of GEO satellites allows a regional service with the potential to be expanded gradually with additional satellites [7].

Frayssinhes investigated satellite constellation geometries with genetic algorithms for data collection purposes. He stressed the efficiency of genetic algorithms in optimizing satellite constellations and noted the effectiveness of the GA for optimizing add-on satellites to the GPS. He proposed relying on real encoding instead of a binary encoding mechanism. He used the GA to distribute the orbital planes on the equator and to distribute the satellites on the orbital planes (i.e., optimization of the right ascension of ascending node and the initial mean anomaly). He concluded that the GA with a binary encoding mechanism was not suitable to manage circular configurations that are both distribution of satellites in an orbital plane and distribution of the orbit ascending nodes over the equator [12].

Ferringer and Spencer studied satellite constellation design optimization via multiple-objective evolutionary algorithms (Non-Dominated Sorting Genetic Algorithm II) for remote sensing purposes. They made optimization of a six-satellite

[1]HEO: period = 12 hrs, apogee/perigee altitude = 39105/1250 km, inclination = 63.45
[2]Tundra: period = 24 hrs, apogee/perigee altitude = 46340/25231 km, inclination = 63.45

constellation considering the distribution of orbits on the equator, distribution of satellites on those orbits, and the same inclination value for each orbit [11].

Ely, Crossley and Williams introduced a method for applying a GA approach for multi-objective design of constellations for zonal coverage. Their study has shown that genetic algorithms and eccentric orbits are useful in designing efficient constellations. Their approach provides an opportunity to identify constellation designs with elliptic orbits that require less launch effort and cost less than designs using circular orbits [30].

1.5 Thesis Overview

In Chapter two, a background of position estimation in GPS and Genetic Algorithms is presented. In Chapter three, the structure of the simulation, the implementation of the GA, and the orbit propagation are described. In Chapter four, the data generated by the simulation is analyzed. In the chapter five, the results of the simulation and the possible benefits the study are discussed.

II. Background

2.1 Overview

The purpose of this chapter is to acquaint the reader with the key concepts used in this research. In Section 2.2, a brief explanation of GPS and its segments is covered. More information about the GPS can be found in [24]. In Section 2.3, definition of common terms to describe the performance of a satellite navigation system is given. In Section 2.4, the position estimation in GPS and the Dilution of Precision concept are explored. In Section 2.5, a basic definition of GA and common operators are provided.

2.2 Global Positioning System

GPS, declared operational in 1995, consists of three segments: the user segment, the control segment, and the space segment [24]. The user segment consists of all kinds of civilian and military receivers. The control segment deals with the management of satellite operations. The space segment comprises the satellites. GPS space segment nominally consists of 24 satellites in nearly circular orbit with a radius of 26560 km, a period of approximately 12 hours, and stationary ground tracks. The satellites are arranged in six equally spaced orbital planes with an inclination of 55 degrees. Each plane hosts four satellites unevenly distributed around the plane. This nominal constellation assures that a receiver anywhere in the world would see at least four satellites at all times. Figure 2.1 illustrates the nominal GPS constellation. In order

to provide better performance to the user community, currently 31 functional GPS satellites are in space (as of January 16, 2008) [2].

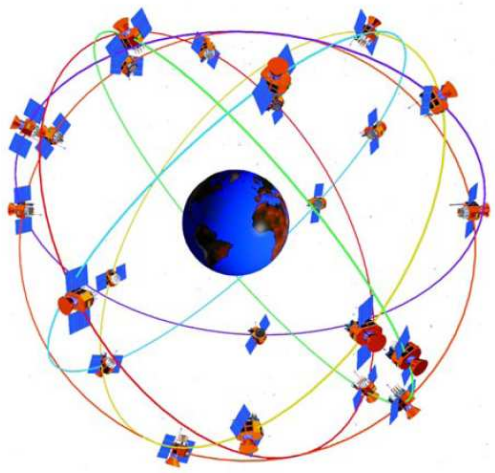

Figure 2.1: Nominal GPS Constellation [3].

2.3 Performance of a Navigation System

The performance evaluation of a navigation system is usually described in terms of accuracy, availability, and integrity.

Accuracy is defined as the difference between the calculated position at any given time and the true position. The accuracy of a navigation system depends on the accuracy of the navigation signal received by the user and the relative geometry of the navigation satellites of which signals are being received [26].

Availability is the ability of a navigation system to provide position information whenever it is needed by the user. The accuracy of a navigation system over the time is not constant. When the accuracy of the system is better than a specified value, the system is called available [26].

Integrity is the ability of a navigation system to provide timely warnings to users or to shut itself down when the accuracy is worse than a specified value [26].

2.4 Position Estimation and Dilution of Precision (DOP)

A GPS receiver needs signals from at least four satellites to estimate its position. The GPS satellites transmit data signals which includes the information of their own position in space and the time of transmission. The GPS receiver calculates its range to each visible satellite by using time-of-arrival (TOA) method. In order to utilize the TOA, the GPS receiver must have the information of the time of signal transmission, the speed of signal propagation, and the time of signal reception. The speed of signal propagation for GPS signals is the speed of the light, which is already known. The time of the signal transmission is provided in the GPS signal. Although satellites have very accurate atomic clocks, the time information is not as precise as GPS receiver needs. However, the correction for satellite clock error is also provided in the GPS data signal. The time of signal reception is determined by the receiver clocks which are generally inexpensive quartz clocks which has relatively less stability than GPS satellite clocks. The receiver clock error is not a problem, because it can be explicitly solved for by the fourth satellite signal. Therefore, a GPS receiver needs at least four satellite signals to determine its own position.

Figure 2.2 illustrates the vectors from the receiver to the satellites in Cartesian coordinate system, where (x_u,y_u,z_u) is the receiver position vector and (x_k,y_k,z_k) are the position vectors of k^{th} satellite for $k = 1, 2, .., n$.

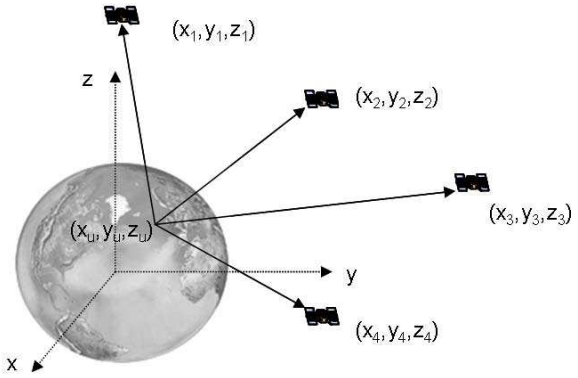

Figure 2.2: Receiver-to-satellite vectors

In order to determine receiver position in three dimensions (x_u, y_u, z_u) and the clock offset t_u, pseudorange measurements should be made to four satellites which can be written as follows (assuming the only error is receiver clock error):

$$\rho_k = \|\mathbf{x}_k - \mathbf{x}_u\| + ct_u \tag{2.1}$$

where ρ_k is the pseudorange between the receiver and the k^{th} satellite, $\mathbf{x}_k$ is the k^{th} satellite position vector, and $\mathbf{x}_u$ is the receiver position vector. Equation 2.1 can be expanded as:

$$\begin{aligned} \rho_k &= \sqrt{(x_k - x_u) + (y_k - y_u) + (z_k - z_u)} + ct_u \\ &= f(x_u, y_u, z_u, t_u) \end{aligned} \tag{2.2}$$

These nonlinear equations can be solved by employing iterative techniques based on linearization. If the approximate receiver position is known, the offset of the true position (x_u, y_u, z_u) can be denoted from the approximate receiver position $(\hat{x}_u, \hat{y}_u, \hat{z}_u)$ by a displacement $(\Delta x_u, \Delta y_u, \Delta z_u)$. The position offset $(\Delta x_u, \Delta y_u, \Delta z_u)$ can be obtained as linear functions of the known coordinates and pseudorange measurements by expanding Equation 2.2. By using the approximate position location $(\hat{x}_u, \hat{y}_u, \hat{z}_u)$ and time bias estimate $\hat{t}_u$, an approximate pseudorange can be calculated:

$$\begin{aligned} \hat{\rho}_k &= \sqrt{(x_k - \hat{x}_u) + (y_k - \hat{y}_u) + (z_k - \hat{z}_u)} + c\hat{t}_u \\ &= f(\hat{x}_u, \hat{y}_u, \hat{z}_u, \hat{t}_u) \end{aligned} \tag{2.3}$$

The receiver position and receiver clock offset is considered to consist of an approximate and an incremental component:

$$\begin{aligned} x_u &= \hat{x}_u + \Delta x_u \\ y_u &= \hat{y}_u + \Delta y_u \\ z_u &= \hat{z}_u + \Delta z_u \\ t_u &= \hat{t}_u + \Delta t_u \end{aligned} \tag{2.4}$$

Therefore, it can be written as:

$$f(x_u, y_u, z_u, t_u) = f(\hat{x}_u + \Delta x_u, \hat{y}_u + \Delta y_u, \hat{z}_u + \Delta z_u, \hat{t}_u + \Delta t_u) \tag{2.5}$$

Equation 2.5 can be expanded about the approximate point and associate predicted receiver clock offset $(\hat{x}_u, \hat{y}_u, \hat{z}_u, c\hat{t}_u)$ using a Taylor series expansion:

$$f(\hat{x}_u + \Delta x_u, \hat{y}_u + \Delta y_u, \hat{z}_u + \Delta z_u, \hat{t}_u + \Delta t_u) = f(x_u, y_u, z_u, t_u) + \tag{2.6}$$

$$\frac{\partial f(\hat{x}_u, \hat{y}_u, \hat{z}_u, \hat{t}_u)}{\partial \hat{x}_u} \Delta x_u + \frac{\partial f(\hat{x}_u, \hat{y}_u, \hat{z}_u, \hat{t}_u)}{\partial \hat{y}_u} \Delta y_u + \frac{\partial f(\hat{x}_u, \hat{y}_u, \hat{z}_u, \hat{t}_u)}{\partial \hat{z}_u} \Delta z_u +$$

$$\frac{\partial f(\hat{x}_u, \hat{y}_u, \hat{z}_u, \hat{t}_u)}{\partial \hat{t}_u} \Delta t_u + higher\ order\ terms$$

In order to eliminate nonlinear terms, the higher order terms are truncated. The partial derivatives evaluate as follows:

$$\begin{aligned}
\frac{\partial f(\hat{x}_u, \hat{y}_u, \hat{z}_u, \hat{t}_u)}{\partial \hat{x}_u} &= -\frac{x_k - \hat{x}_u}{\hat{r}_k} \\
\frac{\partial f(\hat{x}_u, \hat{y}_u, \hat{z}_u, \hat{t}_u)}{\partial \hat{y}_u} &= -\frac{y_k - \hat{y}_u}{\hat{r}_k} \\
\frac{\partial f(\hat{x}_u, \hat{y}_u, \hat{z}_u, \hat{t}_u)}{\partial \hat{z}_u} &= -\frac{z_k - \hat{z}_u}{\hat{r}_k} \\
\frac{\partial f(\hat{x}_u, \hat{y}_u, \hat{z}_u, \hat{t}_u)}{\partial \hat{t}_u} &= c
\end{aligned} \tag{2.7}$$

where $\hat{r}_k$ is the magnitude of the vector from the approximate user position to the k^{th} satellite and defined as:

$$\hat{r}_k = \sqrt{(x_k - \hat{x}_u)^2 + (y_k - \hat{y}_u)^2 + (z_k - \hat{z}_u)^2} \tag{2.8}$$

Substituting Equations 2.4 and 2.7 into Equation 2.6 yields:

$$\rho_k = \hat{\rho}_k - \frac{x_k - \hat{x}_u}{\hat{r}_k}\Delta x_u - \frac{y_k - \hat{y}_u}{\hat{r}_k}\Delta y_u - \frac{z_k - \hat{z}_u}{\hat{r}_k}\Delta z_u + c\Delta t_u \tag{2.9}$$

Equation 2.9 is the linearized form of Equation 2.3 with respect to the unknowns $\Delta x_u, \Delta y_u, \Delta z_u$, and Δt_u. Rearranging the the expression with the known quantities on the left yields:

$$\hat{\rho}_k - \rho_k = \frac{x_k - \hat{x}_u}{\hat{r}_k}\Delta x_u + \frac{y_k - \hat{y}_u}{\hat{r}_k}\Delta y_u + \frac{z_k - \hat{z}_u}{\hat{r}_k}\Delta z_u - c\Delta t_u \tag{2.10}$$

By introducing new variables, Equation 2.10 can be simplified as:

$$\begin{aligned} \Delta\rho &= \hat{\rho}_k - \rho_k \\ a_{xk} &= \frac{x_k - \hat{x}_u}{\hat{r}_k} \\ a_{yk} &= \frac{y_k - \hat{y}_u}{\hat{r}_k} \\ a_{zk} &= \frac{z_k - \hat{z}_u}{\hat{r}_k} \end{aligned} \tag{2.11}$$

In these equations, (a_{xk}, a_{yk}, a_{zk}) defines the unit vector pointing from the approximate user position to the k^{th} satellite. Substituting the new variables into Equation 2.10 yields:

$$\Delta\rho_k = a_{xk}\Delta x_u + a_{yk}\Delta y_u + a_{zk}\Delta z_u - c\Delta t_u$$

The four unknowns $\Delta x_u, \Delta y_u, \Delta z_u$, and Δt_u can be solved for by making ranging measurements to at least four satellites, and then solving the following linear equations:

$$\begin{aligned}
\Delta\rho_1 &= a_{x1}\Delta x_u + a_{y1}\Delta y_u + a_{z1}\Delta z_u - c\Delta t_u \\
\Delta\rho_2 &= a_{x2}\Delta x_u + a_{y2}\Delta y_u + a_{z2}\Delta z_u - c\Delta t_u \\
\Delta\rho_3 &= a_{x3}\Delta x_u + a_{y3}\Delta y_u + a_{z3}\Delta z_u - c\Delta t_u \\
\vdots &= \vdots \\
\Delta\rho_n &= a_{xn}\Delta x_u + a_{yn}\Delta y_u + a_{zn}\Delta z_u - c\Delta t_u
\end{aligned} \tag{2.12}$$

These equations can be expressed in matrix form as:

$$\mathbf{\Delta}\rho = \begin{bmatrix} \Delta\rho_1 \\ \Delta\rho_2 \\ \Delta\rho_3 \\ \vdots \\ \Delta\rho_n \end{bmatrix} \quad \mathbf{H} = \begin{bmatrix} a_{x1} & a_{y1} & a_{z1} & -1 \\ a_{x2} & a_{y2} & a_{z2} & -1 \\ a_{x3} & a_{y3} & a_{z3} & -1 \\ \vdots & \vdots & \vdots & \vdots \\ a_{xn} & a_{yn} & a_{zn} & -1 \end{bmatrix} \quad \mathbf{\Delta x} = \begin{bmatrix} \Delta x_u \\ \Delta y_u \\ \Delta z_u \\ c\Delta t_u \end{bmatrix}$$

where $\mathbf{\Delta}\rho$ is pseudorange difference vector, $\mathbf{H}$ is measurement matrix and $\mathbf{\Delta x}$ is user position displacement vector. This matrix equation can be written as:

$$\mathbf{\Delta}\rho = \mathbf{H}\,\mathbf{\Delta x} \tag{2.13}$$

where there are three cases:

1. $n < 4$: Underdetermined case
    - Cannot solve for $\mathbf{\Delta x}$
2. $n = 4$: Uniquely determined case
    - One valid solution for $\mathbf{\Delta x}$
    - Solved by calculating $\mathbf{H}^{-1}$ ($\mathbf{\Delta x} = \mathbf{H}^{-1}\mathbf{\Delta}\rho$)
3. $n > 4$: Overdetermined case
    - No perfect solution that solves equation
    - Least-squares techniques can be used to make an estimate

The solution for the third case, which is more common, based on the least-squares solution is as follows:

$$\mathbf{\Delta x} = (\mathbf{H}^T\mathbf{H})^{-1}\mathbf{H}^T\mathbf{\Delta}\rho \tag{2.14}$$

Once the $\mathbf{\Delta x}$ is calculated, the receiver's coordinates x_u, y_u, z_u and the receiver clock offset t_u are calculated using Equation 2.4. This linearization works well as

long as the displacement $(\Delta x_u, \Delta y_u, \Delta z_u)$ is within the close proximity of the known approximate receiver position. When the position estimation error is above an acceptable value, taking the solution as new approximate known receiver position and repeating the linearization will provide a better estimate. The iteration process may go on until the desired accuracy is reached [16].

The position estimation accuracy also depends on the relative geometry of the location of the receiver and the satellites which is represented by $\mathbf{H}$ matrix. In the beginning of the position estimation calculation, the only error was assumed to be the receiver clock error. In a real world situation, the receiver-to-satellite measurements are corrupted by independent errors, such as measurement noise, satellite position error (ephemeris error), multipath error. In other words, $\mathbf{\Delta}\rho$ includes all of the measurement errors, and these errors are amplified by $(\mathbf{H}^T\mathbf{H})^{-1}$ matrix when solving for $\mathbf{\Delta x}$. Therefore, a badly distributed satellite geometry reduces the accuracy of the position estimation which is called Dilution of Precision (DOP). The good and poor DOP situation is illustrated in Figure 2.3.

The DOP concept is a way to characterize the impact of measurement geometry on the position solution. By defining the covariance matrix of measurements $(\mathbf{C}_\rho)$ and the covariance matrix of calculated position and clock error $(\mathbf{C}_\mathbf{x})$ as:

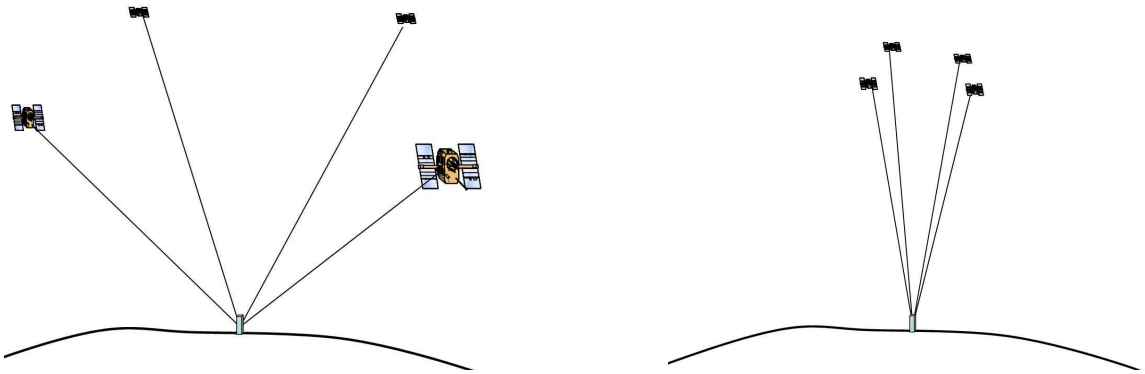

(a) (b)

Figure 2.3: (a) Well distribution of satellites provides a good DOP. (b) Clustered satellites give poor DOP values.

$$\mathbf{C}_\rho = \begin{bmatrix} \sigma_{\rho_1}^2 & \sigma_{\rho_1\rho_2} & \dots & \sigma_{\rho_1\rho_n} \\ \sigma_{\rho_2\rho_1} & \sigma_{\rho_2}^2 & \dots & \sigma_{\rho_2\rho_n} \\ \vdots & \vdots & \ddots & \vdots \\ \sigma_{\rho_n\rho_1} & \sigma_{\rho_n\rho_2} & \dots & \sigma_{\rho_n}^2 \end{bmatrix} \tag{2.15}$$

$$\mathbf{C}_x = \begin{bmatrix} \sigma_{x_u}^2 & \sigma_{x_u y_u} & \sigma_{x_u z_u} & \sigma_{x_u \delta t_u} \\ \sigma_{y_u x_u} & \sigma_{y_u}^2 & \sigma_{y_u z_u} & \sigma_{y_u \delta t_u} \\ \sigma_{z_u x_u} & \sigma_{z_u y_u} & \sigma_{z_u}^2 & \sigma_{z_u \delta t_u} \\ \sigma_{\delta t_u x_u} & \sigma_{\delta t_u y_u} & \sigma_{\delta t_u z_u} & \sigma_{\delta t_u}^2 \end{bmatrix} \tag{2.16}$$

and making the following assumptions;

- Measurement errors are zero-mean
- Measurement errors have a Gaussian distribution

- All measurements have the same variance
- Measurement errors are uncorrelated

the following definitions can be made:

$$\mathbf{C}_\rho = \mathbf{I}{\sigma_\rho}^2 \tag{2.17}$$

$$\mathbf{C}_\mathbf{x} = (\mathbf{H}^T\mathbf{H})^{-1}{\sigma_\rho}^2 \tag{2.18}$$

The matrix $(\mathbf{H}^T\mathbf{H})^{-1}$ is called the DOP matrix and directly relates the measurement errors to position errors. In Equation 2.18 the $\mathbf{H}$ is defined in Earth-Centered Earth-Fixed (ECEF) frame, but DOP values should describe errors in geodetic (local-level) coordinate frame. Therefore, the $\mathbf{H}$ matrix should be modified so that the unit LOS vectors are expressed in the local-level frame. When the $\mathbf{H}$ matrix is thus modified as $\mathbf{H}^G$, the Equation 2.18 is redefined as:

$$\mathbf{C}_\mathbf{x} = (\mathbf{H}^{G_T}\mathbf{H}^G)^{-1}{\sigma_\rho}^2 \tag{2.19}$$

where

$$\mathbf{C}_x = \begin{bmatrix} \sigma_e^2 & \sigma_{en} & \sigma_{eu} & \sigma_{e\delta t_u} \\ \sigma_{ne} & \sigma_n^2 & \sigma_{nu} & \sigma_{n\delta t_u} \\ \sigma_{ue} & \sigma_{un} & \sigma_u^2 & \sigma_{u\delta t_u} \\ \sigma_{\delta t_u e} & \sigma_{\delta t_u n} & \sigma_{\delta t_u u} & \sigma_{\delta t_u}^2 \end{bmatrix} \tag{2.20}$$

It is desirable to characterize the $\mathbf{C}_x$ matrix using a number. The Geometric Dilution of Precision (GDOP) can be calculated directly from the modified DOP matrix;

$$(\mathbf{H}^T\mathbf{H})^{-1} = \begin{bmatrix} D_{11} & D_{12} & D_{13} & D_{14} \\ D_{21} & D_{22} & D_{23} & D_{24} \\ D_{31} & D_{32} & D_{33} & D_{34} \\ D_{41} & D_{42} & D_{43} & D_{44} \end{bmatrix} \tag{2.21}$$

as follows:

$$GDOP = \sqrt{D_{11} + D_{22} + D_{33} + D_{44}} \tag{2.22}$$

The GDOP relates User Equivalent Range Error (UERE) with root-sum-square of errors as:

$$\sqrt{\sigma_e^2 + \sigma_n^2 + \sigma_u^2 + \sigma_{\delta t_u}^2} = GDOP\ \sigma_{UERE} \tag{2.23}$$

where σ_{UERE} is the standard deviation of UERE.

There are other DOP parameters which are useful to characterize the accuracy of various components of the position/time solution. These are Position Dilution of Precision (PDOP), Horizontal Dilution of Precision (HDOP), Vertical Dilution of Precision (VDOP), and Time Dilution of Precision (TDOP). The definitions of these DOP parameters are as follows:

$$\begin{aligned} PDOP &= \sqrt{D_{11} + D_{22} + D_{33}} \\ HDOP &= \sqrt{D_{11} + D_{22}} \\ VDOP &= \sqrt{D_{33}} \\ TDOP &= \sqrt{D_{44}}/c \end{aligned} \tag{2.24}$$

and the relationships with σ_{UERE} are as follows:

$$\begin{aligned} \sqrt{\sigma_e^2 + \sigma_n^2 + \sigma_u^2} &= PDOP \ \ \sigma_{UERE} \\ \sqrt{\sigma_e^2 + \sigma_n^2} &= HDOP \ \ \sigma_{UERE} \\ \sigma_u &= VDOP \ \ \sigma_{UERE} \\ \sigma_{\delta t_u} &= TDOP \ \ \sigma_{UERE} \end{aligned} \tag{2.25}$$

2.5 Genetic Algorithms

Genetic Algorithms (GAs) are adaptive methods which are used to solve search and optimization problems. GAs are based on the genetic processes of biological organisms. Natural populations evolve over many generations according to the principles of natural selection and survival of the fittest. When they are suitably encoded, GAs are able to evolve solutions to real world problems by mimicking the biological evolutionary process [6].

GAs operate on a population of potential solutions applying the principle of survival of the fittest to generate better approximations to a solution. At each generation, a new set of potential solutions is generated by the process of selecting individuals according to their level of fitness in the population and breeding them using operators borrowed from natural genetics. This process leads to the evolution of populations of individuals which have better levels of fitness than the individuals that they were created from [34].

The implementation of GAs begins with an initial set of parameter combinations. Each individual of the population is evaluated by a fitness function. A selection process is used to select a group of parents among the individuals with the highest fitness values in the population. The resulting parent chromosomes (individuals) are paired off. The string content is swapped between the parents in a pair during a crossover process, according to a specified crossover probability. The resulting chromosomes are called children [5]. The crossover operation is shown in Figure 2.4.

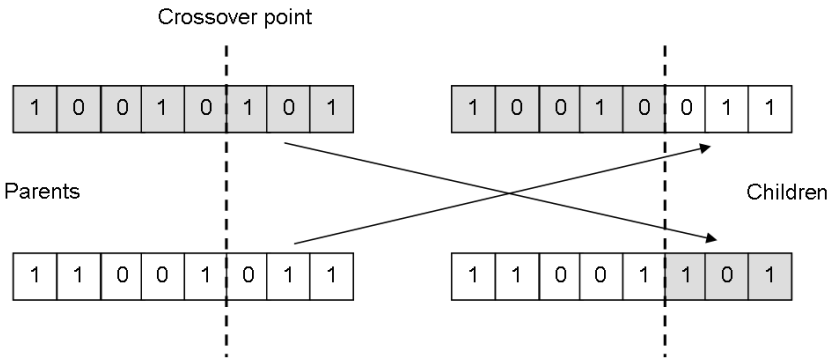

Figure 2.4: Crossover operator cuts both chromosomes at a determined point and swaps the tails.

A mutation operation is applied to each child after crossover. It basically alters each gene with a small probability [6]. An example of mutation is shown in Figure 2.5.

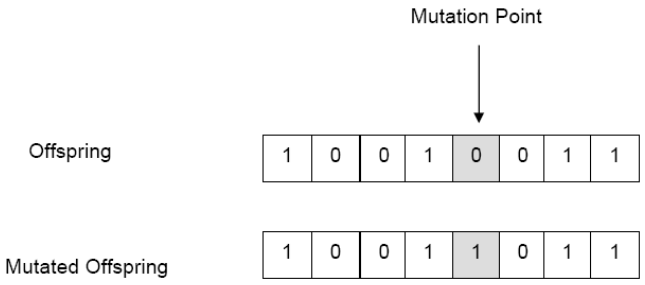

Figure 2.5: Mutation operator flips the value of the bit at determined point.

After selection, crossover, and mutation operations applied to the current *generation*, a whole new generation is produced. This new generation inherits a higher proportion of the characteristics possessed by the good members of the previous generation. In this way, good characteristics are spread throughout the population over many generations. By favoring the mating of the more fit individuals, the most promising regions of the search space are explored to find the optimum solution. If

the GA has been well designed for the nature of the problem, the population *converge*s to an optimal or a close solution to the problem [6]. This process is shown in Figure 2.6:

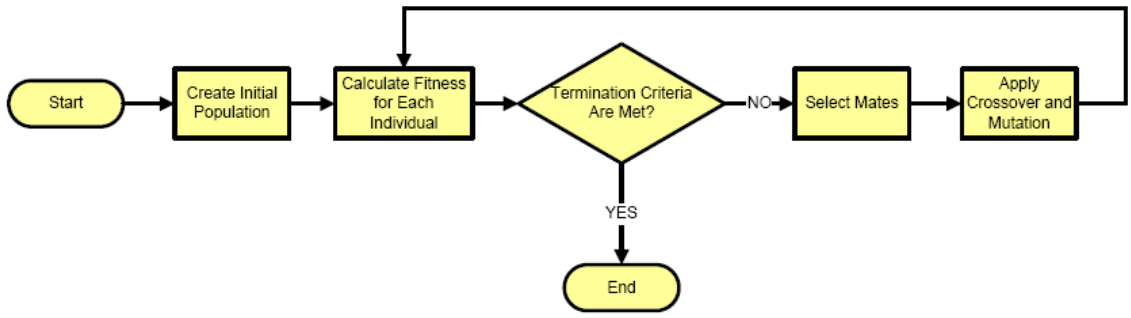

Figure 2.6: Basic GA Flowchart

2.5.1 Selection. Selection involves choosing the individuals in the population that will create children for the next generation. The purpose of the selection is to emphasize the fitter individuals in the population in hopes that their children will in turn have even better fitness. Selection has to be balanced: too-strong selection means that sub-optimal highly fit individuals takes over the population, reducing the diversity needed for further progress; too-weak selection results in slow convergence. Numerous selection schemes have been proposed in the GA literature [22]. The *roulette wheel selection* and *tournament selection* are explained briefly.

A selection mechanism in GA is simply a process that selects better individuals in the population for the mating pool. The *selection pressure* is the degree to which better individuals are selected: the higher the selection pressure, the more the better individuals are selected. This selection pressure drives the GA to improve the population fitness over succeeding generations. The convergence rate of a GA is largely

determined by the selection pressure. If the selection pressure is too low, the convergence rate will be slow, which causes the GA to unnecessarily take longer to find the optimal solution. If the selection pressure is too high, there is an increased probability for the GA to converge to an incorrect (sub-optimal) solution [21].

2.5.1.1 Roulette Wheel Selection. This approach is the commonly used type of fitness-proportional selection. With the roulette wheel selection approach, the probability of selection is proportional to an individual's fitness value. The selection probability is the rate of individual's fitness to the sum of the population's fitness. With this approach, fitter individuals have more probability of being selected. However, even the fittest may not be selected for parenthood [9].

2.5.1.2 Tournament Selection. The tournament selection is made by taking s competitors from the population and selecting the the fittest one, with s being the tournament size. Therefore, the selected individuals have a better average fitness than the population. This difference drives the GA to improve the fitness of each succeeding generation. Increased number of competitors causes increased probability of early convergence [21].

2.5.1.3 Elitism. Fitness-proportional selection does not guarantee the selection of fitter individuals, including the fittest. Therefore, the best solution to the problem discovered might be thrown away. This is sometimes advantageous, because that causes the algorithm to explore more search space before convergence.

For many applications, the search performance can be greatly improved by keeping the best individual between generations. Designing the algorithm so that the best, or *elite*, will not die is termed *elitism*. In elitism, the elite is kept undisrupted between generations while it is the best [9].

2.5.2 Exploration and Exploitation. In order to find a global minimum, an efficient optimization algorithm must use two techniques: *exploration* to investigate new and unknown areas in the search space, and *exploitation* to make use of knowledge found at points previously visited to help find better points. Since these requirements are contradictory, a good search algorithm must find a tradeoff between exploration and exploitation. A good combination of these strategies can be quite effective, but it is hard to find the balance between them to find an acceptable solution [5].

2.6 Summary

Brief overview of the GPS is given in the beginning of this chapter. The outlines of position estimation and Dilution of Precision concept in GPS are discussed. The fundamental concepts and operations for GA are introduced and explained. In Chapter III, the methodology of the thesis is explained.

III. Methodology

3.1 Overview

The purpose of this chapter is to describe the development of the Matlab® simulation for this study. In Section 3.2, the structure of the simulation is provided to give a big picture of the process. In Section 3.3, the implementation of the GA and reason for each adopted approach are explained. In Section 3.4, the formulas used for orbit propagation are given. In Section 3.5, DOP calculation is explained. In Section 3.6, the cost function to evaluate the candidate solutions is introduced.

3.2 The Structure of the Simulation

The simulation is developed in Matlab® environment for this study [1]. The simulation includes a Genetic Algorithm module, an orbit propagator module, and a performance evaluation module. The Genetic Algorithm module generates candidate solutions and provides them to orbit propagator module. The orbit propagator calculates the satellite positions over time. The performance evaluation module exploits the satellite positions calculated by the orbit propagator module and the given receiver positions to find out the cost of each candidate solution. The cost is then provided to Genetic algorithm module. The Genetic Algorithm module assesses the cost of each candidate solution and generates new candidates. This process repeats until the predetermined criteria are met. This process is illustrated in Figure 3.1.

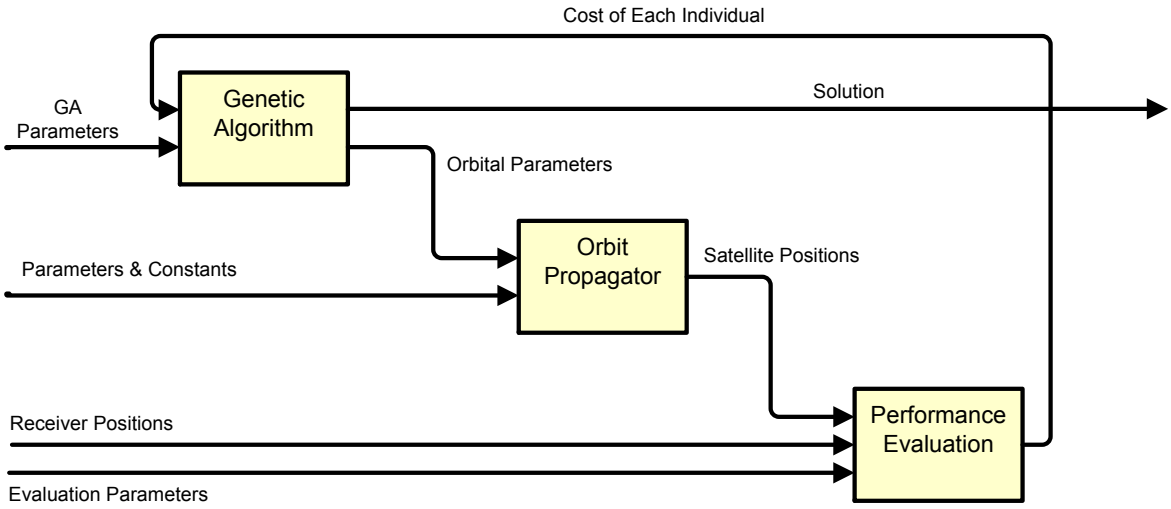

Figure 3.1: Top-Level Simulation Structure

3.3 Genetic Algorithm Implementation

Since there is no unique genetic algorithm that works for all types of optimization problems, a special algorithm has been developed for this study. Since the optimization problem of this study is a minimization problem, using the term *cost* is more sensible than fitness. An initial population is generated randomly, and cost for each individual is calculated. The individuals are mated randomly and the individuals selected by a tournament selection as parents for crossover operation to generate an intermediate population. After the crossover operation, the mutation operation is applied to the intermediate population to create the children population. The cost for each child is calculated. A second tournament selection is made over the initial (old) population and the children generation completely to create the new generation. This process repeats until the stopping criteria for the algorithm are met. The implementation of GA for this study is illustrated in Figure 3.2.

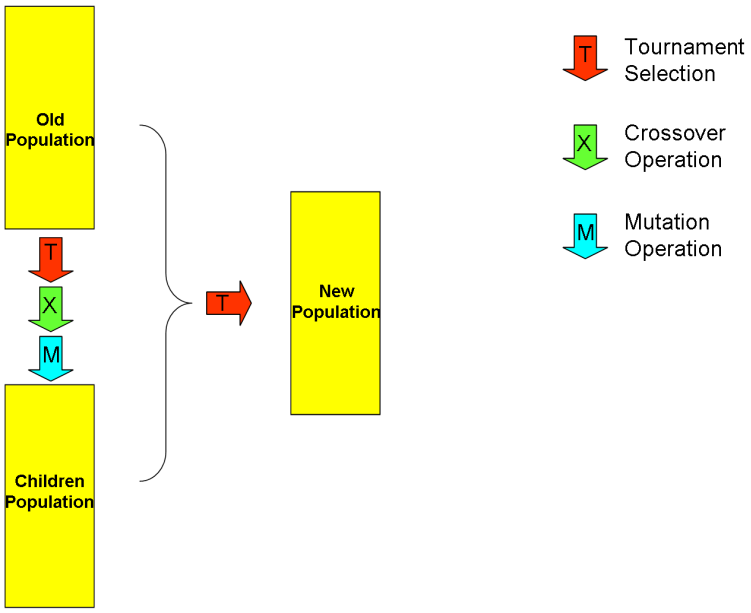

Figure 3.2: Process for Generating New Populations (Also Referred to as a New Generation)

3.3.1 Representation.

3.3.1.1 Encoding. The GA developed for this study relies on binary encoding, which is the traditional GA approach [13]. Providing the required quantization level for desired resolution of parameters, the binary encoding is capable of creating a large enough search space.

In order to encode the parameter values in binary format, the number of the required bits should be determined using Equation 3.1 [13], where l_ξ is the chromosome length (number of bits) of the parameter, ξ_{min} is the minimum parameter value, ξ_{max} is the maximum parameter value and R is the desired resolution (number of digits after the decimal point).

$$2^{(l_\xi - 1)} < (\xi_{max} - \xi_{min})10^R \leq 2^{l_\xi} - 1 \tag{3.1}$$

Calculating the required chromosome length for the parameter value allows to represent the parameter value in the Matlab code for GA operations. Then the binary coded parameter value (ξ_{bin}) can be converted to its decimal value (ξ_{dec}). The decimal value (ξ_{dec}) should be converted to its adjusted or real value (ξ_{real}) by using Equation 3.2 for calculations.

$$\xi_{real} = \xi_{min} + \frac{\xi_{max} - \xi_{min}}{2^{l_\xi} - 1}\xi_{dec} \tag{3.2}$$

3.3.1.2 Population Size. It is very important to create an initial population which provides a good trade-off between efficiency and effectiveness. When the population is small, the algorithm may not effectively explore the search space. On the other hand, when the population is large, the efficiency of the algorithm is significantly reduced to find an optimal solution in a reasonable time of computation. Therefore, there should be an optimal population size for a given individual bit length. At least, a minimum population size should be determined which enables the algorithm to visit every point in the search space. That minimum population size can be calculated using Equation 3.3 [25].

$$\Pi = (1 - (1/2)^{N_{min} - 1})^l \tag{3.3}$$

Where Π is the probability of points in the search space to be explored and N_{min} is the minimum population size. Using an exponential function approximation the equation can be written as follows:

$$\Pi \approx e^{-\frac{l}{2^{N_{min}-1}}} \tag{3.4}$$

Then minimum population size can be calculated using the following equation:

$$N_{min} \approx 1 + \frac{log(-\frac{l}{ln\Pi})}{log2} \tag{3.5}$$

In this study, the population size is determined so that it is not less than the minimum population size and it is not too large (which decreases the efficiency of the algorithm).

3.3.2 Selection. In Holland's original genetic algorithm, parents are replaced by their children just after they give birth which is called *generational replacement*. Because children may be worse than their parents, some fitter chromosomes will be lost from the evolutionary process with the strategy of replacing each parent with his children directly. Several strategies have been developed to overcome this problem [13]. In this thesis research, most of the generated chromosomes have poor fitness values; in fact, some chromosomes have fitness values of not-a-number (NaN) if there is no solution. Therefore, there is no luxury of losing good chromosomes. By applying Holland's original genetic algorithm and his *generational replacement*, the population

of the problem in this study was not able to converge properly. In order to have an evolving population, *enlarged sampling space* approach has been adopted in this study. When selection is performed on enlarged sampling space, both parents and children have the same chance of competing for survival. This approach evidently has an advantage, in that genetic algorithm performance can be improved by increasing the crossover and mutation rates. There is no need to worry that the high rate introduces too much random perturbation, if selection is performed on the enlarged sampling space [13].

There are many selection schemes for GAs, each with different characteristics. An ideal selection scheme would be simple to implement. It also should be able to adjust its selection pressure to tune its performance for different domains. Tournament selection increasingly being used as a GA selection scheme, because it satisfies above mentioned criteria.

Tournament selection was used in the algorithm due to its resistance to early convergence. The tournament selection approach, which closely mimics mating competition in nature, is to randomly pick a small subset of chromosomes (two or three) from the mating pool, and the chromosome with the lowest cost in this subset becomes a parent. The tournament repeats for every parent needed. Tournament selection works best for larger population sizes, because sorting becomes time-consuming for large populations [14].

The tournament selection with two chromosomes in this study ensures that the best individual does not die and the selection pressure is lowest possible to avoid excessive elitism.

Tournament selection is made twice in a generation in this study. The first one is made to select parents for producing intermediate population; λ number of couples are selected out of N number of parents, where λ is the number of children population size and N is the population size. The second tournament selection is accomplished to produce the next generation from the current population; N number of new parents are selected out of $N + \lambda$ number of parents and children of current population. At each time two random individuals are selected and their fitness values are compared and better one is selected.

3.3.3 Crossover. After having selected the mates for crossover, the question arises: How many crossovers should be made? There are two issues relating to crossover: *bias* and *disruption*. The investigation of biasing effect of crossover showed that there are two sources of bias exist to be exploited in a genetic algorithm: *positional bias*, and *distributional bias*. One-point crossover has considerable positional bias, which causes early convergence to sub-optimal solution. On the other hand, one-point crossover has no distributional bias, because the crossover point is chosen randomly. However, lack of this bias is not always good since it limits the exchange of information between the parents. A completely random number crossover, which

is called *uniform crossover*, is capable of significantly reducing any biases. In uniform crossover, each crossover operation is made in random numbers [25].

Uniform crossover is also capable of improving the performance of algorithm as explained by Spears and De Jong [29]. However, uniform crossover causes disruption. Because the mates are cut multiple times, the good features of the parents are disrupted so that the children are less likely to have good fitness values. Disruption slows down evolution in the beginning of the algorithm, but it may be helpful as the algorithm proceeds. When the population becomes quite homogenous, the ability of crossover to produce new individuals is reduced. This ability is called *crossover productivity*. Uniform crossover is capable of having more productivity as evolution proceeds. Uniform crossover is used in this study because of these factors.

In order to implement uniform crossover, a randomly generated vector, which is called *mask*, at the same length of the individuals is used. In the mask vector, a switch from 0 to 1 or from 1 to 0 represents a crossover point at respective bit of mates. This process can be formulated as follows:

$$\begin{aligned} \beta_1^{'} &= \mathbf{m} \otimes \beta_1 \oplus \overline{\mathbf{m}} \otimes \beta_2 \\ \beta_2^{'} &= \overline{\mathbf{m}} \otimes \beta_1 \oplus \mathbf{m} \otimes \beta_2 \end{aligned} \tag{3.6}$$

where β_1 and β_2 are parents, $\mathbf{m}$ is mask vector, $\overline{\mathbf{m}}$ is complement of mask vector, $\beta_1^{'}$ and $\beta_2^{'}$ are children and $\oplus$, $\otimes$ denote component-wise addition and multiplication respectively [25]. This process is illustrated in Figure 3.3.

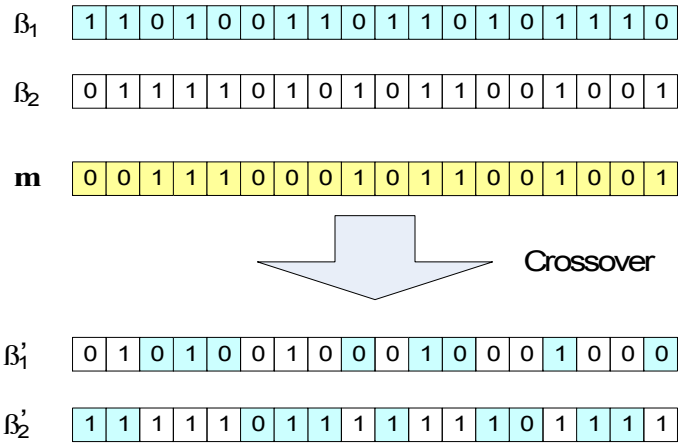

Figure 3.3: In uniform crossover, a switch from 0 to 1 or from 1 to 0 represents a crossover point at respective bit of mates.

3.3.4 Mutation. Mutation operation operation is accomplished by determining the number of bits to be mutated in the population. This number is calculated by multiplying the probability of mutation by the population size and the chromosome length as shown in Equation 3.7 [14].

$$n_m = P_m N l \tag{3.7}$$

where n_m is the number of bits to be mutated, P_m is mutation probability and l is total chromosome length. Then n_m bits are randomly flipped in the population. This process is illustrated in Figure 3.4.

3.4 Orbit Propagation

The orbit propagation module requires six orbital elements to calculate the position of satellites. These elements and their definitions are as follows:

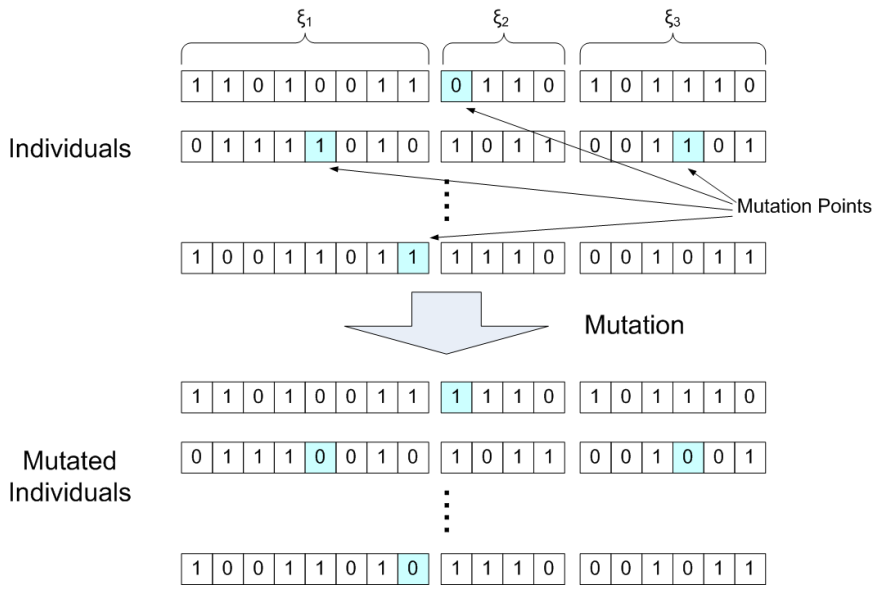

Figure 3.4: In distributed mutation operation, number of bits to be mutated (n_m) are calculated and n_m bits are randomly flipped in the generation.

a Semi-major axis, defines the size and period of the orbit

e Eccentricity, defines the shape of the orbit

i Inclination, defines the angle between orbit plane and the equator

ω Argument of perigee, defines the angle between the ascending node and the orbit's point of closest approach to the earth

ν True anomaly, defines the angle between perigee and the satellite position vector

Ω Right Ascension of Ascending Node (RAAN), defines the angle between vernal equinox and the point where the orbit crosses the equatorial plane from south to north

In Figure 3.5 [4], these elements are illustrated.

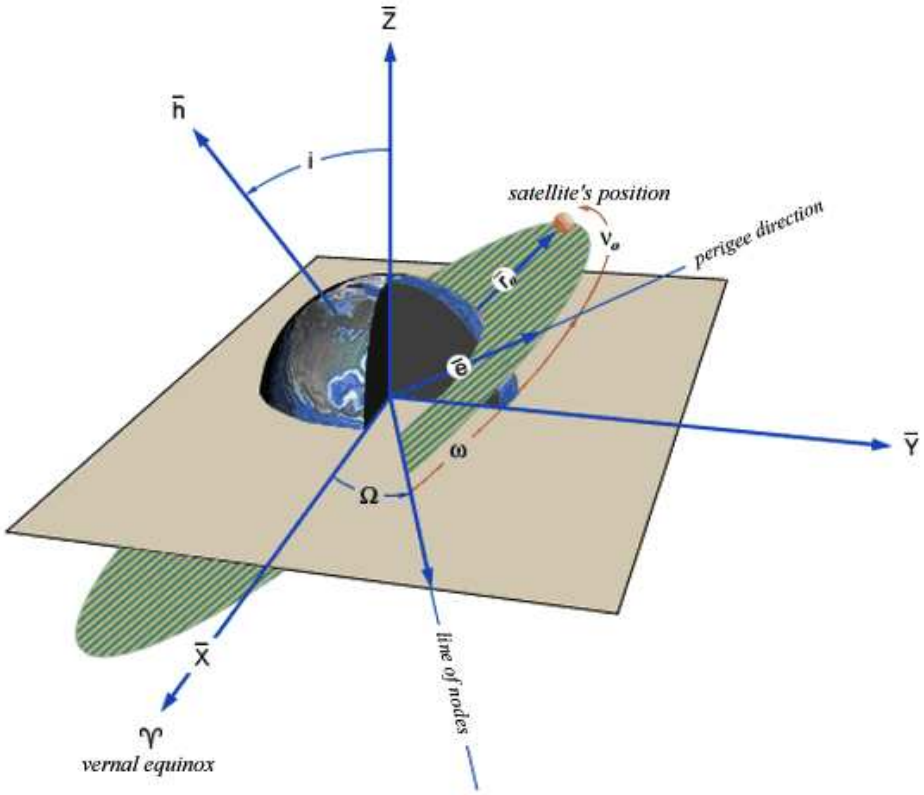

(a)

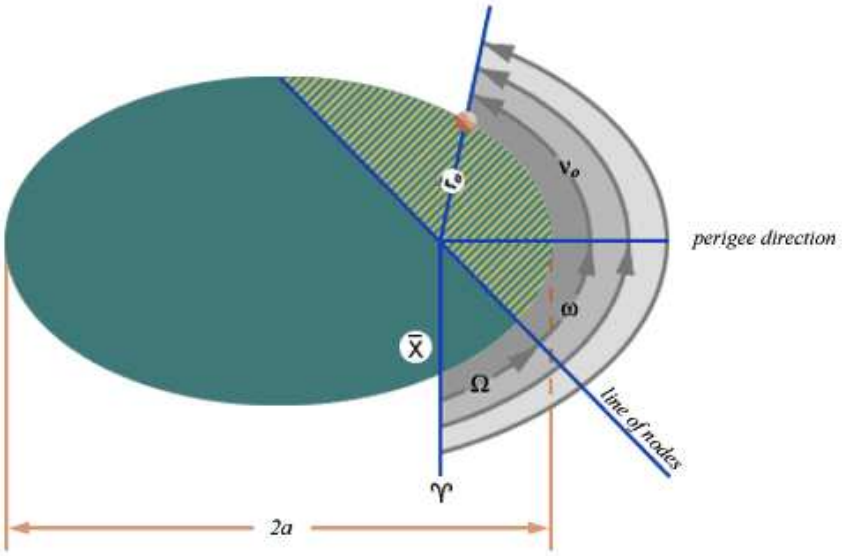

(b)

Figure 3.5: (a) Three dimensional view of the orbital elements.
(b) Orbital elements defined within the orbital plane [4].

In this study, using Longitude of Ascending Node (LAN) (which is defined relative to the earth) is more sensible than RAAN (which is defined relative to the inertial space), because the satellites of the objective constellation should be visible over a specific region of the earth. The input for the orbit propagation is Longitude of Ascending Node, but the corrected RAAN is used for calculation of the actual orbit. This calculation ensures that the ground track of the satellite will be same for different true anomaly values where the other parameters are constant. Therefore, it will be possible to make an optimization of true anomaly. In Figure 3.6, the ground tracks of Sat1 (red) and Sat2 (blue) are shown, which have the same orbital parameters except the true anomaly. The true anomaly values are 180^o and 210^o respectively. Because the RAAN is not corrected to reflect the LAN, the ground track of Sat2 drifts approximately 30^o towards east. The angular difference of two ground tracks on the equatorial plane is the required correction to reflect the same LAN value. Therefore, the corrected RAAN is calculated as follows:

$$\Omega = \Omega_{LAN} - \Omega_{shift} \tag{3.8}$$

where Ω_{LAN} is Longitude of Ascending Node and Ω_{shift} is the required correction for RAAN.

Argument of perigee has a similar effect on the ground track too. Therefore, the effect of both argument of perigee and true anomaly should be calculated. The value of total effect can be calculated as follows:

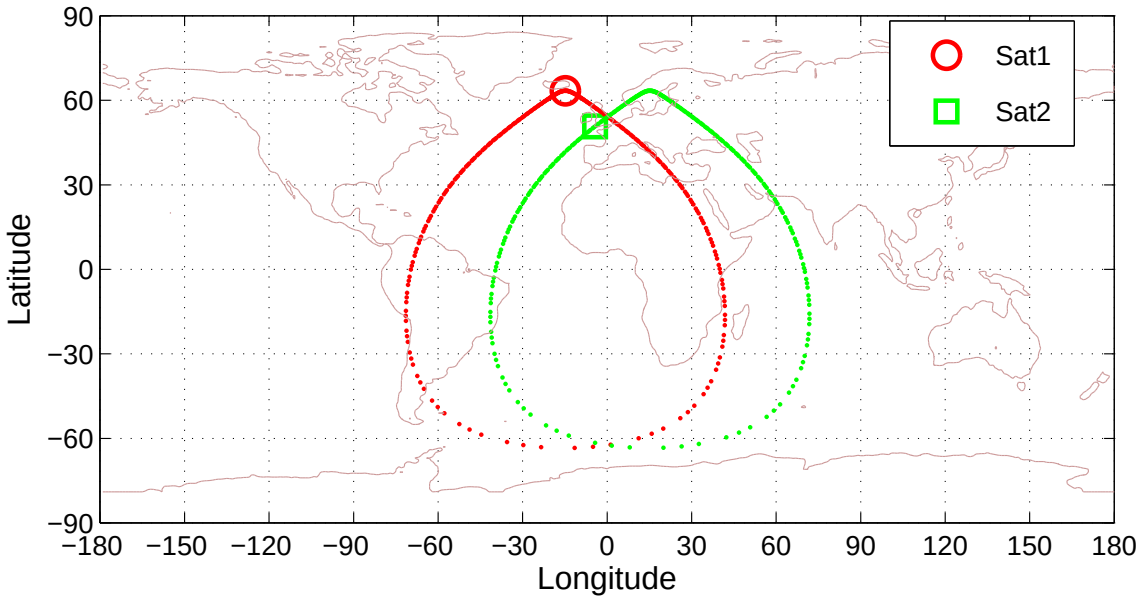

Figure 3.6: The Effect of the Uncorrected RAAN. If the RAAN is not corrected to represent LAN, the ground track drifts when the true anomaly is changed.

$$\Omega_{shift} = \frac{M_\omega + M_\nu}{n} \dot{\Omega}_e + \theta_{GMST} \tag{3.9}$$

where M_ω is the mean anomaly equivalent of argument of perigee, M_ν is the mean anomaly equivalent of true anomaly, n is mean motion, $\dot{\Omega}_e$ is the earth's rotation rate, and θ_{GMST} is Greenwich mean sidereal time. θ_{GMST} can be assumed zero for simplification and mean motion is defined as:

$$n = \sqrt{\frac{\mu}{a^3}} \tag{3.10}$$

where μ is the earth's gravitational constant. Before calculating the mean anomaly equivalent of true anomaly and argument of perigee, their eccentric anomaly equivalents should be calculated.

$$\tan(\frac{E_\omega}{2}) = \sqrt{\frac{1-e}{1+e}}\ \tan(\frac{\omega}{2}) \tag{3.11}$$

$$\tan(\frac{E_\nu}{2}) = \sqrt{\frac{1-e}{1+e}}\ \tan(\frac{\nu}{2}) \tag{3.12}$$

where E_ω is the eccentric anomaly equivalent of argument of perigee and E_ν is eccentric anomaly equivalent of true anomaly. Then the equivalent mean anomaly values are calculated as follows:

$$M_\omega = E_\omega - e\ \sin(E_\omega) \tag{3.13}$$

$$M_\nu = E_\nu - e\ \sin(E_\nu) \tag{3.14}$$

The position of the satellites are calculated a for period of simulation time (t_{sim}) at simulation steps (t_{step}).

$$M_{step} = n\,t + M_\nu \tag{3.15}$$

$$E_{step} = M_{step} + e\ \sin(E_{step}) \tag{3.16}$$

$$\tan(\frac{\nu_{step}}{2}) = \sqrt{\frac{1+e}{1-e}}\,\tan(\frac{E_{step}}{2}) \tag{3.17}$$

Now, the position and velocity vectors can be calculated using two-body equations as follows [33]:

$$p = a\,(1-e^2) \tag{3.18}$$

$$\mathbf{r}_{PQW} = \begin{bmatrix} \frac{p\,\cos(\nu_{step})}{1+e\cos(\nu_{step})} \\ \frac{p\,\sin(\nu_{step})}{1+e\cos(\nu_{step})} \\ 0 \end{bmatrix} \tag{3.19}$$

$$\mathbf{v}_{PQW} = \begin{bmatrix} -\sqrt{\frac{\mu}{p}}\,\sin(\nu_{step}) \\ \sqrt{\frac{\mu}{p}}\,(e+\cos(\nu_{step})) \\ 0 \end{bmatrix} \tag{3.20}$$

where p is orbit semiparameter, $\mathbf{r}_{PQW}$ is position vector in perifocal coordinate system and $\mathbf{v}_{PQW}$ is velocity vector in perifocal coordinate system. It is required to convert those vectors from perifocal coordinate system to ECI frame. The following rotation matrices should be calculated to do this conversion:

$$\mathbf{R}_{\omega} = \begin{bmatrix} \cos(-\omega) & \sin(-\omega) & 0 \\ -\sin(-\omega) & \cos(-\omega) & 0 \\ 0 & 0 & 1 \end{bmatrix} \tag{3.21}$$

$$\mathbf{R}_{i} = \begin{bmatrix} 1 & 0 & 0 \\ 0 & \cos(-i) & \sin(-i) \\ 0 & -\sin(-i) & \cos(-i) \end{bmatrix} \tag{3.22}$$

$$\mathbf{R}_{\Omega} = \begin{bmatrix} \cos(-\Omega) & \sin(-\Omega) & 0 \\ -\sin(-\Omega) & \cos(-\Omega) & 0 \\ 0 & 0 & 1 \end{bmatrix} \tag{3.23}$$

Using the above matrices, the position and velocity vectors can be converted as follows:

$$\mathbf{r}_{ECI} = \mathbf{R}_{\Omega}\,\mathbf{R}_{i}\,\mathbf{R}_{\omega}\,\mathbf{r}_{PQW} \tag{3.24}$$

$$\mathbf{v}_{ECI} = \mathbf{R}_{\Omega}\,\mathbf{R}_{i}\,\mathbf{R}_{\omega}\,\mathbf{v}_{PQW} \tag{3.25}$$

Coordinate frame conversion is not complete yet. Conversion from ECI frame to ECEF frame is also required. In order to convert ECI frame to ECEF frame, how far the earth rotated in t_{step} seconds should be found.

$$\theta = \dot{\Omega}_e \, t_{step} \tag{3.26}$$

where θ is the earth's rotation angle. The following rotation matrix can be calculated using θ:

$$\mathbf{T}_{ECItoECEF} = \begin{bmatrix} \cos(\theta) & \sin(\theta) & 0 \\ -\sin(\theta) & \cos(\theta) & 0 \\ 0 & 0 & 1 \end{bmatrix} \tag{3.27}$$

where $\mathbf{T}_{ECItoECEF}$ is rotation matrix from ECI to ECEF frame. Using this rotation matrix, the position and velocity vectors can be converted from ECI to ECEF frame as follows:

$$\mathbf{r}_{ECEF} = \mathbf{T}_{ECItoECEF} \, \mathbf{r}_{ECI} \tag{3.28}$$

$$\mathbf{v}_{ECEF} = \mathbf{T}_{ECItoECEF} \, \mathbf{v}_{ECI} \tag{3.29}$$

The position vector of a satellite in ECEF frame ($\mathbf{r}_{ECEF}$) calculated in Equation 3.28 is needed to calculate DOP value. In the simulation two-body equations of motion are used to optimize the constellation. The accuracy of two-body equations are enough for short term simulations. However, two-body equations are not realistic for long term simulations, where higher order terms have a larger impact. Therefore,

J_2 perturbation is included in computation for long term analysis of the solutions. In order to include J_2 perturbation effect, the initial condition of satellites should be calculated using Equation 3.11 through Equation 3.25. The calculation of initial position and velocity vectors enables to form the current 6x1 state matrix. One can calculate the next state including the J_2 perturbation as follows:

$$\begin{bmatrix} \mathbf{r}_{1x3} \\ \mathbf{v}_{1x3} \end{bmatrix}_{t+1} = \begin{bmatrix} 0_{3x3} & I_{3x3} \\ \mathbf{G}_{3x3} & 0_{3x3} \end{bmatrix} \begin{bmatrix} \mathbf{r}_{1x3} \\ \mathbf{v}_{1x3} \end{bmatrix}_t + \begin{bmatrix} 0_{3x3} & 0_{3x3} \\ \mathbf{a}_{3x3} & 0_{3x3} \end{bmatrix} \begin{bmatrix} \mathbf{r}_{1x3} \\ \mathbf{v}_{1x3} \end{bmatrix}_t \tag{3.30}$$

where 0_{3x3} is zero matrix and I_{3x3} is identity matrix. $\mathbf{G}_{3x3}$ and $\mathbf{a}_{3x3}$ are defined as follows:

$$\mathbf{G} = \begin{bmatrix} -\frac{\mu}{\sqrt{\|r\|^3}} & 0 & 0 \\ 0 & -\frac{\mu}{\sqrt{\|r\|^3}} & 0 \\ 0 & 0 & -\frac{\mu}{\sqrt{\|r\|^3}} \end{bmatrix} \tag{3.31}$$

$$\mathbf{a} = \begin{bmatrix} a_I & 0 & 0 \\ 0 & a_J & 0 \\ 0 & 0 & a_K \end{bmatrix} \tag{3.32}$$

a_I, a_J and a_K are the accelerations due to J_2 perturbation in the respective axis in ECI frame. J_2 acceleration components are defined as follows [33]:

$$a_I = -\frac{3J_2\mu R_\oplus^2}{2\|r\|^5}(1 - \frac{5\|r_K\|^2}{\|r\|^2}) \tag{3.33}$$

$$a_J = -\frac{3J_2\mu R_\oplus^2}{2\|r\|^5}(1 - \frac{5\|r_K\|^2}{\|r\|^2}) \tag{3.34}$$

$$a_K = -\frac{3J_2\mu R_\oplus^2}{2\|r\|^5}(3 - \frac{5\|r_K\|^2}{\|r\|^2}) \tag{3.35}$$

where $R_\oplus$ is earth's radius. After the satellite positions are calculated in ECI frame, they are converted to ECEF frame using the equations 3.26, 3.27 and 3.28.

3.5 DOP Calculation

The DOP should be calculated for different receiver positions in the desired region. The receiver position coordinates, which are defined in the World Geodetic System 1984 (WGS84) reference system, should be converted to ECEF frame. In this study, this conversion is accomplished using the *lla2ecef* function of *Aerospace* toolbox in MATLAB. After having the receiver positions converted to ECEF frame, one can determine the elevation angle of the Line-of-Sight (LOS) vectors from receiver to satellites using the *elevation* function of *Mapping* toolbox in MATLAB. Then elevation angles (El) for each satellite should be more than mask angle (El_{mask}):

$$El > El_{mask} \tag{3.36}$$

The satellites which are below mask angle are assumed as non-visible. If there are fewer than four visible satellite, DOP is undefined and valued as NaN. If there are at least four satellites, the unit LOS vectors are calculated as follows:

$$\mathbf{u}_k = \mathbf{r}_k - \mathbf{r}_u \tag{3.37}$$

where $\mathbf{u}_k$ is the receiver to satellite LOS unit vector, $\mathbf{r}_k$ is position vector of k^{th} satellite in ECEF frame (calculated as $\mathbf{r}_{ECEF}$ in the previous section) and $\mathbf{r}_u$ is receiver position vector in ECEF frame. Then the $\mathbf{H}$ is formed as follows:

$$\mathbf{H} = \begin{bmatrix} \mathbf{u}_1 & -1 \\ \mathbf{u}_2 & -1 \\ \vdots & \\ \mathbf{u}_n & -1 \end{bmatrix} \tag{3.38}$$

The DOP matrix is calculated using Equation 2.21. Because GDOP represents the overall satellite geometry, GDOP value is calculated to analyze the navigation performance of the constellation using Equation 2.22. The system is considered available if the GDOP value is less than a threshold value ($GDOP_T$). Therefore, the system must meet the following criterion:

$$GDOP < GDOP_T \tag{3.39}$$

After calculating GDOP value and availability for all receivers and time steps, the proposed solution can be evaluated. In this study, performance evaluation of the constellation is made considering accuracy and availability.

3.6 Cost Calculation

The GA developed for this study requires a single cost value for each candidate solution. The cost function is developed to evaluate the candidate solutions based on the following criteria:

1. The availability should be 100%, if possible.
2. Average GDOP should be the lowest possible.
3. The system should perform better over the region of interest.

The cost function developed to meet the above requirements is as follows:

$$C_f = W_{GDOP} \sum_{i=1}^{n_r} W_i \, \overline{GDOP}_i + W_\alpha \sum_{i=1}^{n_r} W_i \, (1 - \alpha_i) \tag{3.40}$$

where C_f is cost function, W_{GDOP} is GDOP weight, n_r is number of the receiver points, W_i is weight of i^{th} receiver point, $\overline{GDOP}_i$ is average GDOP value at the i^{th} receiver, W_α is availability weight, and α_i is availability at the i^{th} receiver (expressed as a decimal notability, where 1 is always available and 0 is never available). *NaN* GDOP values are disregarded for average GDOP calculation.

For most applications, which are using satellite based navigation, it is desired to have the system at all times with the most accuracy. Therefore, the navigation system should provide a good accuracy with continuous service. The cost function was developed to meet this requirement.

3.7 Summary

In this chapter, the structure of the simulation developed for this study is covered. The adopted approach for each operator of GA is explained in detail. The equations of the orbit propagator and DOP calculation are given. Finally, the cost evaluation function is formed to distinguish the better constellations among the population. In Chapter IV, the obtained data and analysis are given.

IV. Data and Analysis

4.1 Overview

In this chapter, the obtained data are given and analyzed. In Section 4.2, the settings of the developed simulation are given. In Section 4.3, the nature of the search space of this problem is analyzed. In Section 4.4, the designed GA is tested to see if it is effective for generating solutions for the problem of this thesis effort. In Section 4.5, the obtained data for the cases are analyzed in groups, which have similar constraints. Finally, in Section 4.6, the J2 perturbation effect on the designed constellations with different features are analyzed.

4.2 Simulation Settings

All but one constellation proposed in this thesis research are comprised of five satellites. Several cases are designed with different constraints. All cases were run for three different random seeds to mitigate the bias caused by Matlab®'s random number generator. One of the cases was designed to have four satellites.

Based on the constraints determined for the cases and the resolution of the variables, total bit length for each case were calculated according to using Equation 3.5. The resolution of the variables and the required bit length calculation for Case 1 are given in Table 4.1.

The sum of the bit length of each variable for the first case equals 47 for one satellite in Case 1, which is the unconstrained case. Then the total bit length (l) is calculated as (47x5 = 235). The next step is to find the minimum population size.

Table 4.1: The required bit length calculation for the first case

	e	i	Ω_{LAN}	ω	ν
R	2	1	1	0	0
$\xi_{min} : \xi_{max}$	0 : 0.85	0 : 90	0 : 360	0 : 360	0 : 360
l_ξ	7	10	13	9	9

In order to ensure almost a 100% probability of the algorithm to visit every point of the search space with crossover operation and without mutation, the minimum population size for $l = 235$ is calculated as 55. In the simulation for every case, the population size is used as 400 which is more than the minimum required population size and provides a better algorithm performance. The number of the generations for the cases was set to 300, 600, and 900, depending on the convergence rate of the cases.

Case 1 has ($2^{235} = 5.52\text{x}10^{70}$) candidate solutions and is run with a parent population number of 400 and children number of 400 for 600 generations. Calculating the cost of every candidate solution would be impossible, where the GA calculates the cost of only a maximum of (800x600 = 480000) candidate solutions in an effort to find an optimal solution in a reasonable computation time. Obviously, the GA evaluates only very small amount of the possible candidate solutions. That is one of the prominent features of the GA. Because it is not possible to evaluate every possible solutions using the GA with above mentioned parameters, it is not guaranteed that the optimal solution found by the GA is the best one. However, the generated solution is an optimal and reasonable solution.

The parameters and the constants used in the simulation are given in Table 4.2. The constraints for each case are given in Table 4.3.

Table 4.2: The constants and parameters of the simulation.

Symbol	Parameter	Value
a	Semi-major axis	42164169.6 m
μ	Earth's gravitational constant	398600.5 km^3/s^2
$R_\oplus$	Earth's radius	6378137 m
$\dot{\Omega}_e$	Earth's rotation rate	$7.2921151\,\mathrm{x}\,10^{-5}$ rad/s
J_2	J_2 perturbation coefficient	0.0010826269
t_{sim}	Simulation time	259000 s
t_{step}	Simulation time step	900 s
El_{mask}	Elevation mask angle	10^o
$GDOP_T$	GDOP threshold value	10
W_{GDOP}	GDOP weight	1
W_α	Availability weight	300
N	Parent Population size	400
λ	Children population size	400
g	Number of generations	300, 600, and 900
P_c	Crossover Probability	1
P_m	Mutation Probability	$1/l$

Table 4.3: Constraints of the Cases

Case	Eccentricity					Inclination					Longitude of Ascending Node					Argument of Perigee					True Anomaly				
	1	2	3	4	5	1	2	3	4	5	1	2	3	4	5	1	2	3	4	5	1	2	3	4	5
1	0 : 0.85	0 : 0.85	0 : 0.85	0 : 0.85	0 : 0.85	0 : 90	0 : 90	0 : 90	0 : 90	0 : 90	0 : 360	0 : 360	0 : 360	0 : 360	0 : 360	0 : 360	0 : 360	0 : 360	0 : 360	0 : 360	0 : 360	0 : 360	0 : 360	0 : 360	0 : 360
2	0 : 0.85	0 : 0.85	0 : 0.85	0 : 0.85	-	0 : 90	0 : 90	0 : 90	0 : 90	-	0 : 360	0 : 360	0 : 360	0 : 360	-	0 : 360	0 : 360	0 : 360	0 : 360	-	0 : 360	0 : 360	0 : 360	0 : 360	-
3	0	0	0 : 0.85	0 : 0.85	0 : 0.85	0	0	0 : 90	0 : 90	0 : 90	0	70	0 : 360	0 : 360	0 : 360	0	0	0 : 360	0 : 360	0 : 360	0	0	0 : 360	0 : 360	0 : 360
4	0	0	0 : 0.85	0 : 0.85	0 : 0.85	0	0	0 : 90	0 : 90	0 : 90	350 : 10	60 : 80	0 : 360	0 : 360	0 : 360	0	0	0 : 360	0 : 360	0 : 360	0	0	0 : 360	0 : 360	0 : 360
5	0	0	0 : 0.85	0 : 0.85	0 : 0.85	0	0	0 : 90	0 : 90	0 : 90	0 : 360	0 : 360	0 : 360	0 : 360	0 : 360	0	0	0 : 360	0 : 360	0 : 360	0	0	0 : 360	0 : 360	0 : 360
6	0	0	0 : 0.85	0 : 0.85	0 : 0.85	0	0	0 : 90	0 : 90	0 : 90	330 : 110	330 : 110	0 : 360	0 : 360	0 : 360	0	0	0 : 360	0 : 360	0 : 360	0	0	0 : 360	0 : 360	0 : 360
7	0	0	0 : 0.85	0 : 0.85	0 : 0.85	0	0	63.4	63.4	63.4	330 : 110	330 : 110	0 : 360	0 : 360	0 : 360	0	0	0 : 360	0 : 360	0 : 360	0	0	0 : 360	0 : 360	0 : 360
8	0	0	0 : 0.85	0 : 0.85	0 : 0.85	0	0	63.4	63.4	63.4	330 : 110	330 : 110	0 : 360	0 : 360	0 : 360	0	0	270	270	270	0	0	0 : 360	0 : 360	0 : 360
9	0	0	0.3 : 0.7	0.3 : 0.7	0.3 : 0.7	0	0	63.4	63.4	63.4	330 : 110	330 : 110	0 : 360	0 : 360	0 : 360	0	0	270	270	270	0	0	0 : 360	0 : 360	0 : 360
10	0	0	0.3 : 0.7	0.3 : 0.7	0.3 : 0.7	0	0	63.4	63.4	63.4	330 : 110	330 : 110	0 : 360	0 : 360	0 : 360	0	0	0 : 360	0 : 360	0 : 360	0	0	0 : 360	0 : 360	0 : 360
11	0	0	0 : 0.85	0 : 0.85	0 : 0.85	0	0	63.4	63.4	63.4	330 : 110	330 : 110	0 : 180	0 : 180	0 : 180	0	0	270	270	270	0	0	0 : 360	0 : 360	0 : 360
12	0	0	0 : 0.85	0 : 0.85	0 : 0.85	0	0	63.4	63.4	63.4	330 : 110	330 : 110	0 : 180	0 : 180	0 : 180	0	0	180 : 360	180 : 360	180 : 360	0	0	0 : 360	0 : 360	0 : 360
13	0	0	0.3 : 0.7	0.3 : 0.7	0.3 : 0.7	0	0	63.4	63.4	63.4	330 : 110	330 : 110	0 : 180	0 : 180	0 : 180	0	0	180 : 360	180 : 360	180 : 360	0	0	0 : 360	0 : 360	0 : 360
14	0	0	0.3 : 0.7	0.3 : 0.7	0.3 : 0.7	0	0	63.4	63.4	63.4	0 : 360	0 : 360	0 : 180	0 : 180	0 : 180	0	0	180 : 360	180 : 360	180 : 360	0	0	0 : 360	0 : 360	0 : 360
15	0	0	0.3 : 0.7	0.3 : 0.7	0.3 : 0.7	0	0	63.4	63.4	63.4	0 : 360	0 : 360	0 : 360	0 : 360	0 : 360	0	0	0 : 360	0 : 360	0 : 360	0	0	0 : 360	0 : 360	0 : 360
16	0 : 0.85	0 : 0.85	0 : 0.85	0 : 0.85	0 : 0.85	0 : 90	0 : 90	0 : 90	0 : 90	0 : 90	0 : 360	0 : 360	0 : 180	0 : 180	0 : 180	180 : 360	180 : 360	180 : 360	180 : 360	180 : 360	0 : 360	0 : 360	0 : 360	0 : 360	0 : 360
17	0 : 0.85	0 : 0.85	0 : 0.85	0 : 0.85	0 : 0.85	0 : 75	0 : 75	0 : 75	0 : 75	0 : 75	0 : 180	0 : 180	0 : 180	0 : 180	0 : 180	180 : 360	180 : 360	180 : 360	180 : 360	180 : 360	0 : 360	0 : 360	0 : 360	0 : 360	0 : 360
18	0 : 0.85	0 : 0.85	0 : 0.85	0 : 0.85	0 : 0.85	0 : 90	0 : 90	0 : 90	0 : 90	0 : 90	0 : 360	0 : 360	0 : 360	0 : 360	0 : 360	0 : 360	0 : 360	0 : 360	0 : 360	0 : 360	0 : 360	0 : 360	0 : 360	0 : 360	0 : 360
19	0	0	0.5	0.5	0.5	0	0	63.4	63.4	63.4	0	70	60	80	100	0	0	270	270	270	0	0	0 : 360	0 : 360	180
20	0 : 0.85	0 : 0.85	0 : 0.85	0 : 0.85	0 : 0.85	0 : 90	0 : 90	0 : 90	0 : 90	0 : 90	0 : 360	0 : 360	0 : 360	0 : 360	0 : 360	0 : 360	0 : 360	0 : 360	0 : 360	0 : 360	0 : 360	0 : 360	0 : 360	0 : 360	0 : 360

The simulation was run for 20 cases-18 using the GA, one random run without the GA and a benchmark run. The description of the cases are given in Table 4.4.

Table 4.4: The Description of the Cases.

Case	Description
1	Unconstrained
2	Four satellite
3	2 GEO Ω_{LAN}(0,70), 3 GSO
4	2 GEO Ω_{LAN}(350:10,60:80), 3 GSO
5	2 GEO, 3 GSO
6	2 GEO Ω_{LAN}(330:110), 3 GSO
7	2 GEO Ω_{LAN}(330:110), 3 GSO i(63.4)
8	2 GEO Ω_{LAN}(330:110), 3 GSO i(63.4) ω(270)
9	2 GEO Ω_{LAN}(330:110), 3 GSO e(0.3:0.7) i(63.4) ω(270)
10	2 GEO Ω_{LAN}(330:110), 3 GSO e(0.3:0.7) i(63.4)
11	2 GEO Ω_{LAN}(330:110), 3 GSO i(63.4) Ω_{LAN}(0:180) ω(270)
12	2 GEO Ω_{LAN}(330:110), 3 GSO i(63.4) Ω_{LAN}(0:180) ω(180:360)
13	2 GEO Ω_{LAN}(330:110), 3 GSO e(0.3:0.7) i(63.4) Ω_{LAN}(0:180) ω(180:360)
14	2 GEO, 3 GSO e(0.3:0.7) i(63.4) Ω_{LAN}(0:180) ω(180:360)
15	2 GEO, 3 GSO e(0.3:0.7) i(63.4)
16	5 GSO ω(180:360)
17	5 GSO i(0:75) Ω_{LAN}(180:360) ω(180:360)
18	Unconstrained, random
19	2 GEO Ω_{LAN}(0,70), 3 GSO e(0.5) i(63.4) Ω_{LAN}(60,80,100) ω(270) ν(0:360,0:360,180)
20	Benchmark (Same Constraints with Case 19)

The constellations were optimized to have the best performance within the specified region (shown in Figure 1.1) by applying the geographically distributed receiver weights. The coordinates and the weights of thirteen receiver points are given in Table 4.5. They are also shown on the map in Figure 4.1.

Table 4.5: The Coordinates and Weights for Each Receiver Site

Receiver	Latitude (^{o})	Longitude (^{o})	Weight
1	40 00	35 00	5
2	43 00	27 00	5
3	43 00	43 00	5
4	36 00	27 00	5
5	36 00	43 00	5
6	45 00	20 00	4
7	45 00	50 00	4
8	35 00	50 00	4
9	35 00	20 00	4
10	30 00	30 00	3
11	30 00	40 00	3
12	50 00	30 00	2
13	50 00	40 00	2

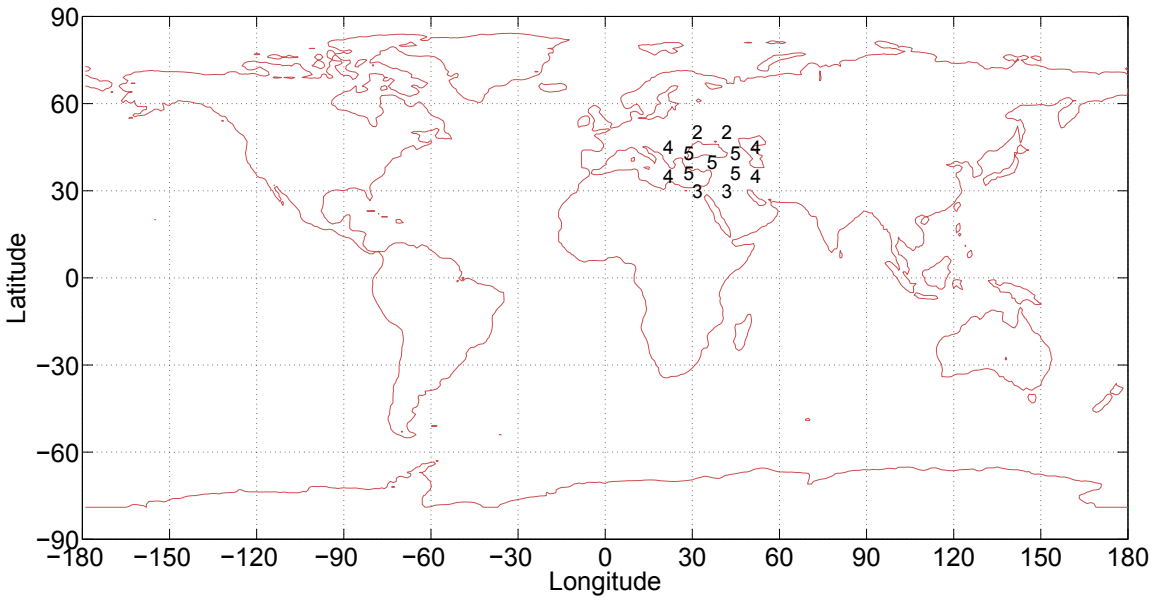

Figure 4.1: Receiver Weights and Geographical Distributions

4.3 The Nature of the Search Space

The level of difficulty to find a solution for this problem can be inferred by analyzing the nature of the search space. Because there are 25 variables in this problem, it is hard to expose all of the relationships between the variables. However, a limited analysis can be made by keeping all variables constant except one variable at a time.

The effect of each variable on the cost was calculated while keeping the other variables constant. It is crucial to state that this analysis does not reflect the exact nature of the search space. Moreover, the results of this analysis is specific to the selected constellation (Case 1 Seed 4). Therefore, for an arbitrary constellation, the relationships between the variables might be different. However, this analysis is enough to give a sense of the roughness of the search space. The ground track of the constellation selected for this analysis is given in Figure 4.7. Parameters of the constellation used for this analysis is given in Table 4.6.

The effect of each variable on the cost for the selected constellation is shown in Figure 4.2. The effect of the eccentricity and the inclination is not very rough. However, the effect of the longitude of ascending node, the argument of perigee, and the true anomaly are very rough. There are lots of peaks and dips in the plots related to those variables. This roughness of the search space shows that there are numerous local minimums, which makes it hard to search for global minimum. This situation is more serious when the variables are unconstrained. Overall, this analysis shows

that the search space of the problem is very rough, it is challenging to find a global minimum.

Table 4.6: The Parameters of the Constellation Used for the Search Space Analysis

Satellite	1	2	3	4	5
Eccentricity	0.2075	0.85	0.8433	0.0335	0.0803
Inclination	23.0499	87.8006	85.8651	5.5425	19.8827
LAN	52.4835	150.6813	84.6593	79.8242	35.7802
Argument of Perigee	286.7319	292.3679	247.9843	348.0235	331.1155
True Anomaly	156.3992	11.9765	208.5323	138.0822	270.5284

4.4 Validation of the Simulation Performance

Before analyzing the solutions generated by the simulation, it should be validated that the GA is designed well for the problem. Two tests were made for this purpose. The first one is to test the GA in a case where the best (or benchmark) solution is already known. The second one is to test if the GA performs in a random manner or it evolves.

4.4.1 Compare Generated Solutions with a Benchmark. Does the developed simulation work well in terms of GA? This question can be answered by determining the best solution after evaluating all possible solutions and comparing it with the solution generated by the GA.

As discussed before, it is impossible to evaluate every possible solution in a reasonable amount of time. However, it is possible to limit the search space so that

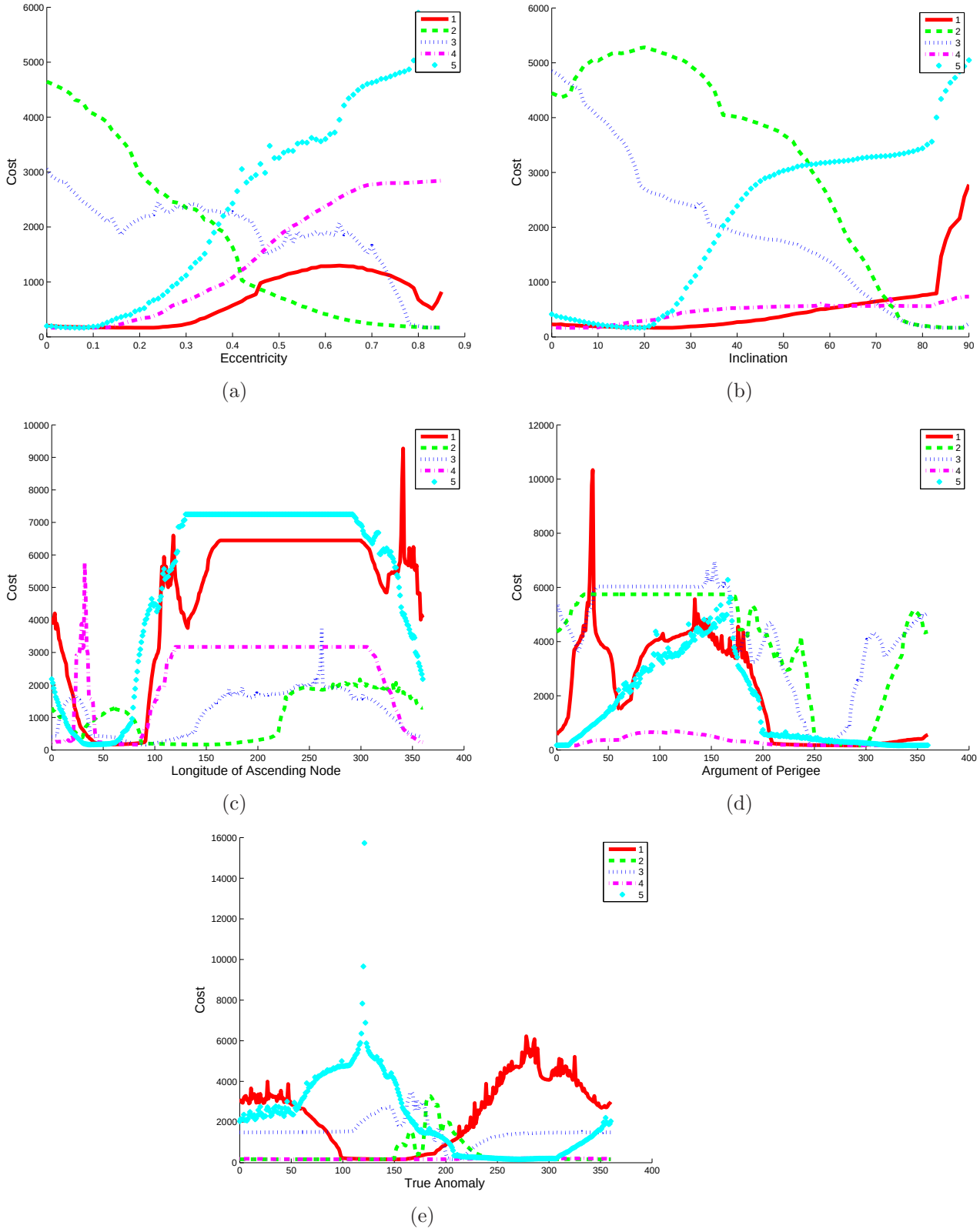

Figure 4.2: (a,b,c,d,e, and f) The effect of each variable on the cost for a selected constellation (e, i, Ω_{LAN}, ω, and ν respectively).

every possible solution in this limited search space can be evaluated in a reasonable amount of time. The benchmark case, with a limited search space, is designed as two GEO satellites at 0^o and 70^o on the equator and three GSO satellites with e(0.5) i(63.4) Ω_{LAN}(60,80,100) ω(270) ν(0:360,0:360,180). Only true anomaly vales (ν) of the third and fourth satellites are not fixed. Because true anomaly (ν) is represented by 9 bits (512 quantization levels from 0 to 360) there are (512x512=262144) possible solutions to be evaluated. This limited search space made it possible to evaluate every solution and find the best one. Another case, Case 19, was designed with the same search space for the GA run. Case 19 is run with a parent population number of 50 and children population number of 50 for 50 generations. So, a maximum of (51x50=2550) points are visited at each run for five different seed numbers. The ratio of the visited points to the number of all points in the search space is ($2550/262144 \approx 0.0097$). It is expected that the GA generates very similar solutions to the solution found in the benchmark case, which is the best one. The solutions generated by the GA and the benchmark runs are given in Table 4.7. The ground tracks of the solutions are depicted in Figure 4.3.

The GA has generated very similar solutions to the best solution. The results of this test showed that the designed GA is evolving and capable of generating good solutions. Therefore, it can be stated that the GA has accomplished the expectations.

4.4.2 Random vs GA. The GA heavily depends heavily upon randomness for its results. Because the solution is generated after evaluation of multiple possible

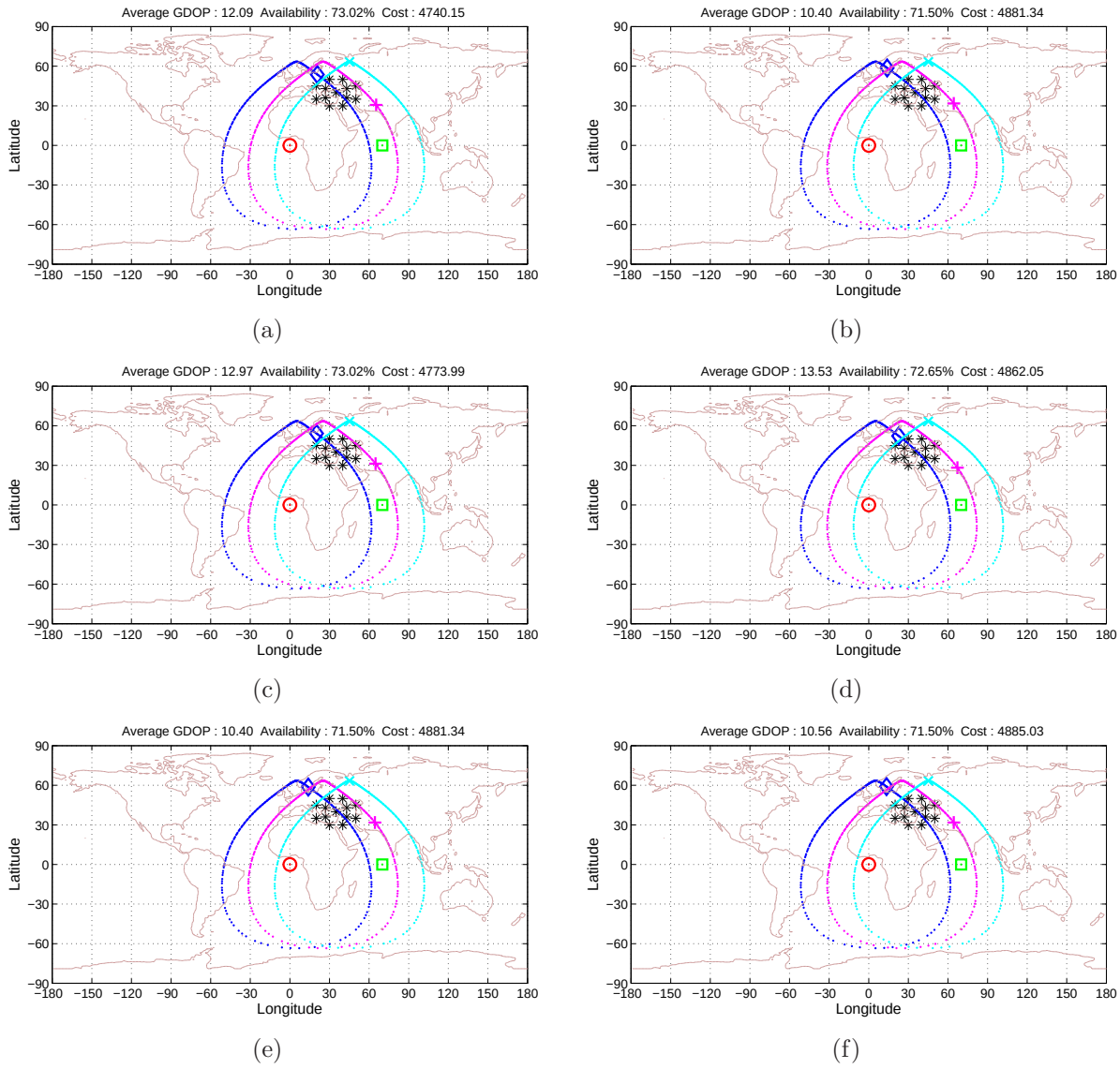

Figure 4.3: (a) Ground track of the optimal solution for benchmark case. (b,c,d,e, and f) Ground tracks of the generated solutions for Case 19 (Random Seed 1,2,3,4 and 5 respectively). Constraints: (2 GEO Ω_{LAN}(0,70), 3 GSO e(0.5) i(63.4) Ω_{LAN}(60,80,100) ω(270) ν(0:360,0:360,180)

Table 4.7: Comparison of the Benchmark and Case 19 Runs

Case	Average GDOP	Availability(%)	Cost	Δ Cost (%)
Benchmark	12.09	73.02	4740.14	0.00
Case 19 Seed 1	10.40	71.50	4881.34	+2.98
Case 19 Seed 2	12.97	73.02	4773.99	+0.71
Case 19 Seed 3	13.53	72.65	4862.05	+2.57
Case 19 Seed 4	10.40	71.50	4881.34	+2.98
Case 19 Seed 5	10.56	71.50	4885.05	+3.06

solutions, one might question whether the GA performs any better than a random search. A test was conducted to see if it is possible to find similar solutions to the GA solutions by searching the search space randomly. If it is possible, then there is no need to use the GA. This issue can be resolved by comparing the GA performance and the random search performance for the same search space. Case 18 was designed to compare the GA performance with a random search. Case 18 is an unconstrained case as Case 1 (i.e., it has the same search space with Case 1). Case 18 was run by evaluating (400x600=240000) random solutions. On the other hand, Case 1 was run with a parent population number of 400 and children population number of 400 for 600 generations using the GA. Therefore, a maximum number of (400x600=240000) solutions are evaluated in Case 1, which is equal to the number of solutions evaluated in Case 18.

The performance of Case 1 and Case 18 are compared in Table 4.8. Case 18 has generated poor solutions at various cost levels. On the other hand, the GA run for Case 1 has generated very good and acceptable solutions. In all cases, the GA

resulted in more than an order of magnitude in cost over the purely random search. Besides, the costs of the GA generated solutions are very close to each other. This shows that the GA designed for this study is mush better than a purely random search tool, and it generates consistent solutions. This demonstrates the value of the GA for efficiently searching for a solution. The generated solutions of Case 1 (GA) and Case 18 (Random) are depicted in Figure 4.4.

Table 4.8: Comparison of Case 1 and Case 18 Runs

	Case 1 (using GA)			Case 18 (best randomly generated result)		
Seed	Av. GDOP	Availability(%)	Cost	Av. GDOP	Availability(%)	Cost
1	4.41	100	223.44	4.81	61.00	6141.29
2	3.61	100	183.79	7.39	75.08	4122.96
3	4.45	99.41	275.10	6.75	73.96	6279.04
4	3.30	100	166.71	8.62	72.30	4729.84
5	4.05	100	206.56	6.10	65.36	5549.88

4.5 Obtained Data

Case 1 is an unconstrained case and has the largest search space. Having the largest search space among the other cases ensures that the search space of Case 1 includes the best possible solution. However, a larger search space makes it harder to find good solutions for the GA. Therefore, it shouldn't be expected that the solutions generated for Case 1 should be better than the solutions generated for the other cases. In order to assist the GA to find better solutions, the search space was constrained in various ways for subsequent cases.

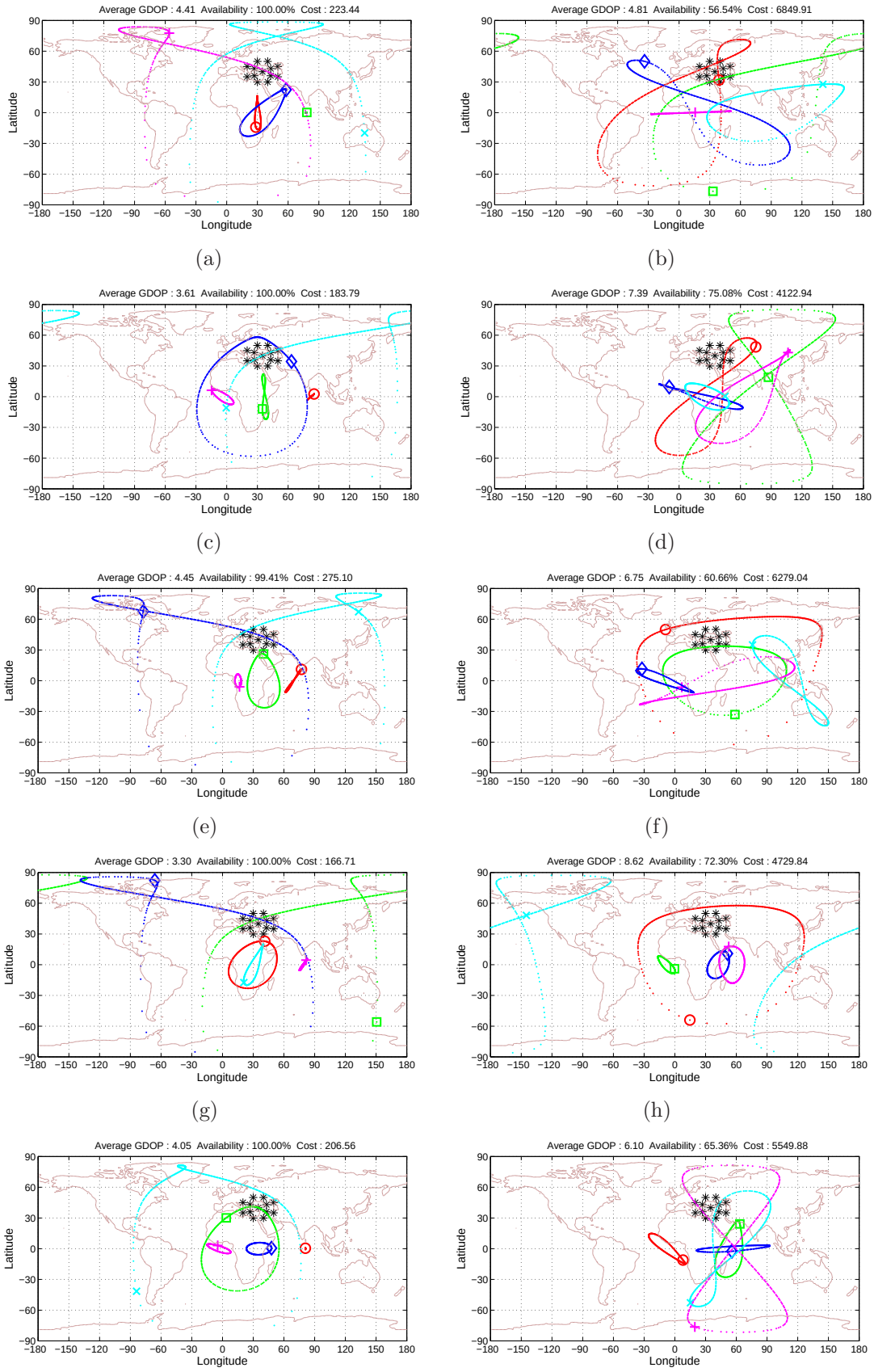

Figure 4.4: Ground tracks of the generated solutions for Case 1 (1^{st} column) and Case 18 (2^{nd} column) (Random Seeds 1,2, and 3 respectively). No Constraints.

First, a detailed analysis of the results obtained for Case 1 is given. Next, the obtained data for the four-satellite case is analyzed. Finally, the rest of the cases are analyzed in groups, which have similar constraints.

4.5.1 Case 1 (Unconstrained case). This case was designed to find a good solution in the whole search space of this thesis. Although Case 1 has the largest search space in this thesis, the GA has generated very good solutions. The GA evolution for Case 1 was able to converge in 600 generations. The progress of the GA evolution for Case 1 Seed 4 is shown in Figure 4.6. The red bars are the average cost values of the populations and the black bars are the cost value of the best individual in each population. The progress of the GA evolution demonstrates that despite the already accepted level of elitism, caused by the use of the enlarged sampling space, it doesn't converge prematurely.

The ground track of the generated constellation for Case 1 Seed 4, one of the best, is shown in Figure 4.7. The average GDOP and the availability values on top of the constellation plots are not weighted for the receivers. Therefore, they shouldn't be used for comparison. They are provided to give an overall idea of the performance of the constellation. This condition applies to all average GDOP and availability values given in the plots and tables except the values for specific receiver sites. However, the cost value can be used for comparison, which is already done to determine the good and bad constellations during the GA process.

The geographical distribution of the average GDOP and availability are given in Figure 4.5 for Case 1 Seed 4 as an example. The contour plots demonstrate that the performance of the constellation does not have fluctuations geographically in the central area of the specified region (Figure 1.1). Therefore, it can be stated that the constellation has a geographically smooth performance.

The generated constellations for Case 1 tend to exploit orbits that are combinations of low inclination orbits, which provide continuous visibility, and high inclination orbits, which provide better satellite geometry (leads to lower GDOP values). The constellations generated for this case provide 100% availability and an average GDOP value of 4.

The visibility of the satellites and the GDOP values over the whole simulation time is shown in Figure 4.8 for Receiver Site 1.

4.5.2 Obtained Data from the Four-Satellite Case (Case 2). In theory, four satellites are enough for creating a navigation satellite constellation, as discussed in Section 2.4. That is still true, because navigation signals transmitted by four satellites are generally sufficient for calculating a position estimate. However, the desired accuracy level may not be achieved by a four-satellite constellation if the satellite geometry is poor. In order to analyze the performance of an optimal four-satellite constellation, Case 2 was run without any constraints. The GA runs for Case 2 were able to converge in 900 generations. The evolutionary progress of the GA for Case 2 Seed 1 is shown in Figure 4.9.

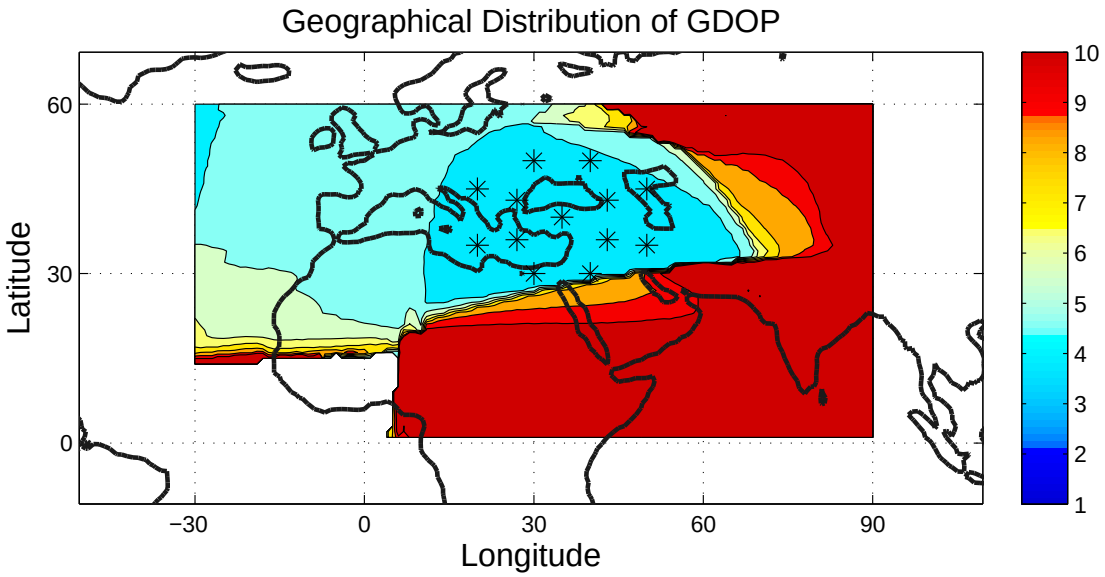

(a)

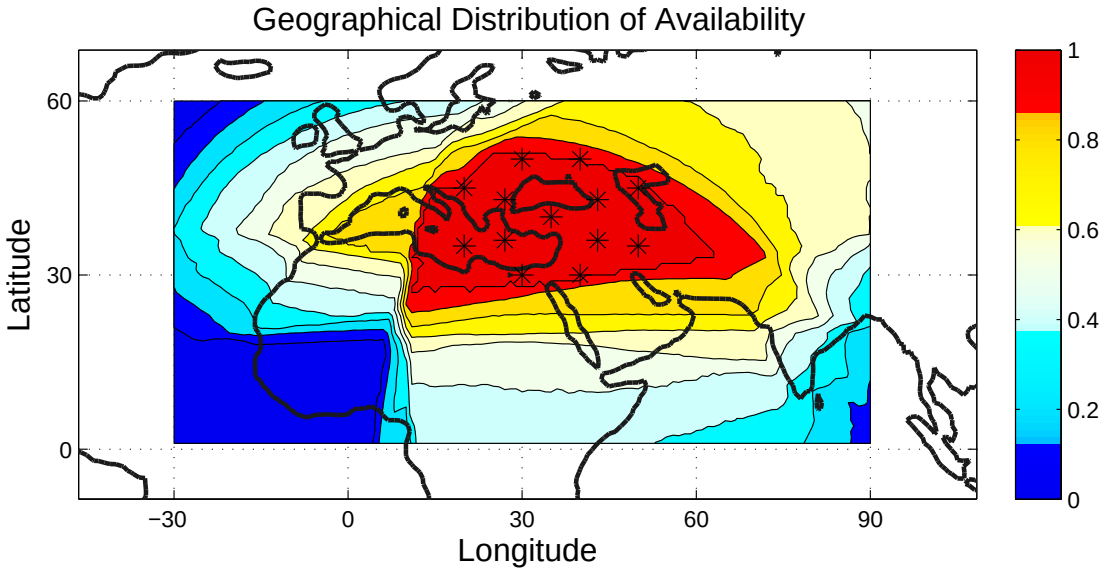

(b)

Figure 4.5: a) Geographical Distribution of Average GDOP for Case 1 Seed 4 b) Geographical Distribution of Availability for Case 1 Seed 4

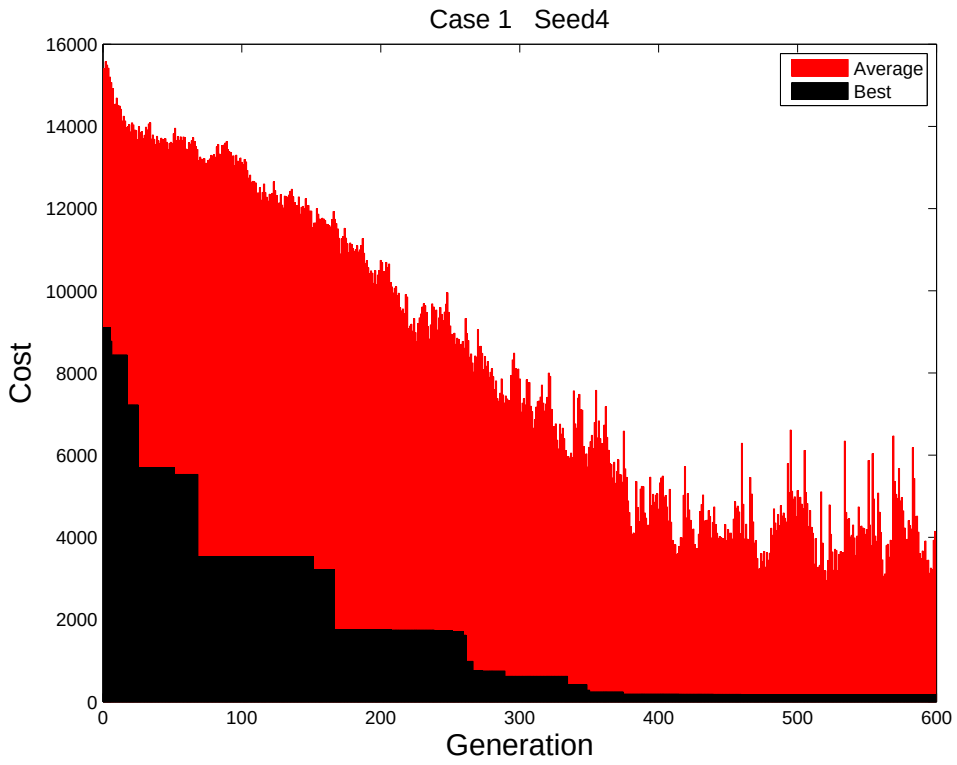

Figure 4.6: GA Evolution for Case 1 Seed 4

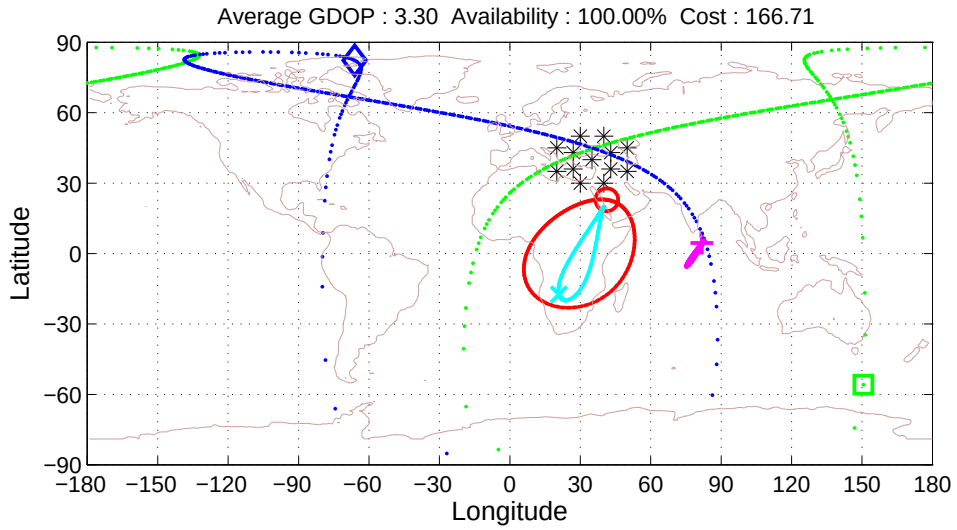

Figure 4.7: Ground Track of the Generated Constellation for Case 1 Seed 4. (Average GDOP is not weighted for the receiver sites)

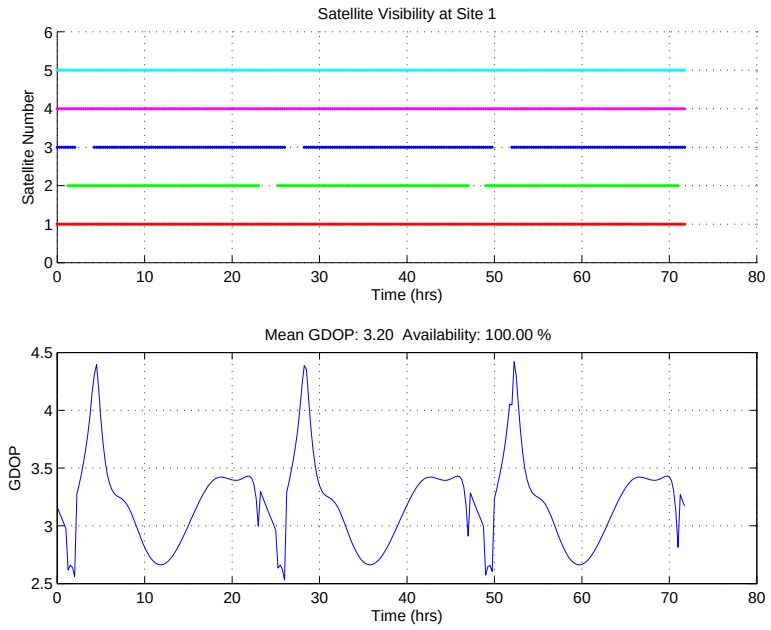

Figure 4.8: Satellite Visibility and GDOP at Receiver Site 1

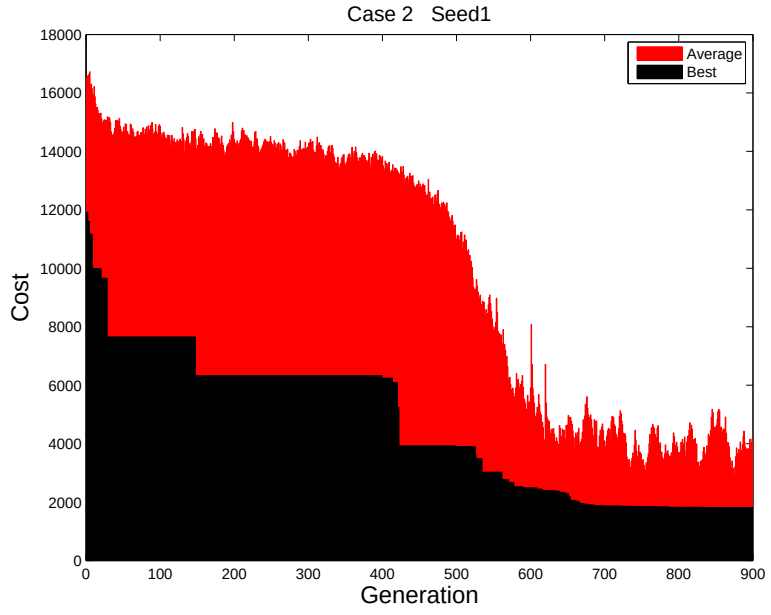

Figure 4.9: GA evolution of four-satellite constellation (Case 2)

The four-satellite case was run to analyze the performance of a four-satellite navigation constellation for a mid-latitude region. The obtained data yields that the algorithm tends to generate constellations with a combination of satellite orbits with very low inclination and high inclination values in order to have a well distributed satellite geometry. However, the performance of the four-satellite constellations are very poor, which are shown in Table 4.9.

Table 4.9: Summary of the Obtained Data for Case 2

Case	Seed	Cost	Av. GDOP	Availability (%)
2	1	1814.07	5.12	89.88
	2	2824.25	6.66	83.33
	3	3518.99	7.99	79.06
	4	4067.38	6.84	75.51
	5	4345.97	5.50	73.34

In the generated constellations for Case 2, there is continuous unavailability for around three hours during the day. The GA-generated constellations for the four-satellite case show that it is hard to have a good navigation performance with a four-satellite constellation over a mid-latitude region. The constellations with highly inclined satellite orbits have long periods of complete system unavailability when the fourth satellite is not visible. The constellations with low inclined satellite orbits don't have complete system unavailability, because the satellites are around the GEO belt and visible. However, their performance values are poor. The ground tracks of the generated constellations for Case 2 are shown in Figure 4.10.

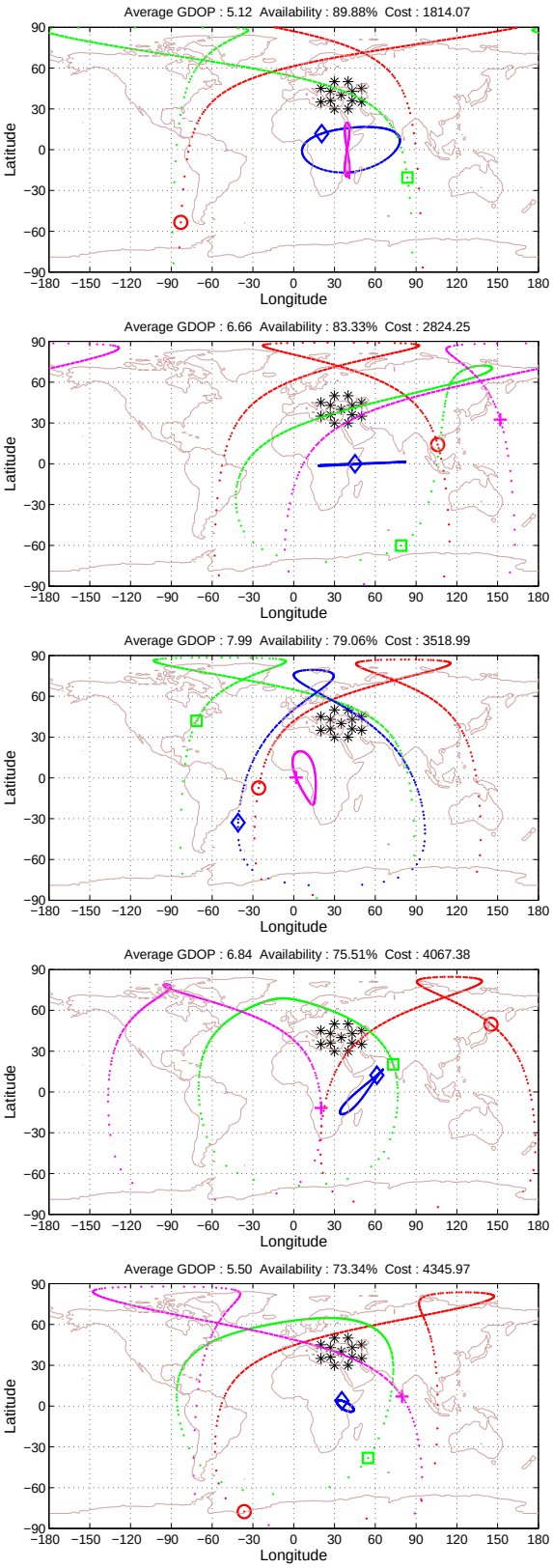

Figure 4.10: Ground Tracks of the Generated Solutions for the Four Satellite Constellation (Case 2)

4.5.3 Group 1 (Case 3,4,5, and 6). This group of cases comprise of three unconstrained GSO satellites and two GEO satellites with different constraints. In Case 3, two GEO satellites are fixed at 0^o and 70^o degrees on the equator. In Case 4, two GEO satellites have twenty degrees of freedom in the range of (350:10) and (60:80). In Case 5, the GEO satellites are free to be placed anywhere on the equator. In Case 6, two GEO satellites have a freedom of 120 degrees on the equator between 330 and 110 degrees. The summary of the obtained performance values for this group is given in Table 4.10.

Table 4.10: Summary of the Obtained Data for Case 3, 4, 5, and 6

Case	Seed	Cost	Av. GDOP	Availability (%)
3	1	281.44	5.55	100
	2	264.19	5.18	100
	3	260.73	5.13	100
	4	278.75	5.48	100
	5	275.36	5.40	100
4	1	176.24	3.49	100
	2	194.48	3.81	100
	3	178.38	3.50	100
	4	178.09	3.49	100
	5	184.02	3.61	100
5	1	196.66	3.86	100
	2	181.35	3.56	100
	3	176.48	3.46	100
	4	161.53	3.17	100
	5	188.25	3.70	100
6	1	192.58	3.78	100
	2	193.54	3.80	100
	3	197.17	3.87	100
	4	171.75	3.37	100
	5	231.03	4.54	100

The generated constellation for Case 4 Seed 2 looks like a manmade constellation design. One of the GSO satellites was put in a nearly circular and very low inclined orbit, which is very close to a GEO orbit. Moreover this satellite was placed almost in the middle of the other GEO satellites on the equator. The other GSO satellites were placed almost on the same orbit with around 140^o phasing. The orbital parameters of this particular constellation is given in Table 4.11. The ground track is depicted in Figure 4.11.

Table 4.11: Orbital Parameters of the Generated Constellation for Case 4 Seed 2.

Satellite	1	2	3	4	5
Eccentricity	0	0	0.01	0.85	0.85
Inclination	0	0	0.44	70.21	70.12
LAN	-10	80	33.67	44.92	44.95
Argument of Perigee	0	0	90.18	270.53	270.53
True Anomaly	0	0	360	319.14	180.35

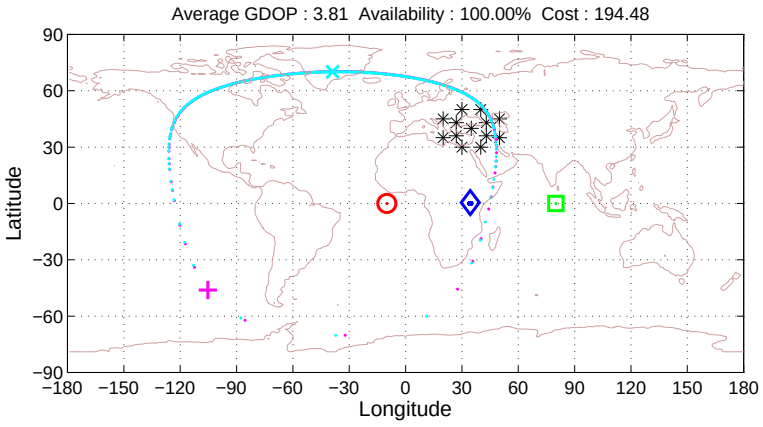

Figure 4.11: Sample Constellation of Case 4 (Seed 2)

The plots of the satellite visibility and GDOP versus time for this constellation (Case 4 Seed 2) are given in Figure 4.12 and 4.13. In these plots, there are two GDOP values 3 and 5. While there are five visible satellites, the GDOP value is almost constant at 3. While there are four visible satellites, the GDOP value is almost constant at 5. Because the three GEO satellites are stationary on the sky and the GDOP value is dependent on the position of the GSO satellites (cyan(x) and magenta(+) in Figure 4.14.d). This kind of a constellation might be optimal for most applications, because the provided GDOP value (which is the only parameter that determines the accuracy in this thesis) is quite predictable. It is approximately 3 or 5.

The common feature of this group of cases is two GEO satellites and three unconstrained GSO satellites. In most cases, the GA generated constellations with a low inclination GSO satellite and two high inclination GSO satellites. The low inclination satellite sometimes appeared as almost a GEO satellite. This result implies that a constellation of three GEO satellites and two highly inclined GSO satellites might be well suited for a mid-latitude regional navigation satellite system. In Figure 4.14, the ground tracks of the generated constellations with this feature are given.

The constellations generated for this group of cases usually exploited 3 GEO satellites, which provides continuous visibility and fixed LOS vectors, and 2 GSO satellites with high inclination and high eccentricity, which provides good satellite geometry for long periods. Therefore, the acquired GDOP values don't have much

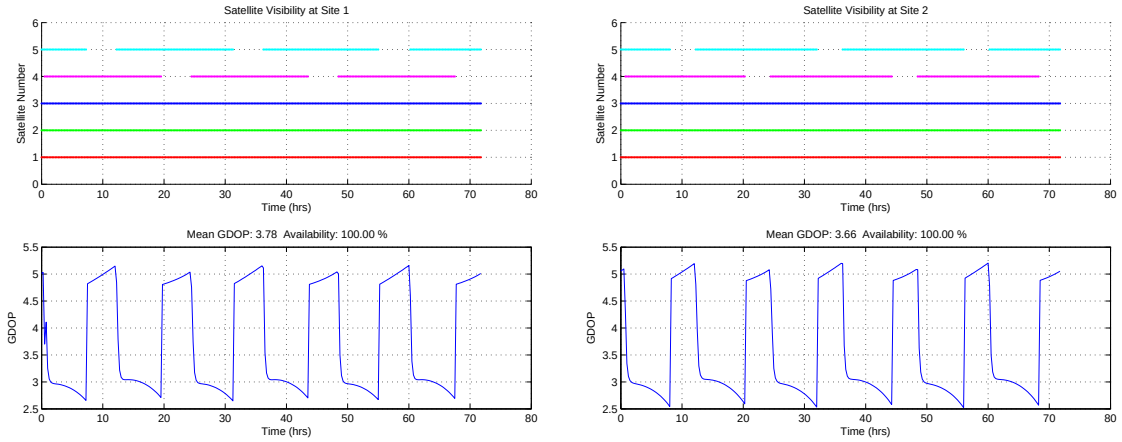

(a)

(b)

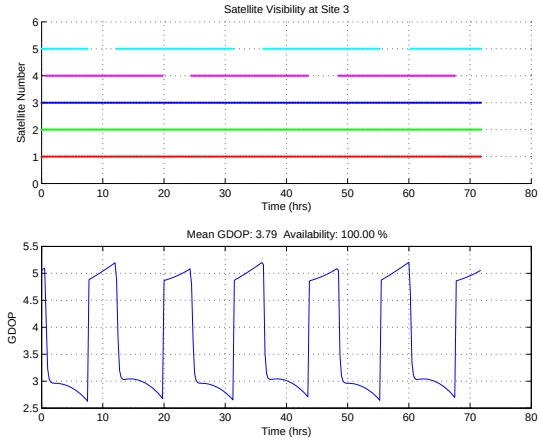

(c)

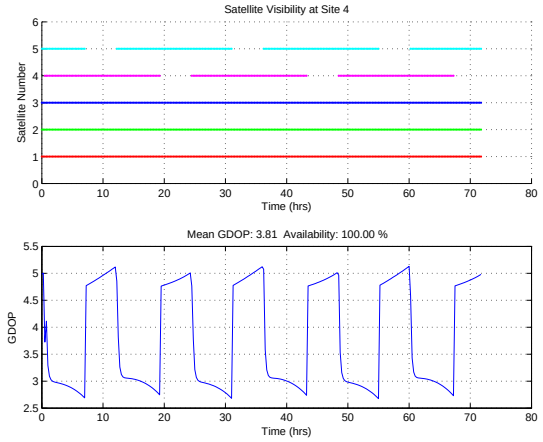

(d)

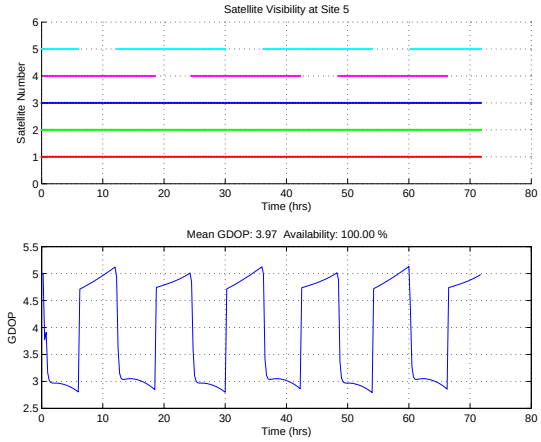

(e)

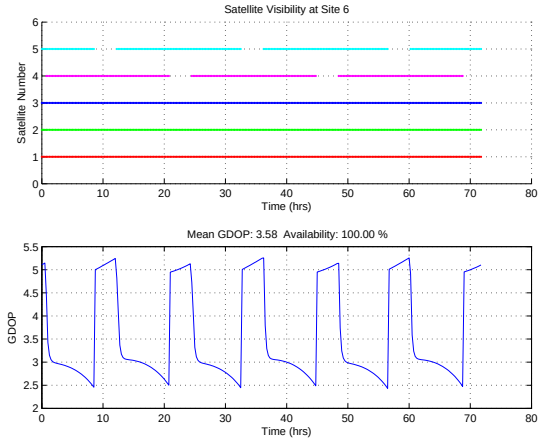

(f)

Figure 4.12: Satellite Visibility and GDOP Plots for Case 4 Seed 2 at Receiver Sites 1 through 6 (a through f, respectively).

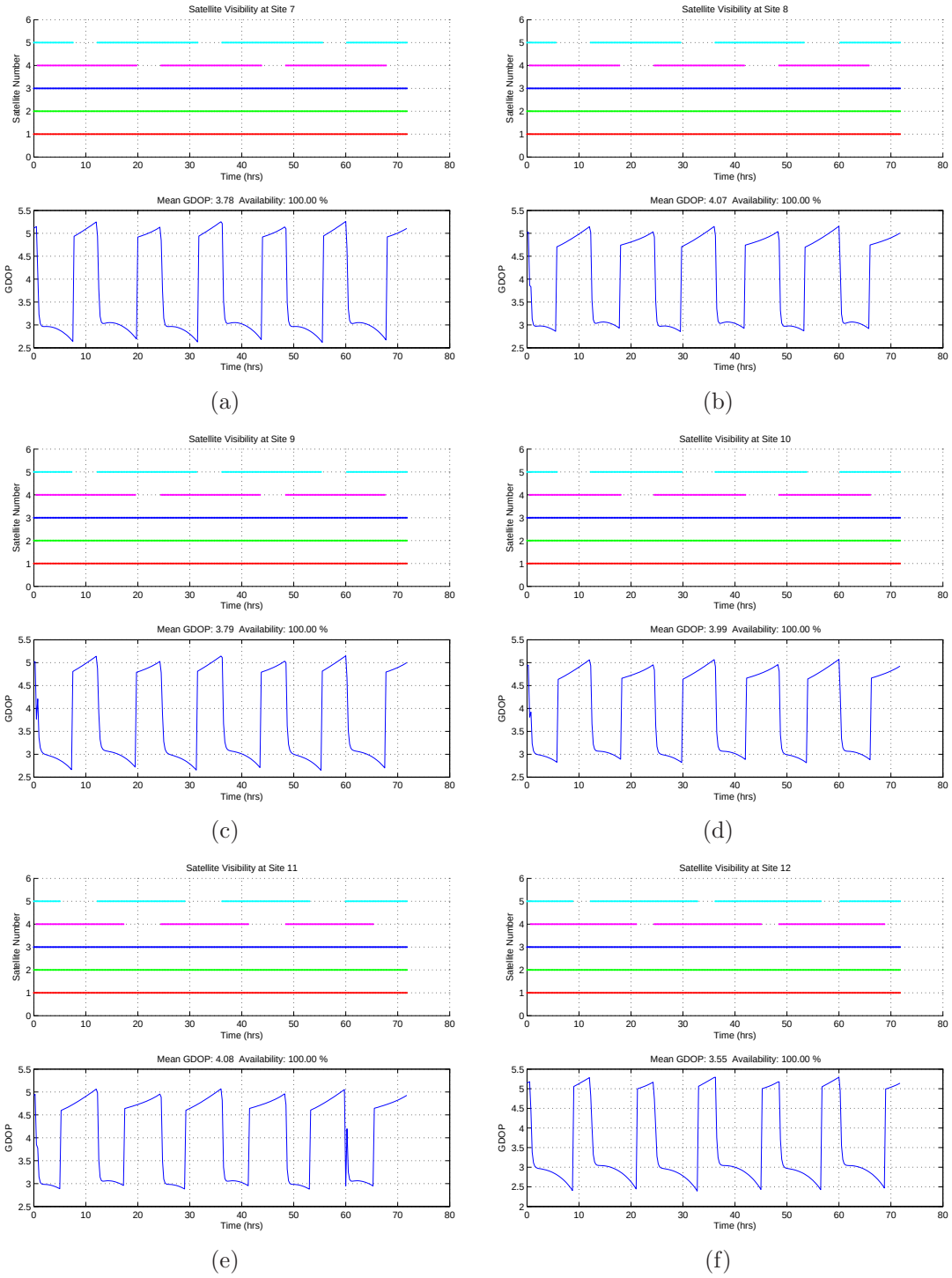

Figure 4.13: Satellite Visibility and GDOP Plots for Case 4 Seed 2 at Receiver Sites 7 through 12 (a through f, respectively).

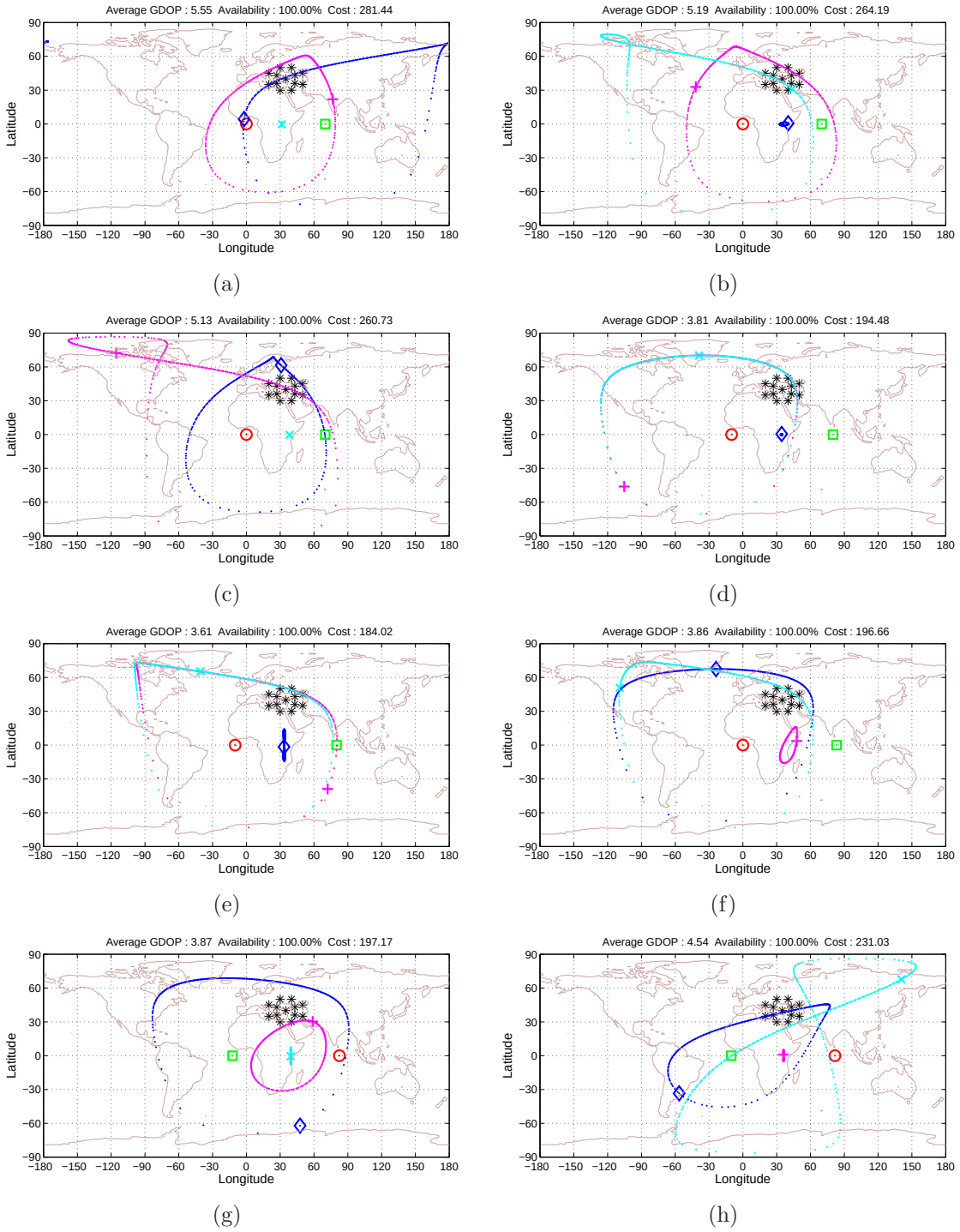

Figure 4.14: Ground Tracks of the Sample Constellations with 2 GEO Satellites and 3 Unconstrained GSO Satellites.
a) Case 3 Seed 1, b) Case 3 Seed 2, c) Case 3 Seed 3, d) Case 4 Seed 2, e) Case 4 Seed 5, f) Case 5 Seed 1, g) Case 6 Seed 3, h) Case 6 Seed 5

fluctuation except the time when a satellite goes out sight and when satellite comes into view.

4.5.4 Group 2 (Case 7,8,9, and 10). In groups 2, 3, and 4, the inclination of the GSO satellites are fixed to *critical inclination* (63.4^o), which provides better resistance against J2 perturbation effect on the parameters of the satellite orbit.

The Group 2 cases are comprised of three GSO satellites with different constraints and two GEO satellites to be placed between 330^o and 110^o on the equator. In Case 7, the inclination values are fixed to 63.4^o for the GSO satellites . In Case 8, the inclination values and the argument of perigee values are fixed to 63.4^o and 270^o respectively for the GSO satellites. In Case 8, in addition to the constraints of Case 7, the eccentricity is limited to be between 0.3 and 0.7. In Case 10, the argument of perigee constraint is removed from those of Case 9. The summary of the obtained performance values for this group is given in Table 4.12.

In Case 7, the GEO satellites of the generated solutions were placed with an average of 85^o separation on the equator. The eccentricity of the GSO satellites were given values between 0.6 and 0.8. The generated values for the argument of perigee of the GSO satellites were between 230^o and 315^o. This range of argument of perigee caused the dwell point of the satellites to be close to each other. The ground track of a sample constellation generated for this case is shown in Figure 4.15.

In Case 8, the GEO satellites of the generated solutions were placed with an average of 70^o separation on the equator. The eccentricity of the GSO satellites were

Table 4.12: Summary of the Obtained Data for Case 7, 8, 9, and 10

Case	Seed	Cost	Av. GDOP	Availability (%)
7	1	178.34	3.50	100
	2	166.33	3.26	100
	3	168.50	3.31	100
	4	222.65	4.37	100
	5	159.14	3.13	100
8	1	247.24	4.77	99.97
	2	193.08	3.78	100
	3	219.52	4.30	100
	4	158.29	3.62	100
	5	190.56	3.73	100
9	1	188.01	3.68	100
	2	223.96	4.39	100
	3	181.11	3.55	100
	4	192.45	3.77	100
	5	209.90	4.11	100
10	1	158.80	3.12	100
	2	155.22	3.05	100
	3	161.64	3.17	100
	4	161.62	3.17	100
	5	158.92	3.12	100

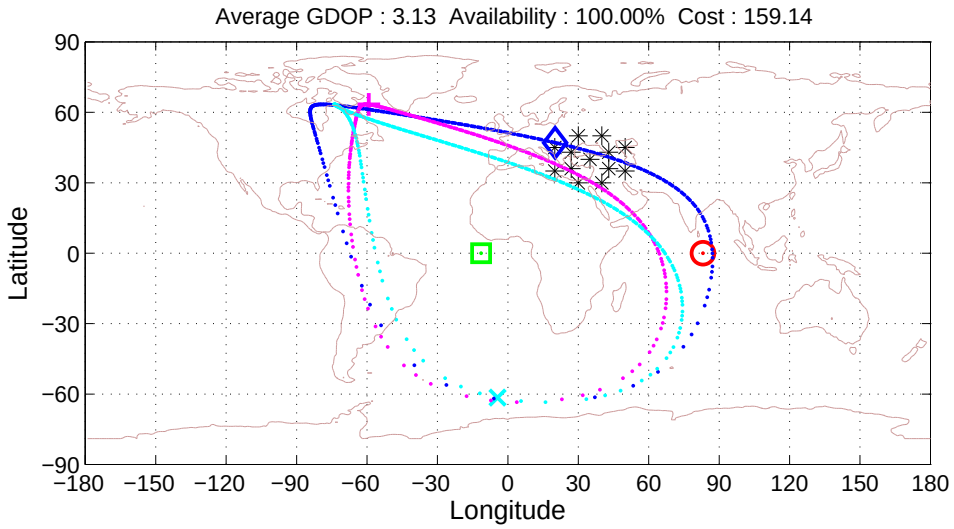

Figure 4.15: Ground Track of a Sample Constellation of Case 7 (Seed 5).

given values between 0.55 and 0.85. The longitude of ascending nodes of the GSO satellites were placed in an average of 20 degree range. The ground track of a sample constellation generated for this case is shown in Figure 4.16.

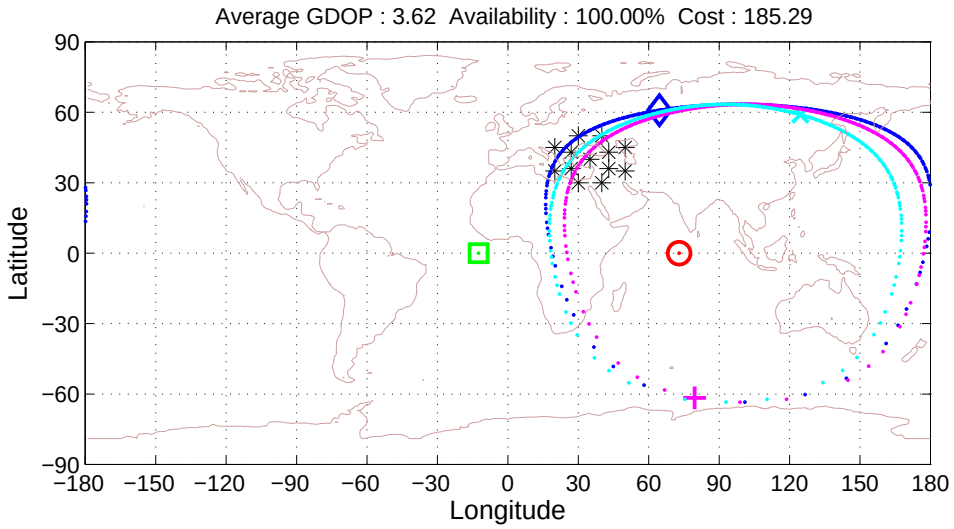

Figure 4.16: Ground Track of a Sample Constellation of Case 8 (Seed 4).

In Case 9, the GEO satellites of the generated solutions were placed with an average of 80^o separation on the equator. The eccentricity of the GSO satellites were given values between 0.6 and 0.7. The longitude of ascending nodes of the GSO satellites were placed in an average of 15 degree range. The very close longitude of ascending node values for the GSO satellites almost put them on the same orbit with different true anomaly values. The ground track of a sample constellation generated for this case is shown in Figure 4.17.

In Case 10, the GEO satellites of the generated solutions were placed with an average of 95^o separation on the equator. The eccentricity of the GSO satellites were given values between 0.4 and 0.7. The longitude of ascending nodes of the GSO

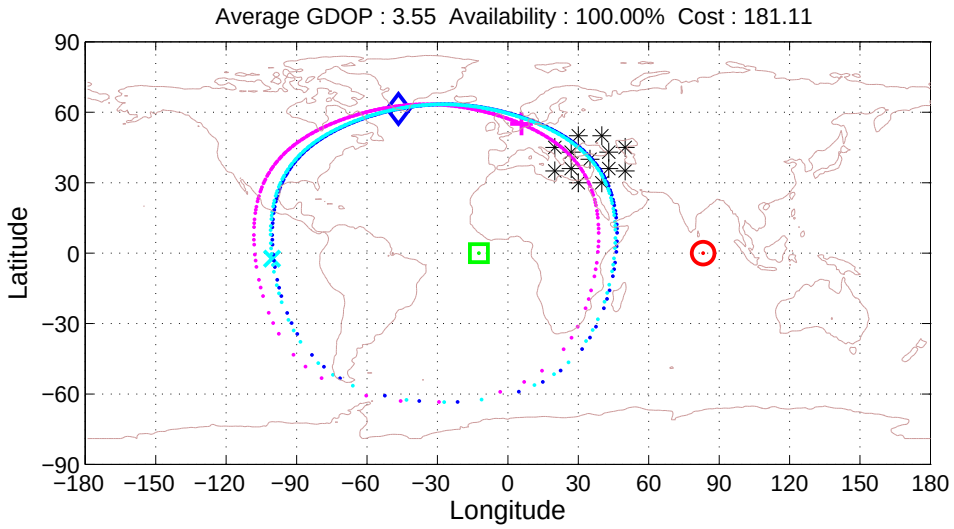

Figure 4.17: Ground Track of a Sample Constellation of Case 9 (Seed 3).

satellites were placed in an average of 20 degree range. The argument of perigee values of the GSO satellites were between 220^o and 270^o. The ground track of a sample constellation generated for this case is shown in Figure 4.18.

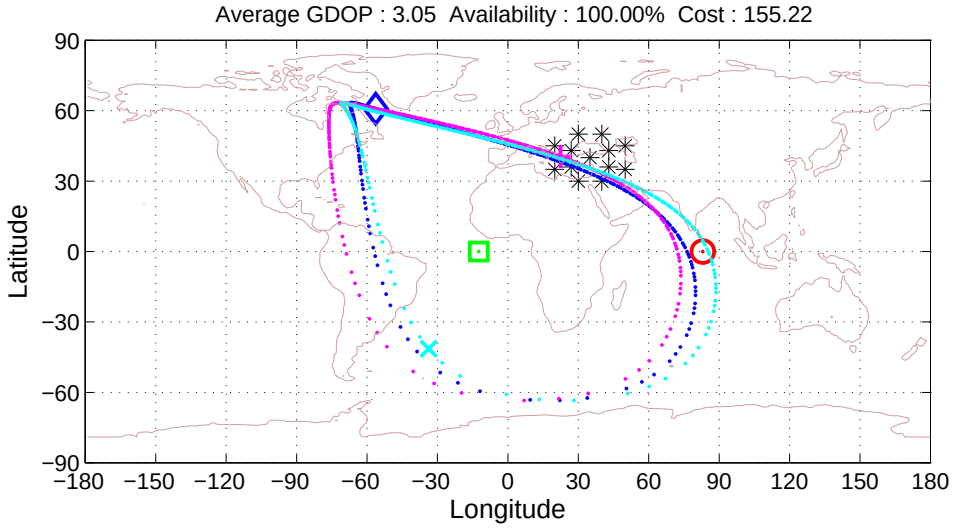

Figure 4.18: Ground Track of a Sample Constellation of Case 10 (Seed 2).

In Group 2, the GEO satellites are generated with an average of 85^o separation between them on the equatorial plane. The GSO satellites tended to have similar

LAN and argument of perigee values. Moreover, in some constellations, the GSO satellites were placed in almost identical orbits. Because of the fixed inclination values of the GSO satellites, the satellite geometry became more unstable than Group 1 constellations. However, the geometric diversity of three GSO satellite improved the performance.

4.5.5 Group 3 (Case 11,12, and 13). This group of cases are comprised of three GSO satellites with different constraints than Group 2 cases and two GEO satellites to be placed between 330^o and 110^o on the equator. In Case 11, the inclination values and the argument of perigee values are fixed to 63.4^o and 270^o respectively and the longitude of ascending node values are constrained to be between 0^o and 180^o on the equator for the GSO satellites. In Case 12, unlike Case 11 the argument of perigee values of the GSO satellites are not fixed and variable between 180^o and 360^o. In Case 13, in addition to the constraints of Case 12, the eccentricity values of the GSO satellites are limited to the range of 0.3 to 0.7. The summary of the obtained performance values for this group is given in Table 4.13.

In Case 11, the GEO satellites of the generated solutions were placed with an average of 70^o separation on the equator. The eccentricity of the GSO satellites were given values between 0.55 and 0.80. The longitude of ascending nodes of the GSO satellites were placed in an average of 25 degree range. The very close longitude of ascending node values for the GSO satellites almost put them on the same orbit with

Table 4.13: Summary of the Obtained Data for Case 11, 12, and 13

Case	Seed	Cost	Av. GDOP	Availability (%)
11	1	261.80	5.13	100
	2	272.05	5.25	99.97
	3	227.23	4.45	100
	4	240.16	4.62	99.97
	5	216.03	4.15	99.97
12	1	155.82	3.06	100
	2	715.93	5.32	97.09
	3	1276.26	6.99	93.83
	4	288.48	4.99	99.76
	5	1091.96	6.74	95.11
13	1	214.77	3.86	99.84
	2	204.92	4.02	100
	3	207.19	4.06	100
	4	239.18	4.69	100
	5	301.47	5.34	99.81

different true anomaly values. The ground track of a sample constellation generated for this case is shown in Figure 4.19.

In Case 12, the GEO satellites of the generated solutions were placed with an average of 65^o separation on the equator. The eccentricity of the GSO satellites were given values between 0.50 and 0.80. The argument of perigee values of the GSO satellites were between 210^o and 300^o. A sample ground track of the constellation generated for this case is shown in Figure 4.20.

In Case 13, the GEO satellites of the generated solutions were placed with an average of 60^o separation on the equator. The eccentricity of the GSO satellites were given values between 0.40 and 0.65. The argument of perigee values of the GSO

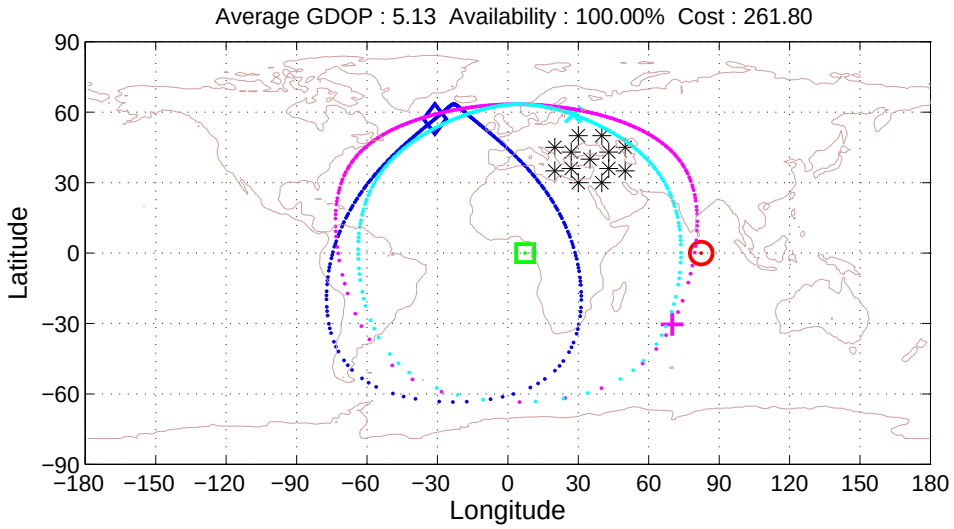

Figure 4.19: Ground Track of a Sample Constellation of Case 11 (Seed 1).

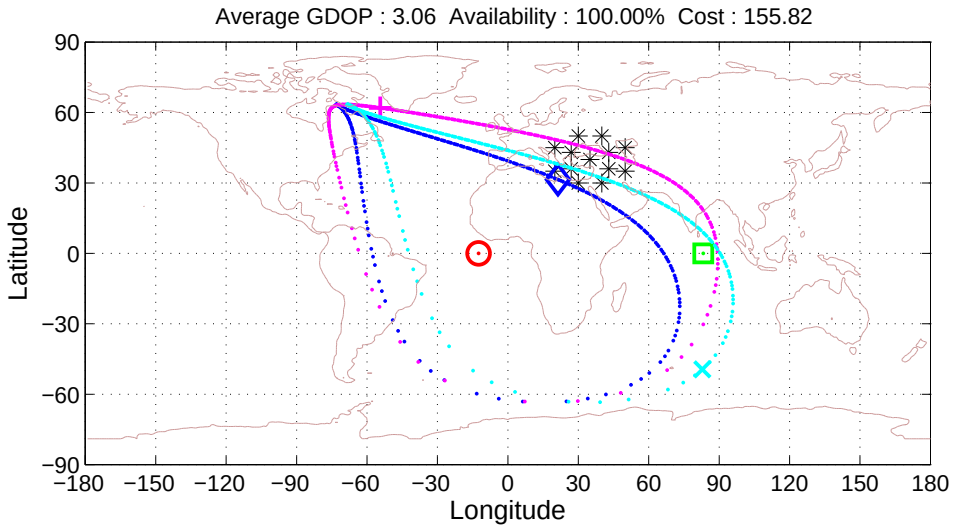

Figure 4.20: Ground Track of a Sample Constellation of Case 12 (Seed 1).

satellites were between 230^o and 290^o. A sample ground track of the constellation generated for this case is shown in Figure 4.21.

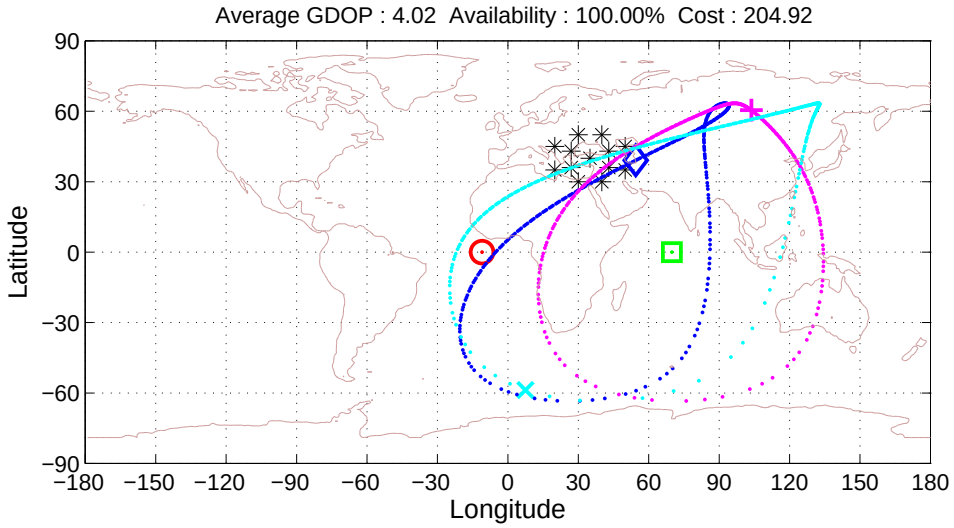

Figure 4.21: Ground Track of a Sample Constellation of Case 13 (Seed 2).

The generated constellations for Group 2 performed well. The longitude of ascending node values of the generated GSO satellites were in the range of 0 to 180. Therefore, constraining the longitude of ascending node values to this range would assist the GA to find even better solutions. The cases of Group 3 were designed with this idea. However, the generated constellations for Group 3 cases performed at the same level of Group 2 constellations. The best cost values in the constellations of Group 2 and 3 are 155.22 (Case 10 Seed 2) and 155.82 (Case 12 Seed 1). Those constellations are also the best of all generated constellations. Therefore, the optimal constellation of this problem might be very similar those solutions. Although those constellations are given in the previous figures, they are given together in Figure 4.22 with their visibility and GDOP versus time plots. For both constellations, the system

is always available ($GDOP < 10$), and the fluctuation of the GDOP value within a range of 2.4 to 3.7. For most applications, that much fluctuation might be within the acceptable limits.

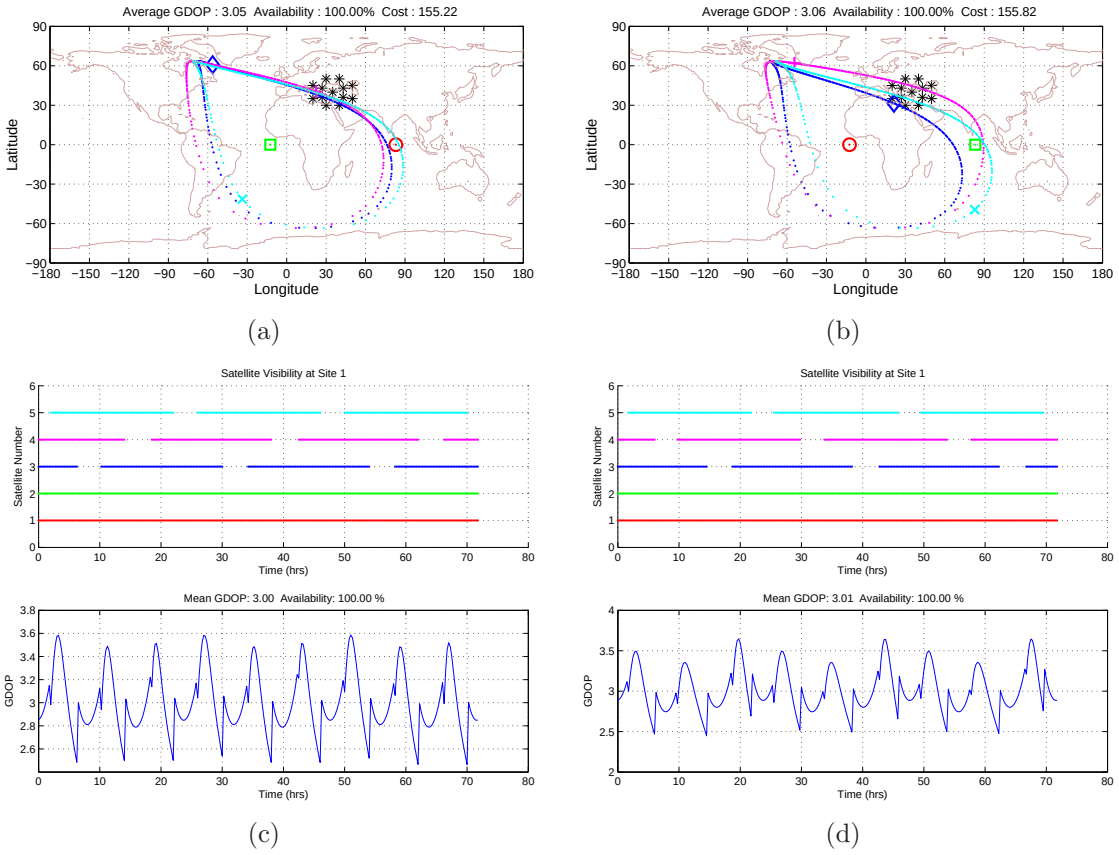

Figure 4.22: The Best Generated Constellations in Group 2 and 3.
a) Case 10 Seed 2
b) Case 12 Seed 1

4.5.6 Group 4 (Case 14 and 15). This group of cases comprise of three GSO satellites with some constraints and two GEO satellites to be placed anywhere on the equator. In Case 14, the inclination values of the GSO satellites are fixed to 63.4^o and the longitude of ascending node values are constrained to be between 0^o and 180^o on the equator for the GSO satellites. Moreover, the eccentricity values and

the argument of perigee values are constrained to be in the range of 0.3 to 0.7 and 180^o to 360^o respectively. In Case 15, unlike Case 14, the constraints for the longitude of ascending node and the argument of perigee values are removed. The summary of the obtained performance values for this group is given in Table 4.14.

Table 4.14: Summary of the Obtained Data for Case 14 and 15

Case	Seed	Cost	Av. GDOP	Availability (%)
14	1	259.46	4.52	99.79
	2	167.732	4.14	100
	3	185.17	3.55	99.97
	4	175.15	3.44	100
	5	270.54	4.82	99.84
15	1	187.89	3.68	100
	2	186.10	3.65	100
	3	206.61	4.05	100
	4	259.66	4.77	99.89
	5	178.45	3.50	100

In Case 14, the GEO satellites of the generated solutions were placed with an average of 80^o separation on the equator. The GSO satellites are generated with different characteristics. The ground track of a sample constellation generated for this case is shown in Figure 4.23.

In Case 15, the GEO satellites of the generated solutions were placed with an average of 70^o separation on the equator. The GSO satellites were generated with different characteristics. The ground track of a sample constellation generated for this case is shown in Figure 4.24.

This group of cases were designed to see if removing the constraint on the longitude of ascending node values of GEO improves the performance of the constellation.

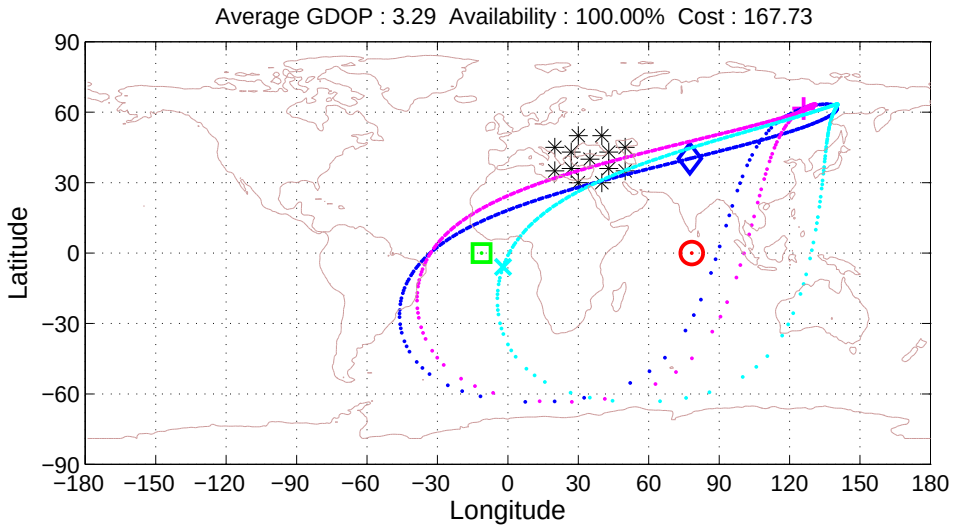

Figure 4.23: Ground Track of a Sample Constellation of Case 14 (Seed 2).

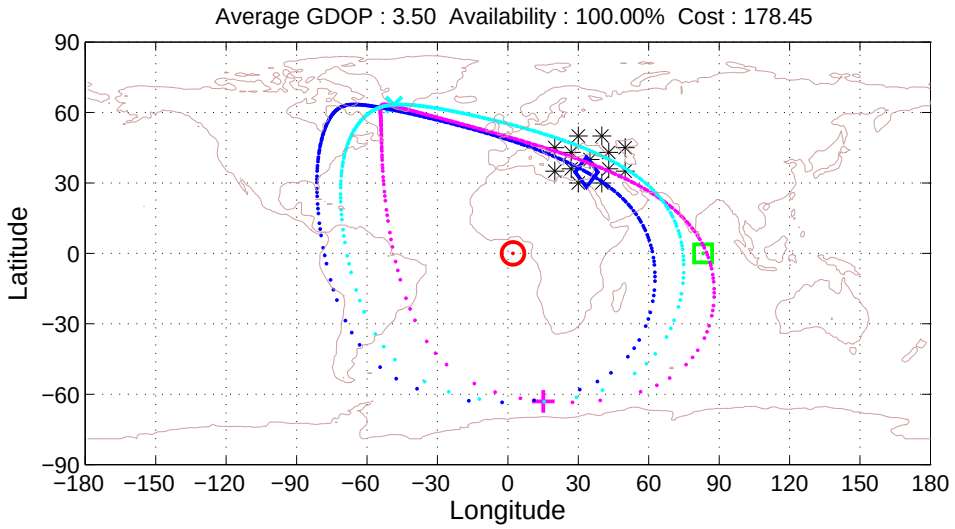

Figure 4.24: Ground Track of a Sample Constellation of Case 15 (Seed 5).

The separation between the GEO satellites of the constellations were 90^o on average, which is not very different from the values obtained in the previous cases. Besides, there were no improvement in the cost value. Therefore, the optimal separation between the GEO satellites for this problem might be 90^o.

4.5.7 Group 5 (Case 16 and 17). This group of cases comprise of five GSO satellites different constraints. In Case 16, only the true anomaly values are constrained to the range of 180^o to 360^o. In Case 17, in addition to the constraints of Case 16, the inclination values and the longitude of ascending node values are limited to the range of 0^o to 75^o and 0^o to 180^o respectively. The summary of the obtained performance values for this group is given in Table 4.15.

Table 4.15: Summary of the Obtained Data for Case 16 and 17

Case	Seed	Cost	Av. GDOP	Availability (%)
16	1	1652.18	6.99	91.56
	2	2158.40	11.70	88.65
	3	1882.42	6.20	89.69
	4	2222.04	10.74	87.77
	5	2533.44	5.70	84.40
17	1	2234.58	7.60	86.78
	2	2487.85	7.85	85.63
	3	685.40	4.83	97.14
	4	2084.21	6.15	87.13
	5	912.81	7.48	95.59

In Case 16, various constellations were generated with nothing in common. Their performance are very poor than most cases. The ground track of a sample constellation for this case is shown in Figure 4.25.

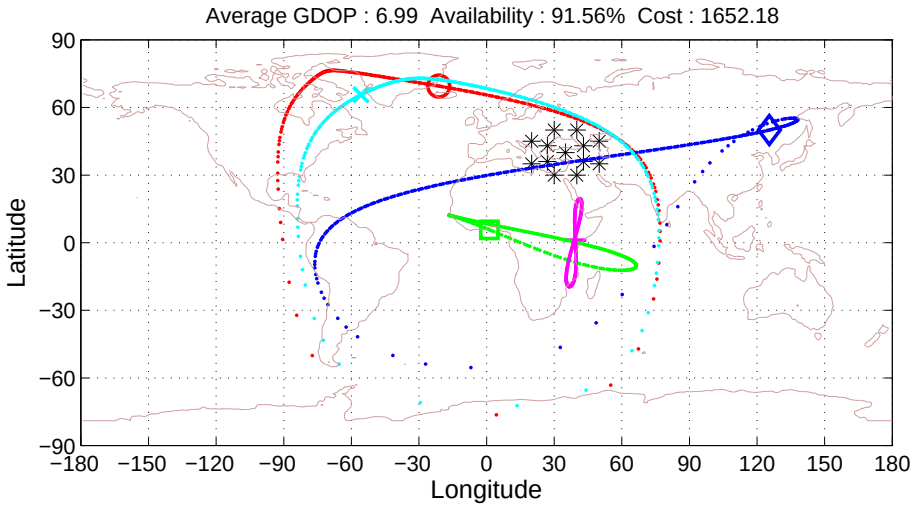

Figure 4.25: Ground Track of a Sample Constellation of Case 16 (Seed 1).

In Case 17, the generated constellations, like Case 16, had nothing in common but poor performance. The ground track of a sample constellation generated for this case is shown in Figure 4.26.

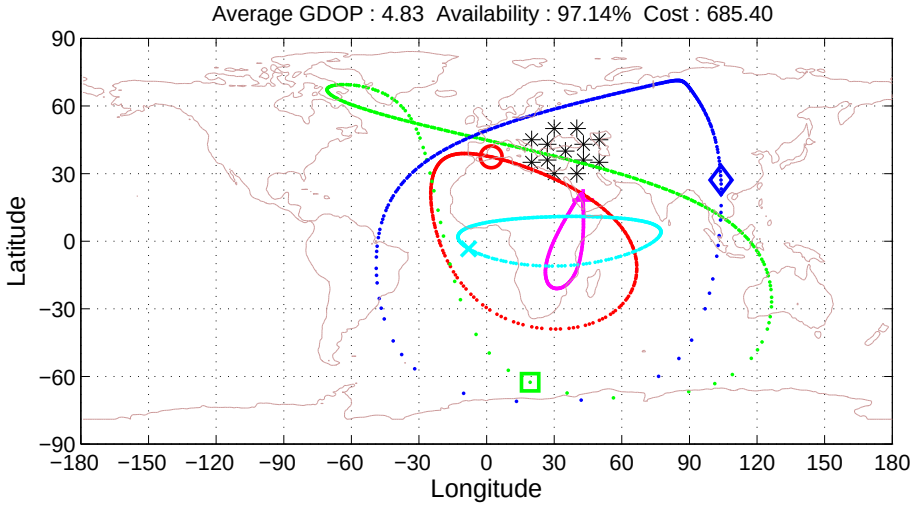

Figure 4.26: Ground Track of a Sample Constellation of Case 17 (Seed 3).

The cases of Group 5 was designed to see if the constellation is able to demonstrate good performance without GEO satellites. The emphasis given to the com-

binations of orbits which have the apogee point over the northern hemisphere. The objective was to increase the visibility over the receiver points. This constraint on the argument of perigee shrank the possible volume of the satellite geometry. Thus, the generated constellations demonstrated poorer performance values than the constellations of most other cases. Some of the constellations of this group performed at the same level of four-satellite constellations (Case 2). Therefore, it is wise to employ GEO satellites in a mid-latitude regional navigation constellation.

4.5.8 Summary of the Results. The summary of the obtained data for all cases are given in tables 4.16, 4.17, and 4.18. The results show that a four-satellite constellation has poor navigation performance over a mid-latitude region. However, the performance of the five-satellite constellations are good. Therefore, a mid-latitude regional navigation system should comprise of at least five satellites. The cases with GEO satellites and three unconstrained GSO satellites generated results with three GEO satellites. Thus, a constellation with three GEO satellites and two GSO satellites appears to be a reasonable solution. Additionally, the constellations which don't have GEO satellites demonstrated poor performance values. Therefore, it can be concluded that the GEO satellites are indispensable for this problem.

4.6 J2 Perturbation Effect on the Performance of the Constellation

The Earth's non-spherical shape causes periodic variations in all of the orbital elements. The dominant effects are in the RAAN and argument of perigee. The rate

Table 4.16: The Summary of the Performance of All Cases (1).

Case	Description	Cost	Average GDOP	Availability	Bit Length
1	Unconstrained	223.44	4.41	100	235
		183.79	3.61	100	
		275.10	4.45	99.41	
		166.71	3.30	100	
		206.56	4.05	100	
2	Unconstrained	1814.07	5.12	89.88	193
		2824.25	6.66	83.33	
	Four-Satellite	3518.99	7.99	79.06	
		4067.38	6.84	75.51	
		4345.97	5.50	73.34	
3	2 GEO Ω_{LAN}(0,70)	281.44	5.55	100	151
		264.19	5.19	100	
	3 GSO	260.73	5.13	100	
		278.75	5.48	100	
		275.36	5.40	100	
4	2 GEO Ω_{LAN}(350:10,60:80)	176.24	3.49	100	165
		194.48	3.81	100	
	3 GSO	178.38	3.50	100	
		178.09	3.49	100	
		184.02	3.61	100	
5	2 GEO	196.66	3.86	100	173
		181.35	3.56	100	
	3 GSO	176.48	3.46	100	
		161.53	3.17	100	
		188.25	3.70	100	
6	2 GEO Ω_{LAN}(330:110)	192.57	3.78	100	171
		193.54	3.80	100	
	3 GSO	197.17	3.87	100	
		171.75	3.37	100	
		231.03	4.54	100	

Table 4.17: The Summary of the Performance of All Cases (2).

Case	Description	Cost	Average GDOP	Availability	Bit Length
7	2 GEO Ω_{LAN}(330:110) 3 GSO i(63.4)	178.34 166.33 168.50 222.65 159.14	3.50 3.26 3.31 4.37 3.13	100 100 100 100 100	144
8	2 GEO Ω_{LAN}(330:110) 3 GSO i(63.4) ω(270)	247.24 193.08 219.52 185.29 190.56	4.77 3.78 4.30 3.62 3.73	99.97 100 100 100 100	120
9	2 GEO Ω_{LAN}(330:110) 3 GSO e(0.3:0.7) i(63.4) ω(270)	188.01 223.96 181.11 192.45 209.90	3.68 4.39 3.55 3.77 4.11	100 100 100 100 100	117
10	2 GEO Ω_{LAN}(330:110) 3 GSO e(0.3:0.7) i(63.4)	158.80 155.22 161.64 161.62 158.92	3.12 3.05 3.17 3.17 3.12	100 100 100 100 100	141
11	2 GEO Ω_{LAN}(330:110) 3 GSO i(63.4) Ω_{LAN}(0:180) ω(270)	261.80 272.05 227.23 240.16 216.03	5.13 5.25 4.45 4.62 4.15	100 100 100 99.97 99.97	117
12	2 GEO Ω_{LAN}(330:110) 3 GSO i(63.4) Ω_{LAN}(0:180) ω(180:360)	155.82 715.93 1276.26 288.48 1091.96	3.06 5.32 6.99 4.99 6.74	100 97.09 93.83 99.76 95.11	138
13	2 GEO Ω_{LAN}(330:110) 3 GSO e(0.3:0.7) i(63.4) Ω_{LAN}(0:180) ω(180:360)	214.77 204.92 207.19 239.18 301.47	3.86 4.02 4.06 4.69 5.34	99.84 100 100 100 99.81	135

Table 4.18: The Summary of the Performance of All Cases (3).

Case	Description	Cost	Average GDOP	Availability	Bit Length
14	2 GEO 3 GSO e(0.3:0.7) i(63.4) Ω_{LAN}(0:180) ω(180:360)	259.46 167.732 185.17 175.15 270.54	4.52 4.14 3.55 3.44 4.82	99.79 100 99.97 100 99.84	137
15	2 GEO 3 GSO e(0.3:0.7) i(63.4)	187.89 186.10 206.61 259.66 178.45	3.68 3.65 4.05 4.77 3.50	100 100 100 99.89 100	143
16	5 GSO ω(180:360)	1652.18 2158.40 1882.42 2222.04 2533.44	6.99 11.70 6.19 10.74 5.69	91.56 88.65 89.69 87.77 84.40	225
17	5 GSO i(0:75) Ω_{LAN}(180:360) ω(180:360)	2234.58 2487.85 685.40 2084.21 912.81	7.60 7.85 4.83 6.15 7.48	86.78 85.63 97.14 87.13 95.59	225
18	Unconstrained Random	6849.91 4122.94 6279.04 4729.84 5549.88	4.81 7.39 6.75 8.62 6.10	56.54 75.08 60.66 72.30 65.36	235
19	2 GEO Ω_{LAN}(0,70) 3 GSO e(0.5) i(63.4) Ω_{LAN}(60,80,100) ω(270) ν(0:360,0:360,180)	4881.34 4773.99 4862.05 4881.34 4885.03	10.40 12.97 13.53 10.40 10.56	71.50 73.02 72.65 71.50 71.50	41
20	Benchmark 2 GEO Ω_{LAN}(0,70) 3 GSO e(0.5) i(63.4) Ω_{LAN}(60,80,100) ω(270) ν(0:360,0:360,180)	4740.15	12.09	73.03	-

of the changes are as follows [19]:

$$\dot{\Omega}_{J_2} = -1.5\, n\, J_2 (\frac{R_\oplus}{a})^2 (\cos i)(1-e^2)^{-2} \quad (4.1)$$

$$\dot{\omega}_{J_2} = 0.75\, n\, J_2 (\frac{R_\oplus}{a})^2 (4 - 5\sin^2 i)(1-e^2)^{-2} \quad (4.2)$$

This perturbation is termed *J2 perturbation*. J2 perturbation disrupts the designed constellation, if orbit maintenance maneuvers are not made, which reduces the usable lifetime of the satellite. An inclination value of 90^o removes the effect on the RAAN (makes $\dot{\Omega}_{J_2}$ zero), but this inclination is not practical for geosynchronous orbits. However, the effect on the argument of perigee can be removed with an inclination value which makes $(4 - 5\sin^2 i)$ zero (also makes $\dot{\omega}_{J_2}$ zero). This inclination value is calculated as 63.4^o or 116.6^o and termed as *critical inclination*.

This effect is not included in the orbit propagation of the GA runs. However, it would be better to know how robust the generated constellation against J2 perturbation is. Therefore, the analysis of the performance of the generated constellations with and without an inclination value of 63.4^o for a 30 day period was made. The parameters of the analyzed constellations are given in Table 4.19. The first three and last three days of ground tracks of the analyzed constellations are depicted in Figure 4.27. The satellite visibility and average GDOP versus time plots at Receiver Site 1 are shown in Figure 4.28.

The analysis of the obtained data shows that the constellations comprising of the satellites, which has inclination values of 63.4^o, are more robust against J2 per-

turbation effect. The summary of the J2 effect on the performance of the analyzed constellations are given in Table 4.20.

Table 4.19: The Constellations for J2 Analysis

	Constellation 1					Constellation 2				
Sat	1	2	3	4	5	1	2	3	4	5
e	0	0	0.85	0.05	0.68	0	0	0.74	0.63	0.74
i	0	0	78.74	19.62	60.09	0	0	63.4	63.4	63.4
Ω_{LAN}	-10	80	58.37	34.02	75.25	-12.49	74.85	81.58	112.44	150.95
ω	0	0	247.28	338.16	269.82	0	0	315.62	309.28	274.76
ν	0	0	7.75	39.45	193.748	0	0	357.18	168.36	204.31

Table 4.20: Summary of the Obtained Data for J2 Effect Analysis

Constellation	Period	Cost	Av. GDOP	Availability (%)
1	First 3 Days	177.45	3.52	100
	Last 3 Days	606.67	4.91	97.29
2	First 3 Days	166.43	3.27	100
	Last 3 Days	196.91	3.62	99.92

4.7 Summary

In this chapter, the obtained data and analysis of the data are given. In Section 4.2, the settings and the parameters of the GA were given. In Section 4.4, the performance of the algorithm to find good solutions was validated. In Section 4.3, a limited version of the search space of the problem was analyzed. In Section 4.5, the obtained data for the groups of cases with similar constraints were analyzed. In Section 4.6, the J2 perturbation effect on the performance of the generated constellations were

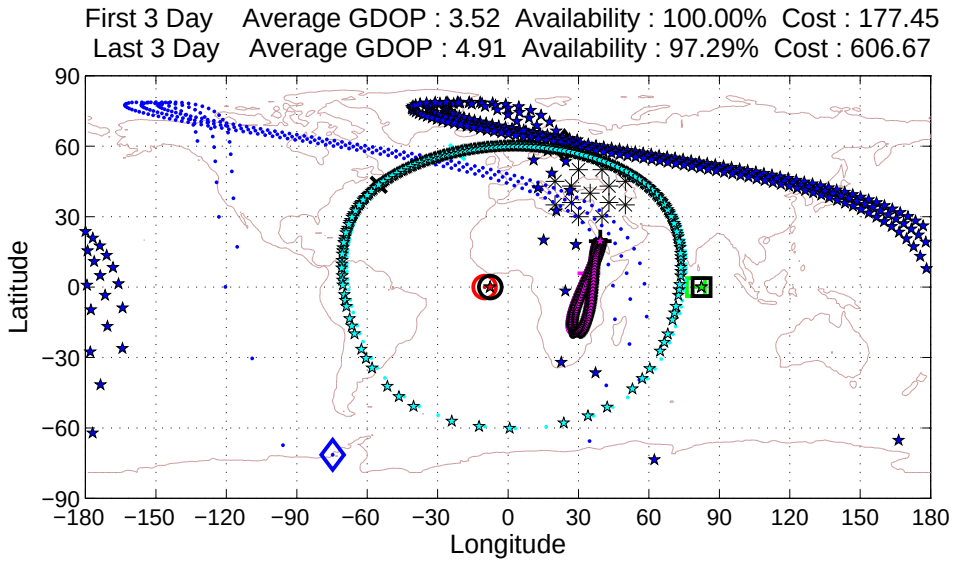

(a)

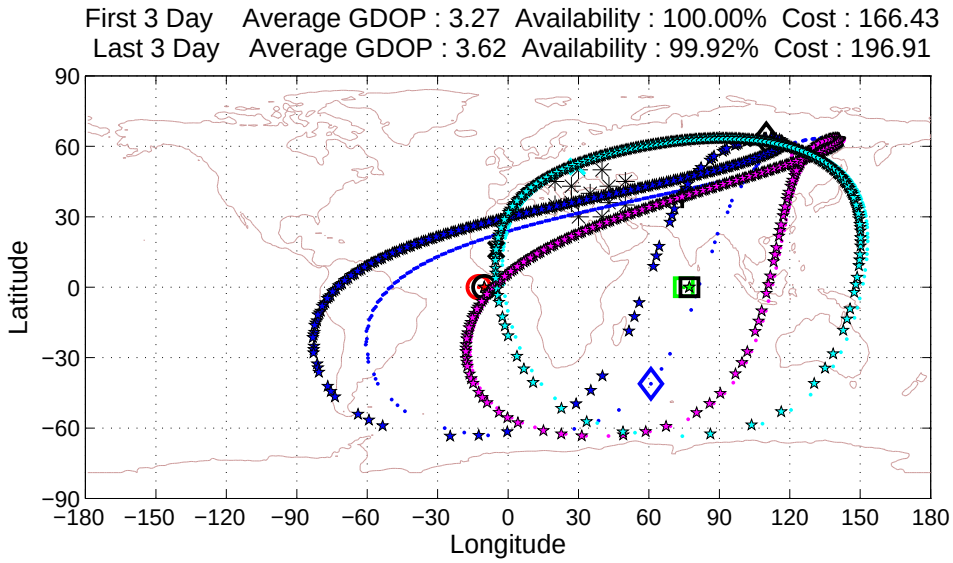

(b)

Figure 4.27: (a) Ground Track of First Constellation.
(b) Ground Track of Second Constellation.
(Light colored ground tracks (dots) show first 3 days, dark colored ground tracks (stars) show last 3 days)

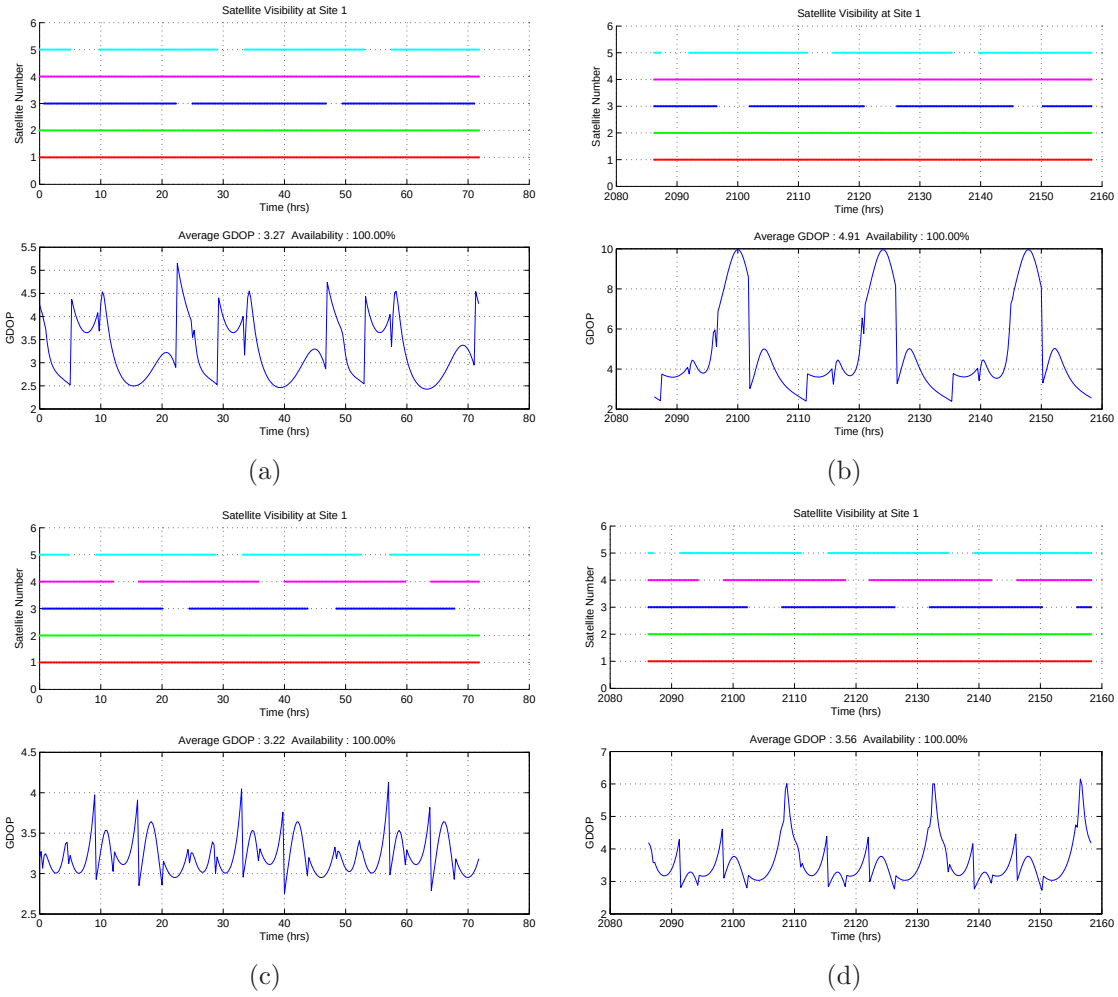

Figure 4.28: (a and b) Satellite visibility and GDOP plots of Constellation 1 for the first 3 and last 3 days respectively.
(c and d) Satellite visibility and GDOP plots of Constellation 2 for the first 3 and last 3 days respectively.

analyzed. In Chapter V, the conclusions and the recommendations for future work is given.

V. Conclusions and Recommendations

5.1 Conclusions

In this thesis investigation, the goal is to design a constellation of geosynchronous navigation satellites which maximizes availability and accuracy over a specified region of the earth by using the GA for optimization. In order to accomplish this goal a simulation tool is developed to find an optimum navigation satellite constellation using Genetic Algorithms. Several cases with different constraints are designed and analyzed for navigation performance over a specified mid-latitude region of the earth. Most of the generated results provide 100% availability with different average GDOP values. The best generated constellation provides 100% availability with an average GDOP value of 3.05. That performance level meets the objectives for the solution of this thesis.

The GAs are problem specific and need to be designed according to the problem. The main objective of designing a GA is to find the global minimum of the problem search space while avoiding the local minimums in the search space. That can achieved by a well designed GA which searches the whole search space while the population evolves. The convergence rate of the GA evolution is a good measure to justify the quality of the designed GA. In the executed runs, GA demonstrates a good convergence rate.

The executed tests to validate the use of the GA to find good solutions for this problem shows that the design and the parameters of the GA are satisfactory. The

tests show that the designed GA is far better than a pure random search. Moreover, the designed GA generates near-optimal solutions in cases where the optimal solution is known. Therefore, the GA developed for this study satisfactorily meets the objectives.

The results of the analysis of the four-satellite constellation indicate that a four-satellite constellation is not suitable for navigation purposes over a mid-latitude region of the earth. The generated solutions either had an average of three-hour unavailability periods or very poor performance values, which resulted in very high cost values.

The cases with two GEO satellites and three GSO satellites without any constraints on the inclination values turned into solutions which have three GEO satellites and two highly inclined GSO satellites after the GA optimization. The GEO satellites are placed on the equator with an average separation of 85^o, when it is not constrained. Moreover, these kind of solutions performed very well among the other generated solutions. Therefore, it can be stated that the GEO satellites are indispensable for this problem.

The constellations with two GEO satellites and three GSO satellites with constraint on the inclination value along with the other constraints also performed well. In those cases, the GSO satellites usually tended to be phased on the nearly same orbital plane.

The cases which are comprised of five GSO satellites are also analyzed. When the apogee point of the satellite constrained to be over the northern hemisphere ($\omega(180:360)$), poor constellations were generated. The reason for the design of cases with this constraint was to increase the visibility over the receiver points. However, this constraint shrank the limits of possible satellite geometry which eventually led to high GDOP values.

The analysis of the effect of J2 perturbation was also made. The results of this analysis show that the constellations comprising of GEO satellites and critically inclined ($i = 63.4$) GSO satellites are more robust against J2 perturbation. Besides, those constellations have good navigation performance values.

5.2 Recommendations

The design of the cost function is vital for the performance of the GA. Because the cost function is used to distinguish the good solutions among the other generated solutions, a badly designed cost function may prevent the GA from finding good solutions. Therefore, the cost function should state the exact performance criteria of the problem. In this research, the designed cost function performed well in terms finding good results. Because the criteria applied to the cost function are average GDOP value and average availability, the algorithm generated availability as high as possible and average GDOP as low as possible values. However, for some applications, the satellite navigation system should provide stable GDOP values along with low GDOP average values. Therefore, an added criteria in the cost function might be to

minimize the magnitude of the peaks of GDOP values. That kind of cost function may generate solution with more stable performance.

As it was discussed in Section 3.3, enlarged sampling space is used in the designed GA. Therefore, a level of elitism was already accepted, which might have resulted early convergence. In order to mitigate this effect of enlarged sampling space, fewer parent population size and more children population size might be used for this problem.

Appendix A. Ground Tracks of the Generated Constellations

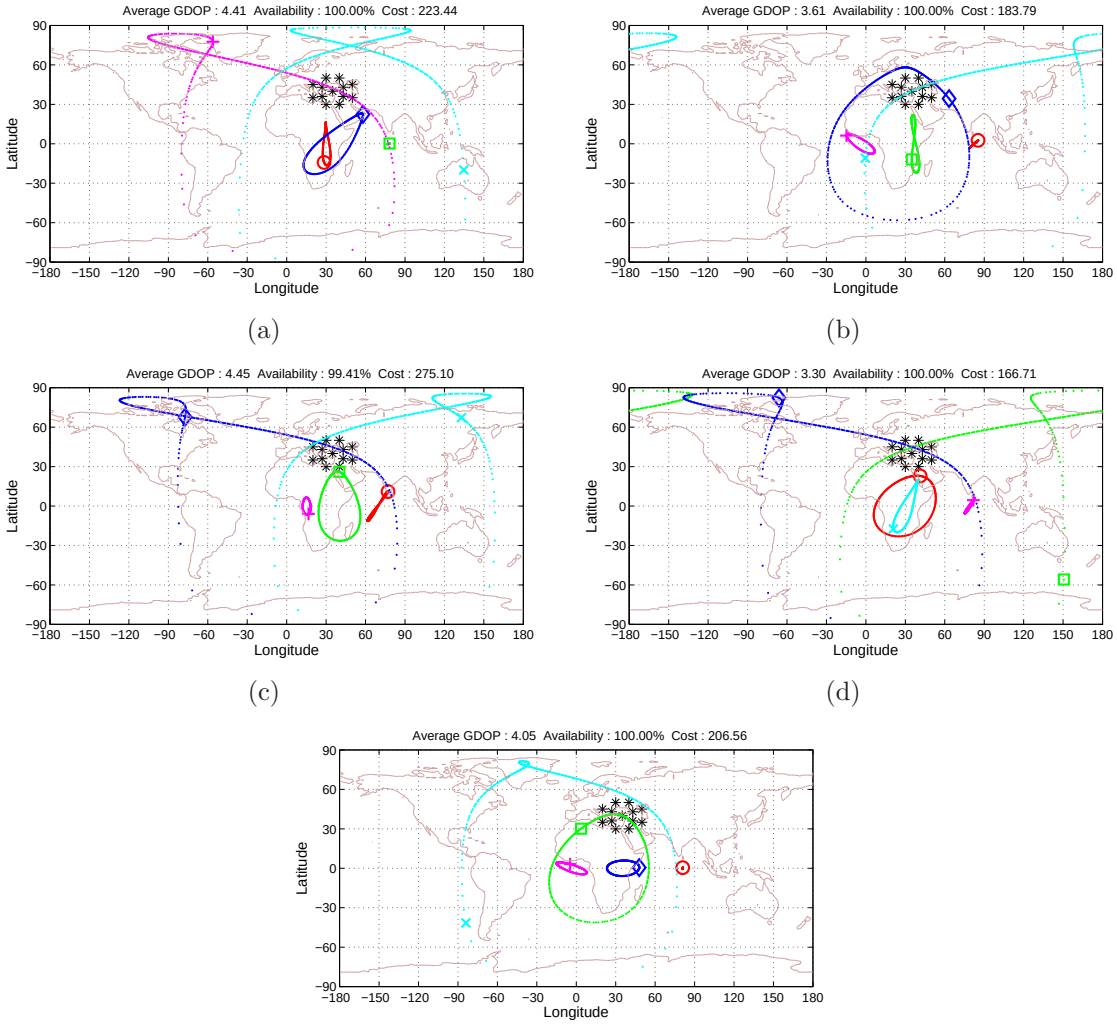

(a) (b) (c) (d) (e)

Figure A.1: a through e) Ground Tracks of the Generated Solutions for Case 1 (Seed 1 trough 5, respectively)

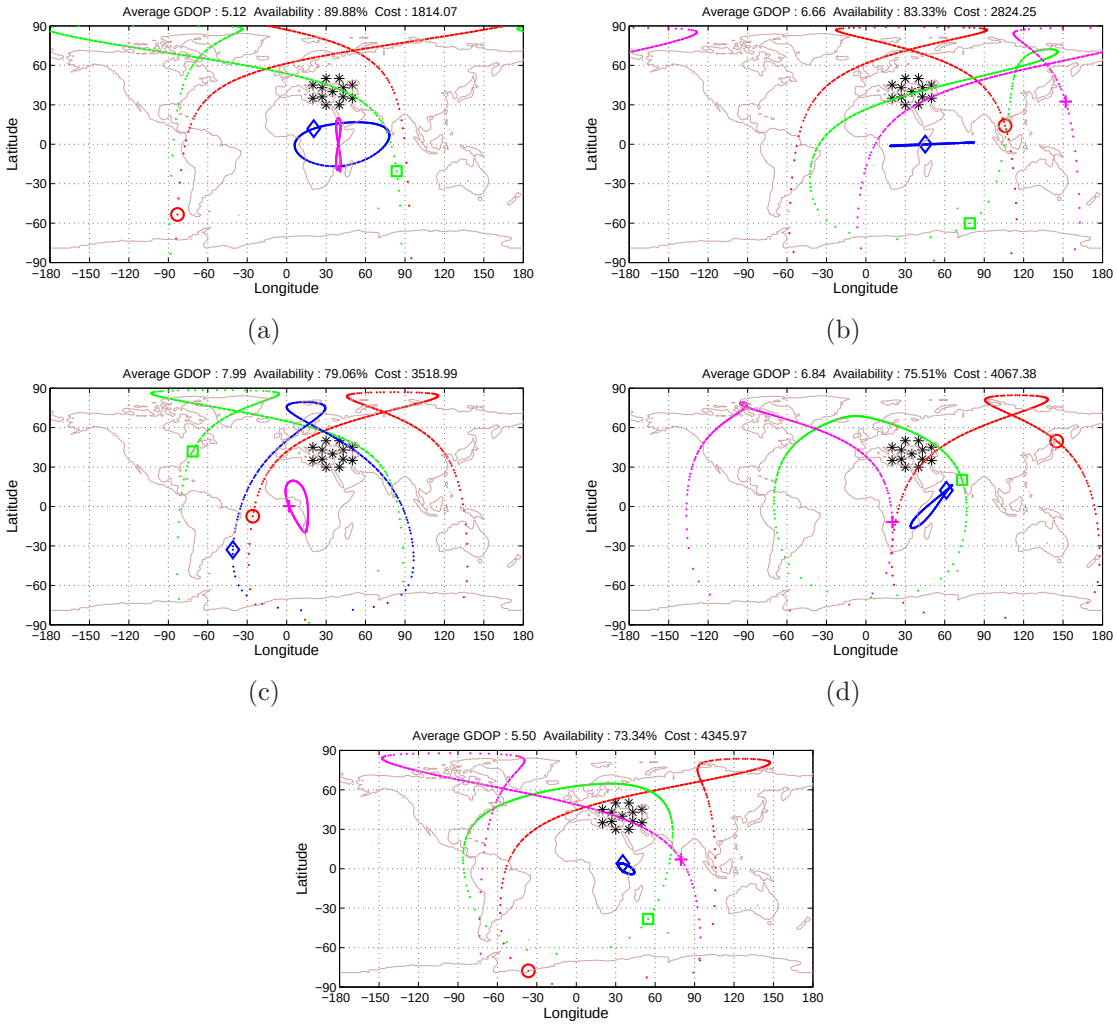

Figure A.2: a through e) Ground Tracks of the Generated Solutions for Case 2 (Seed 1 through 5, respectively)

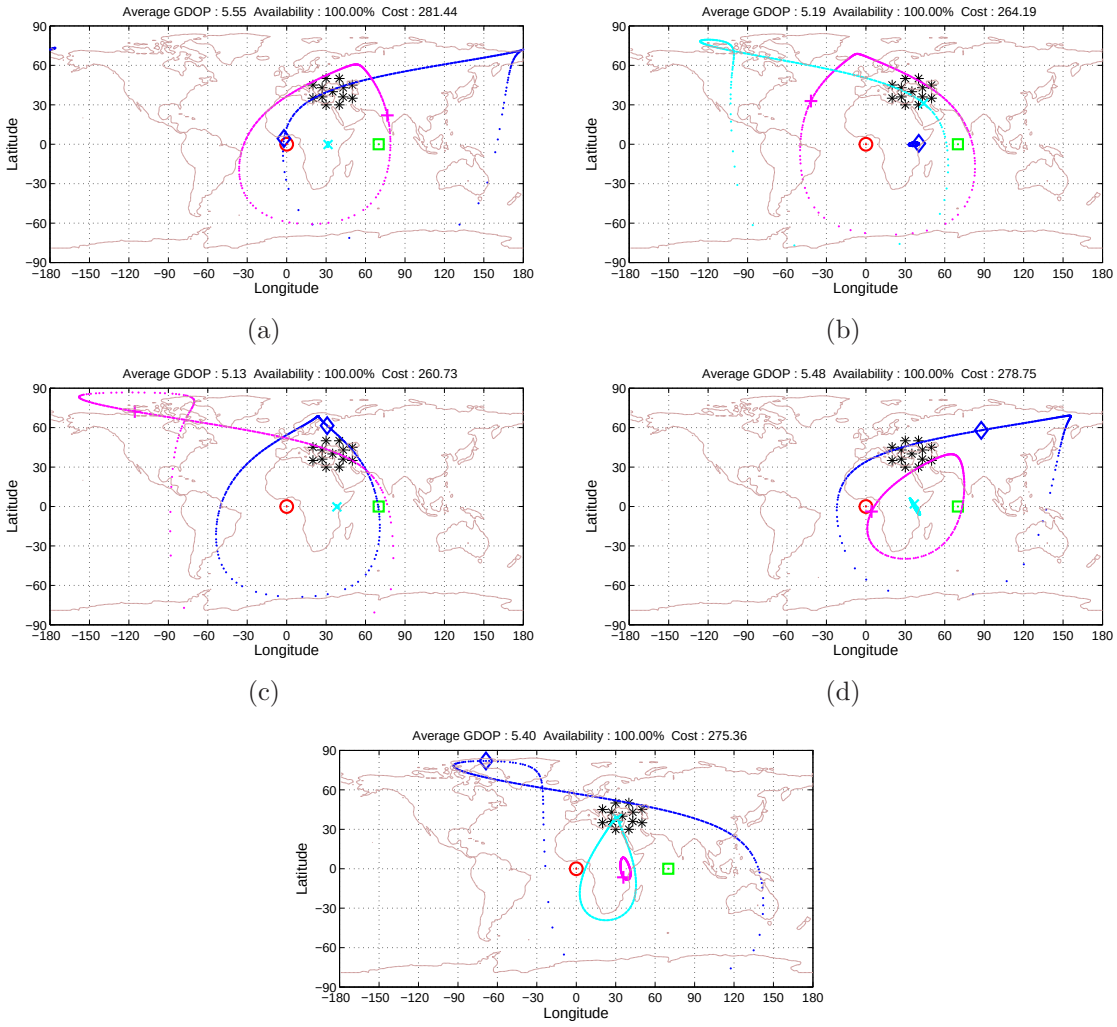

Figure A.3: a through e) Ground Tracks of the Generated Solutions for Case 3 (Seed 1 through 5, respectively)

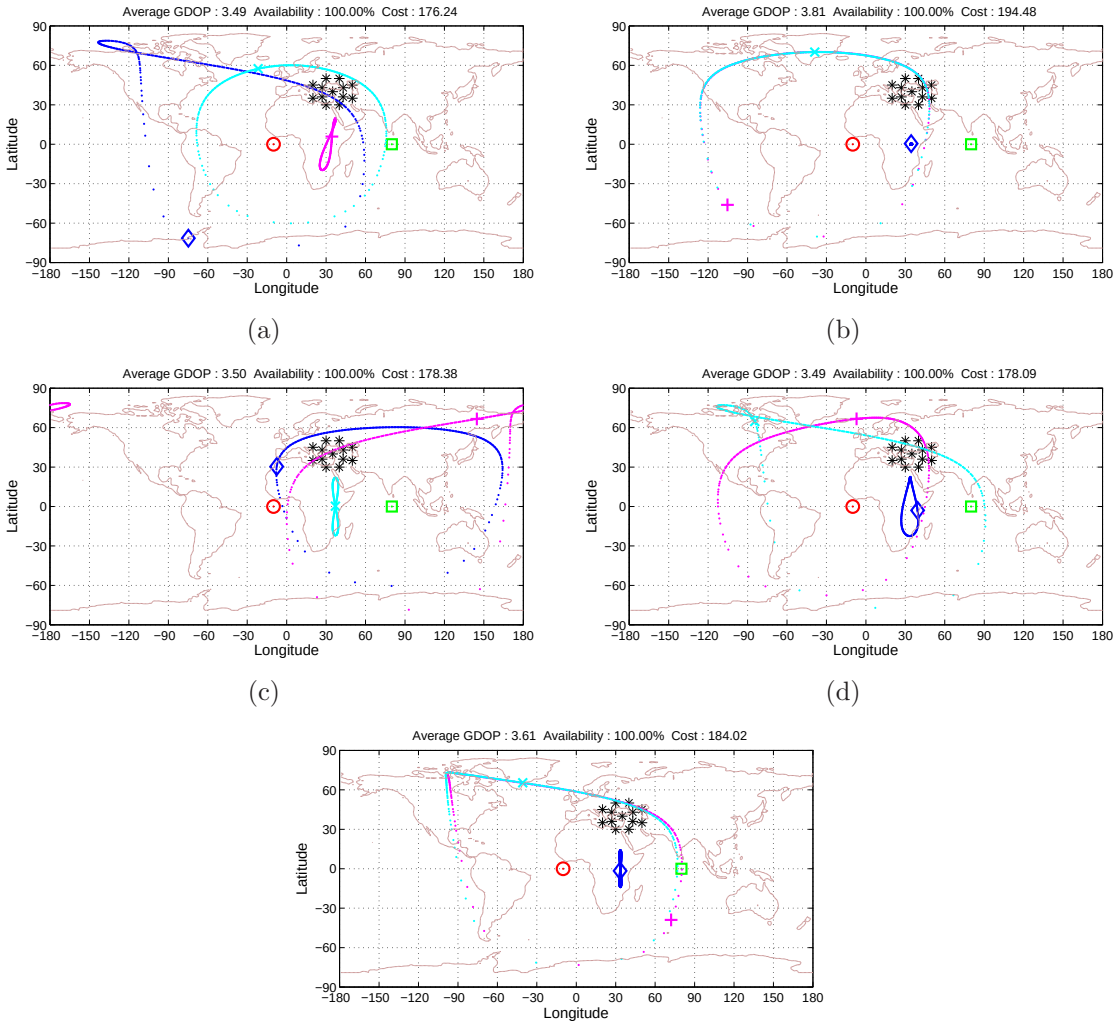

Figure A.4: a through e) Ground Tracks of the Generated Solutions for Case 4 (Seed 1 through 5, respectively)

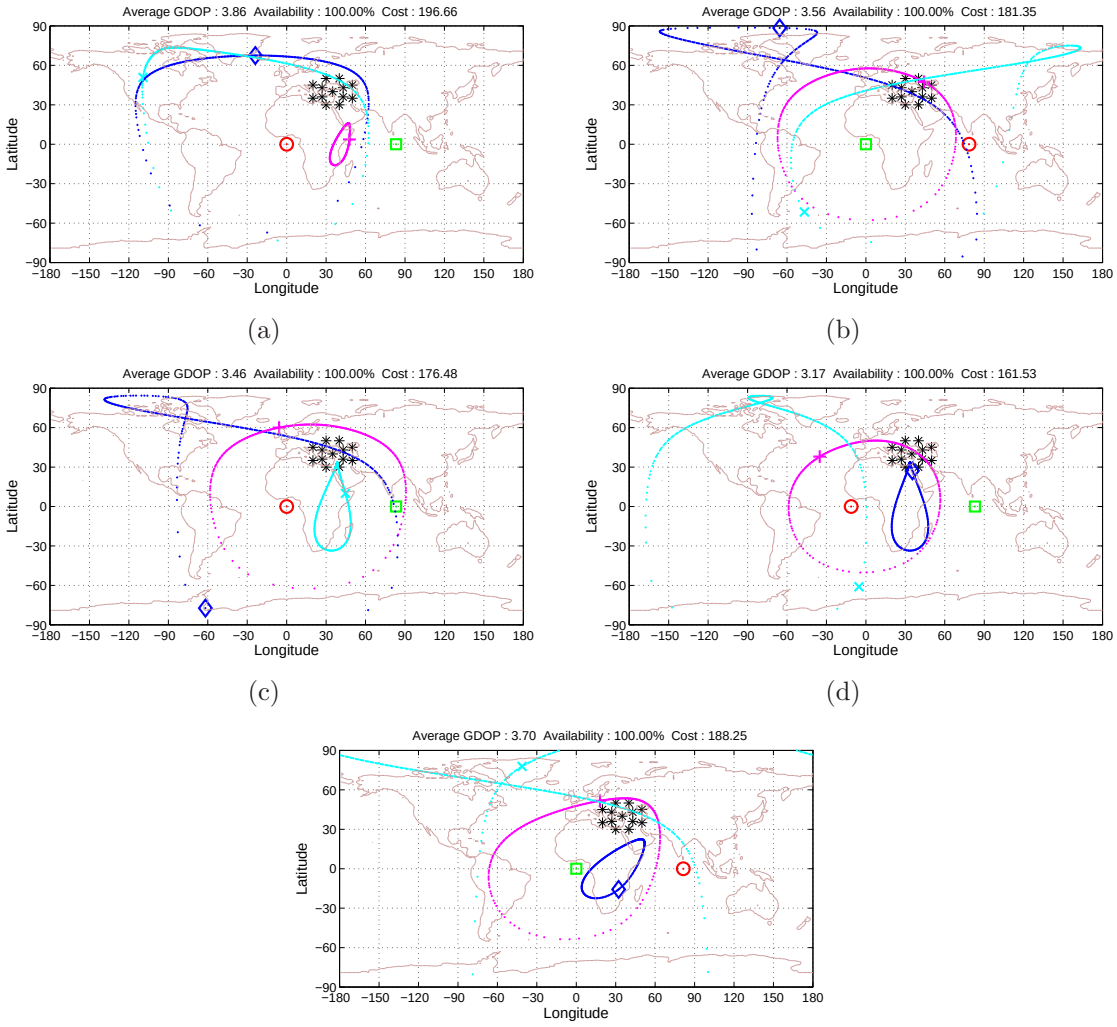

Figure A.5: a through e) Ground Tracks of the Generated Solutions for Case 5 (Seed 1 through 5, respectively)

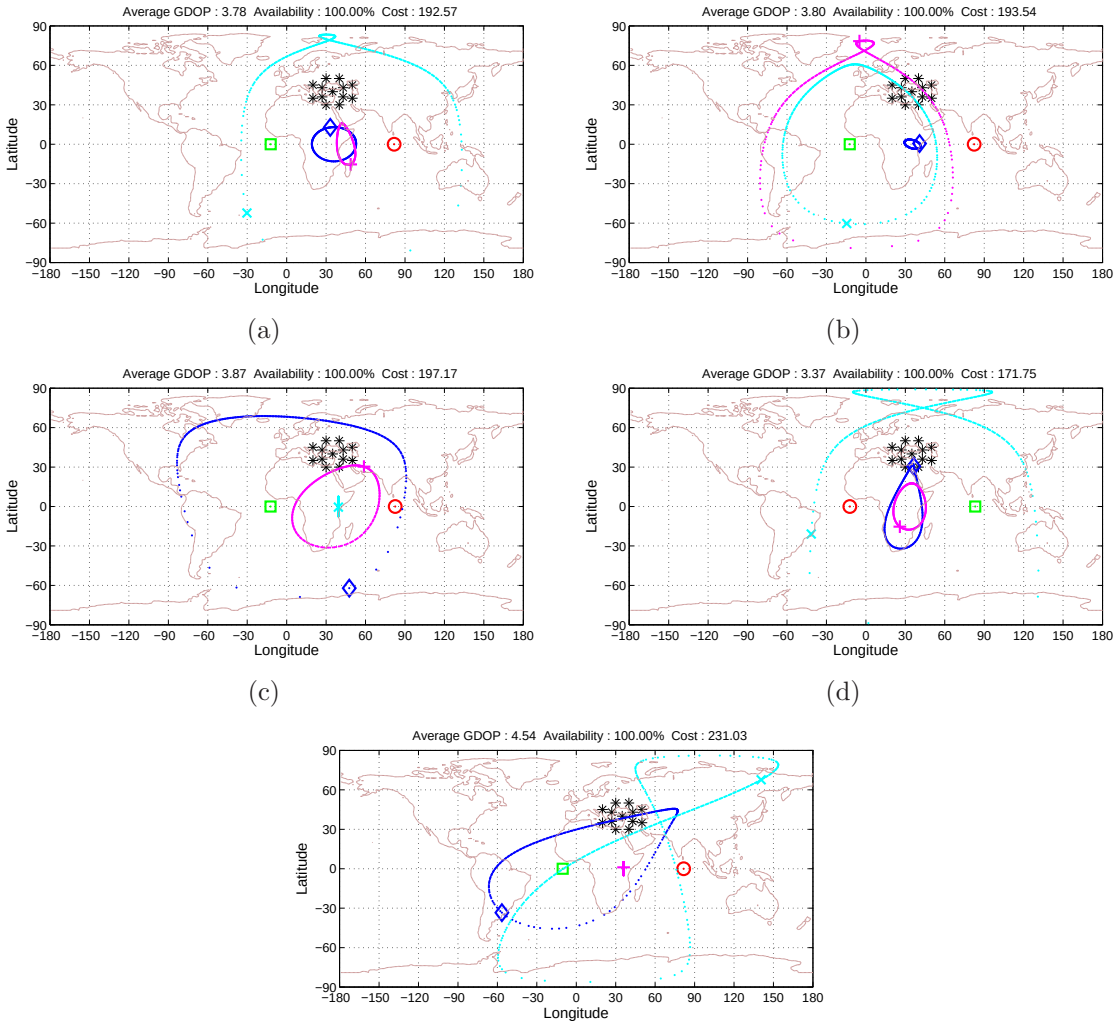

Figure A.6: a through e) Ground Tracks of the Generated Solutions for Case 6 (Seed 1 through 5, respectively)

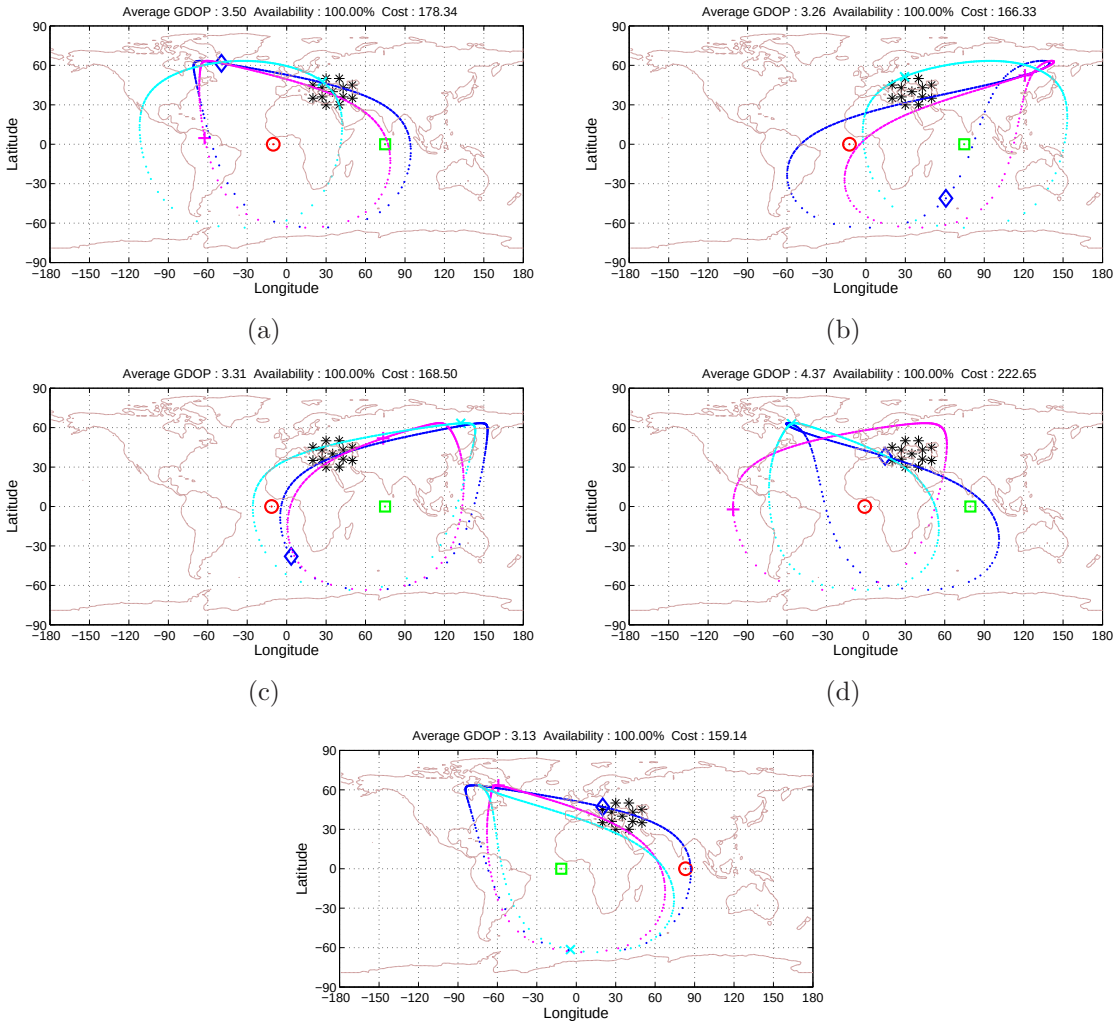

Figure A.7: a through e) Ground Tracks of the Generated Solutions for Case 7 (Seed 1 through 5, respectively)

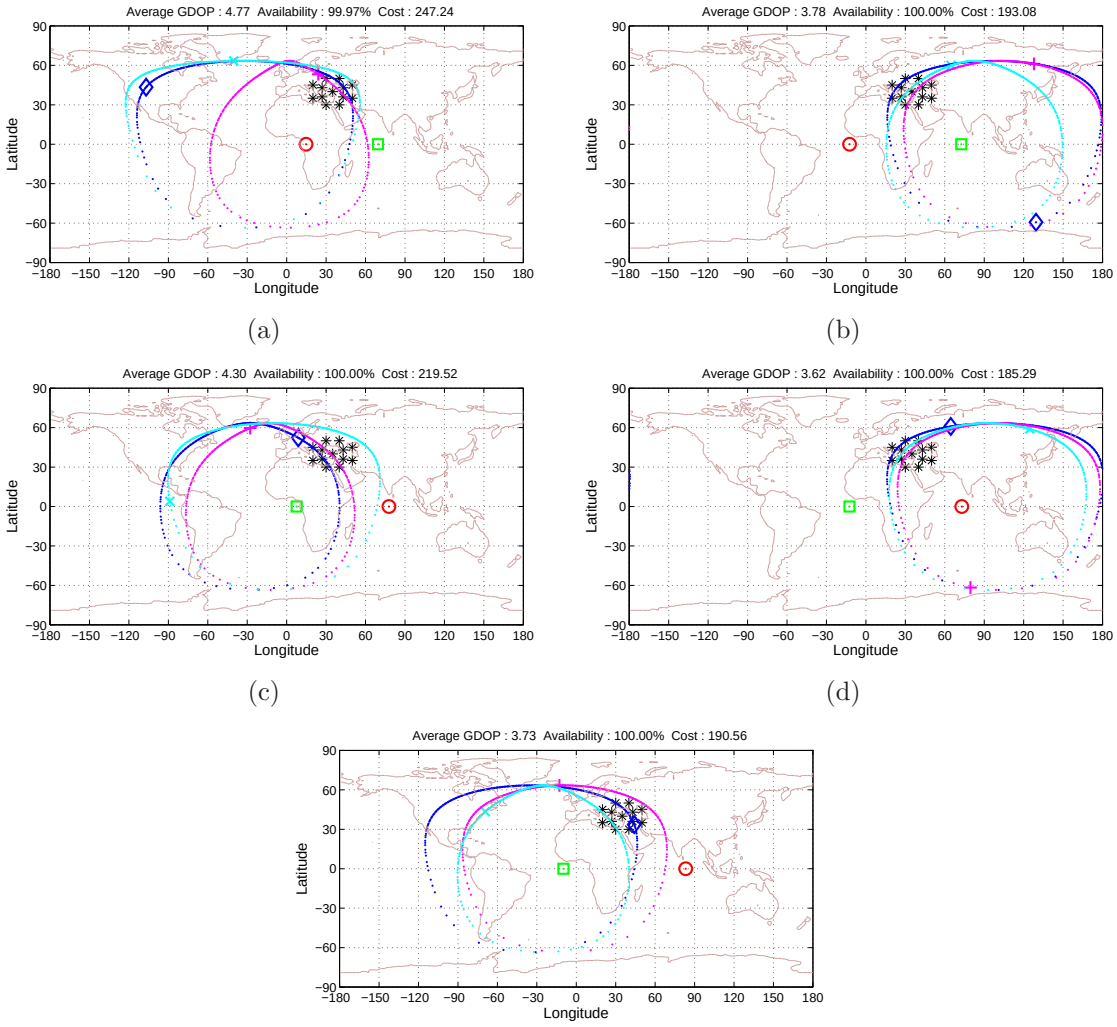

Figure A.8: a through e) Ground Tracks of the Generated Solutions for Case 8 (Seed 1 through 5, respectively)

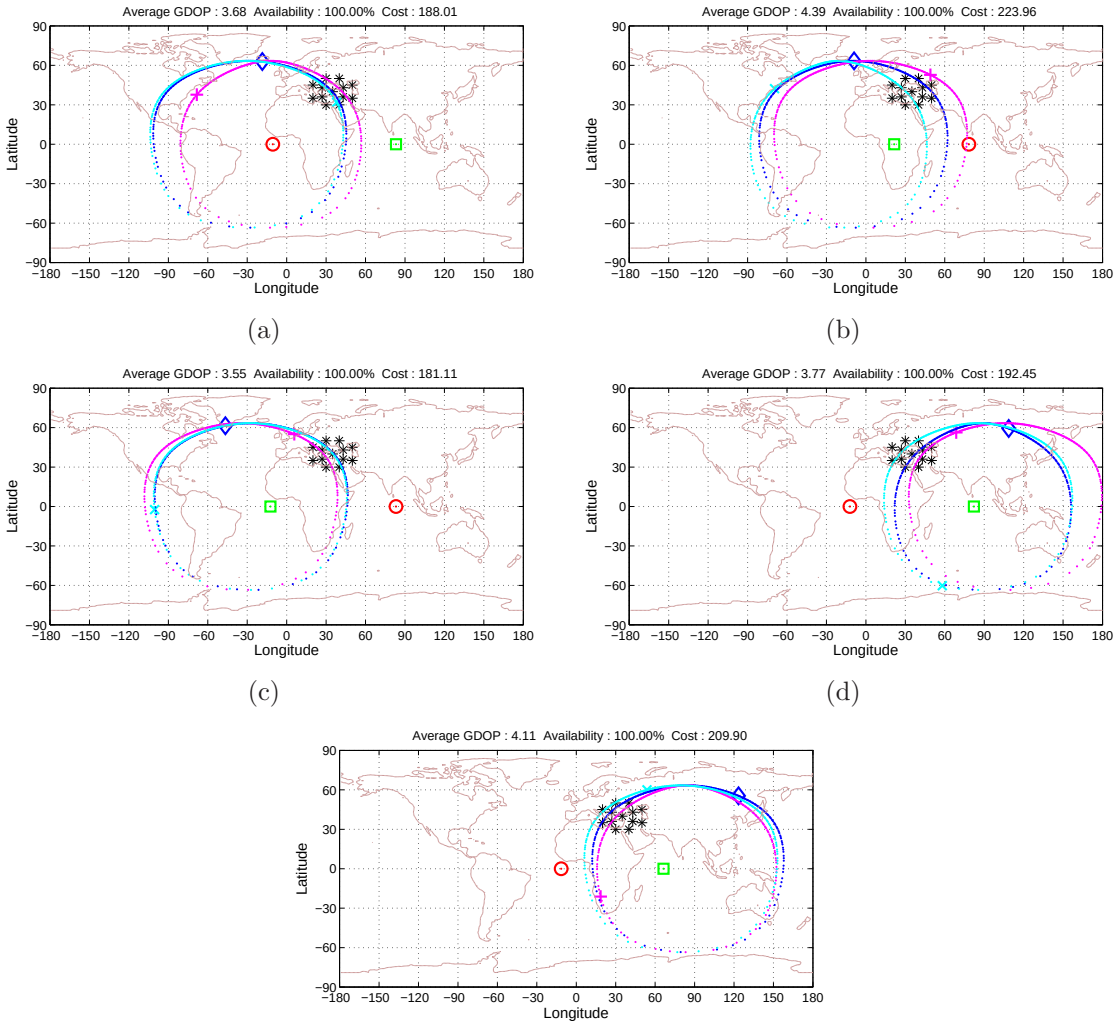

Figure A.9: a through e) Ground Tracks of the Generated Solutions for Case 9 (Seed 1 through 5, respectively)

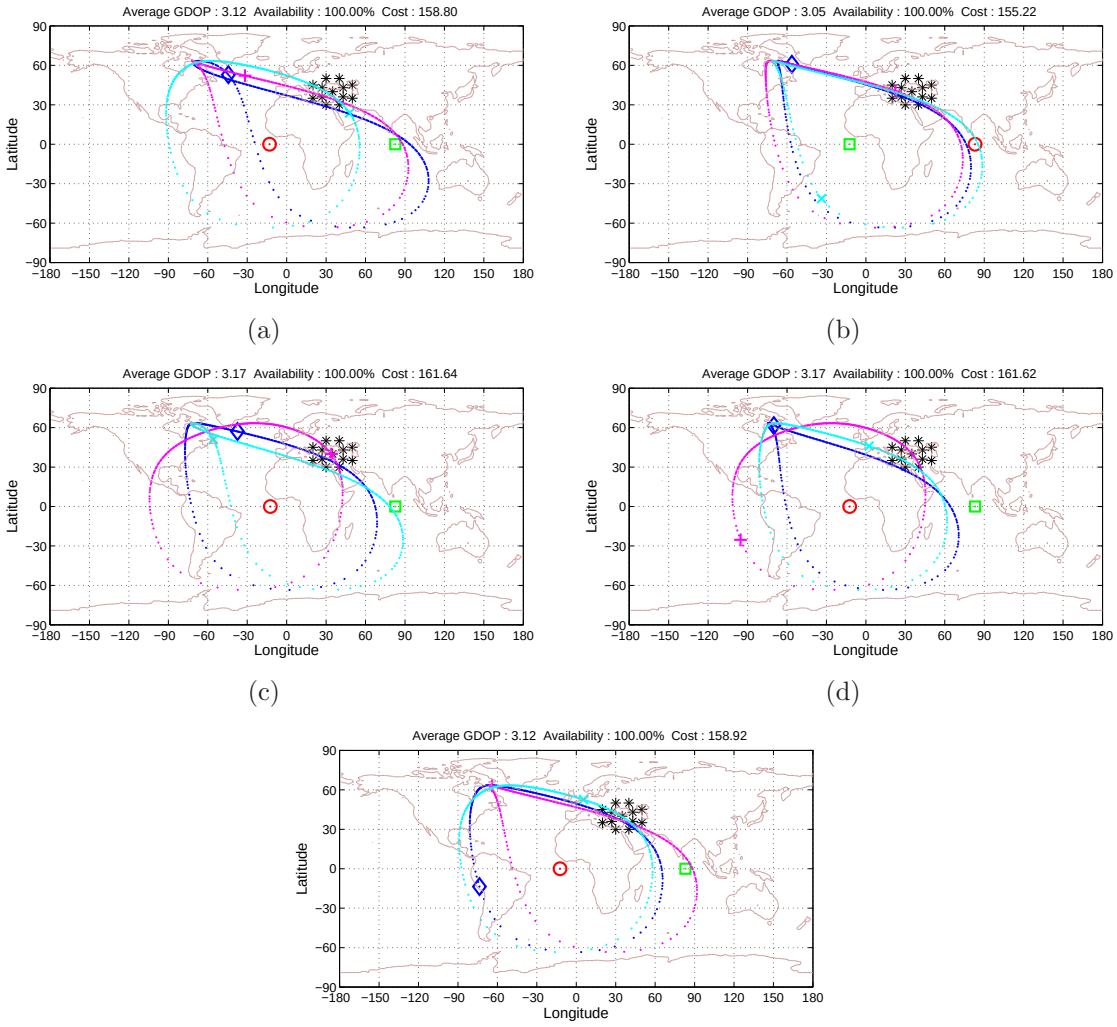

Figure A.10: a through e) Ground Tracks of the Generated Solutions for Case 10 (Seed 1 through 5, respectively)

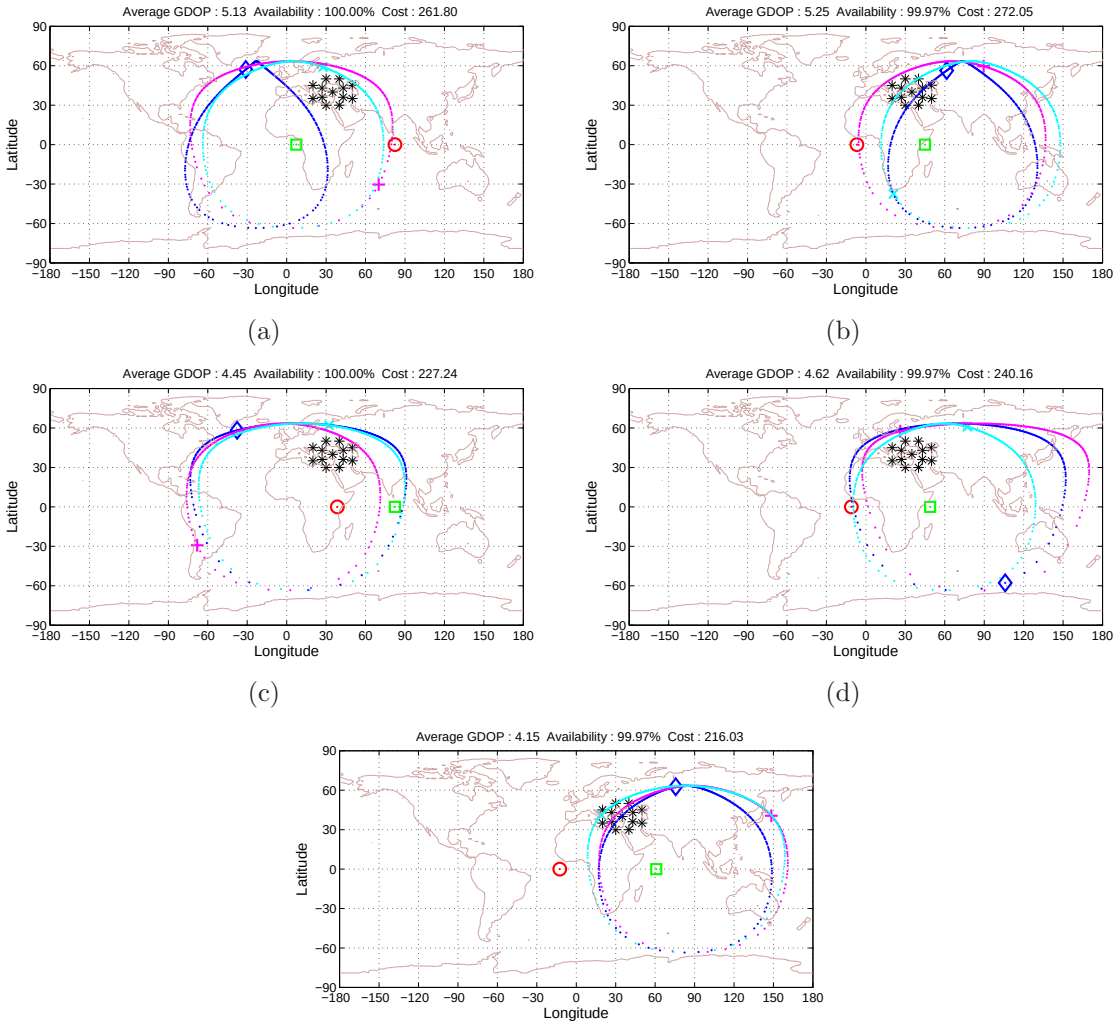

Figure A.11: a through e) Ground Tracks of the Generated Solutions for Case 11 (Seed 1 through 5, respectively)

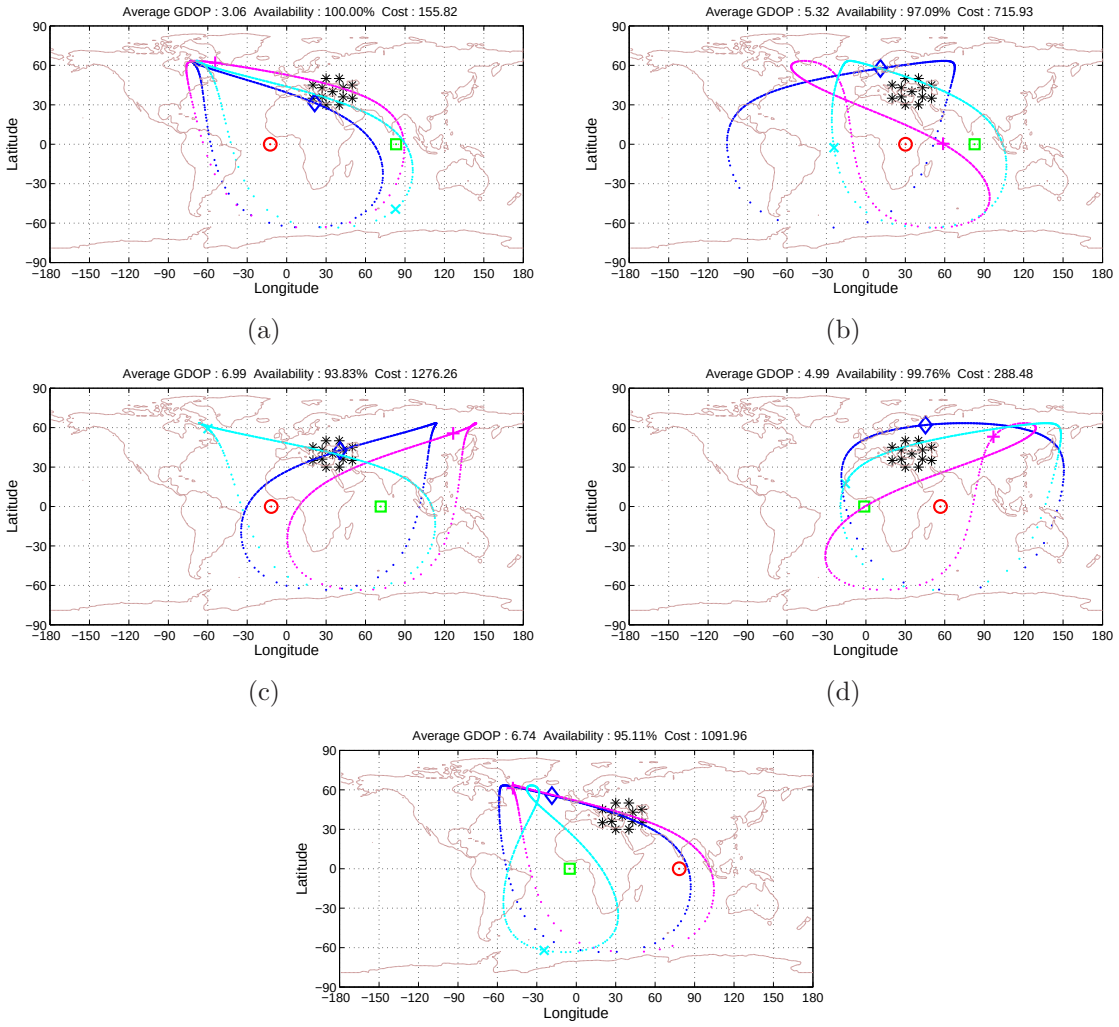

Figure A.12: a through e) Ground Tracks of the Generated Solutions for Case 12 (Seed 1 through 5, respectively)

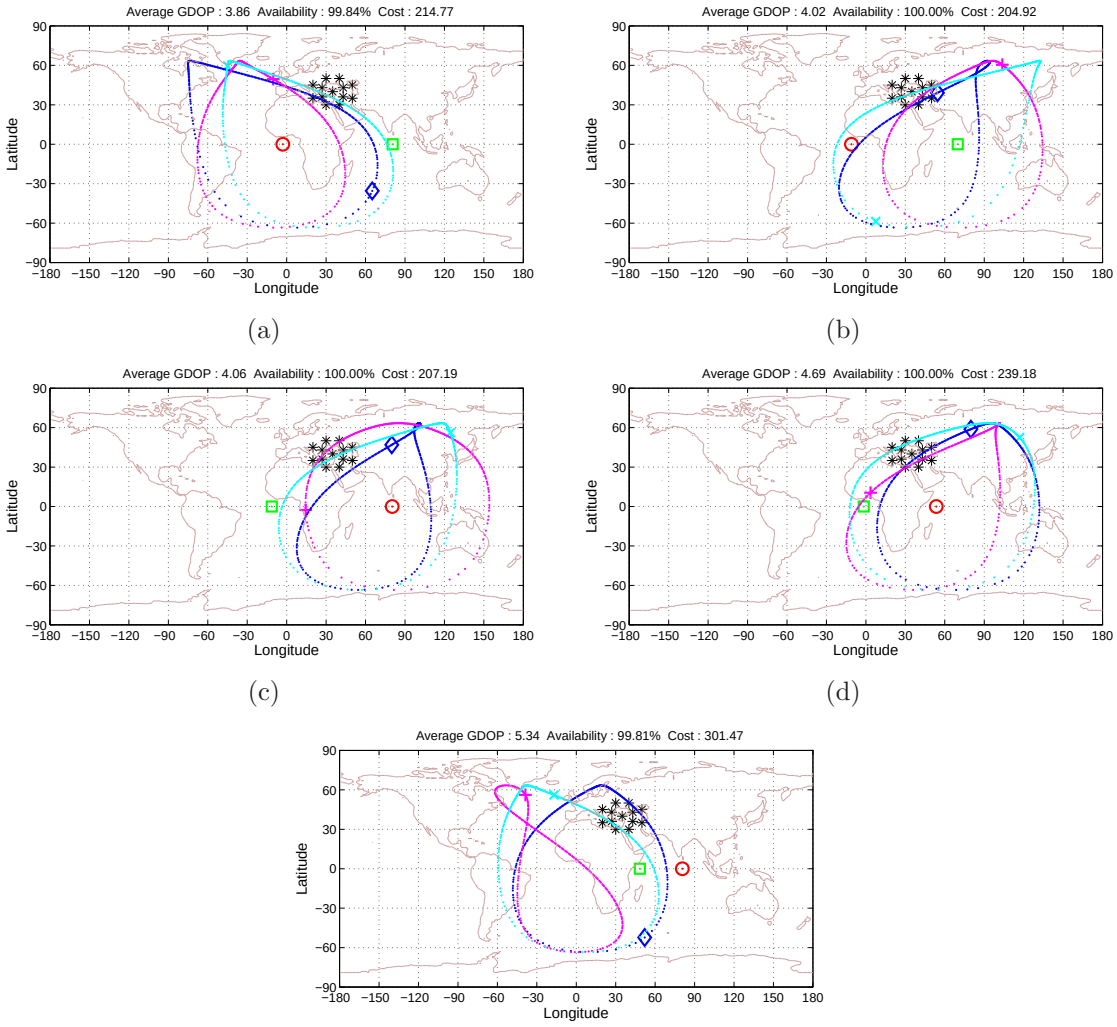

Figure A.13: a through e) Ground Tracks of the Generated Solutions for Case 13 (Seed 1 through 5, respectively)

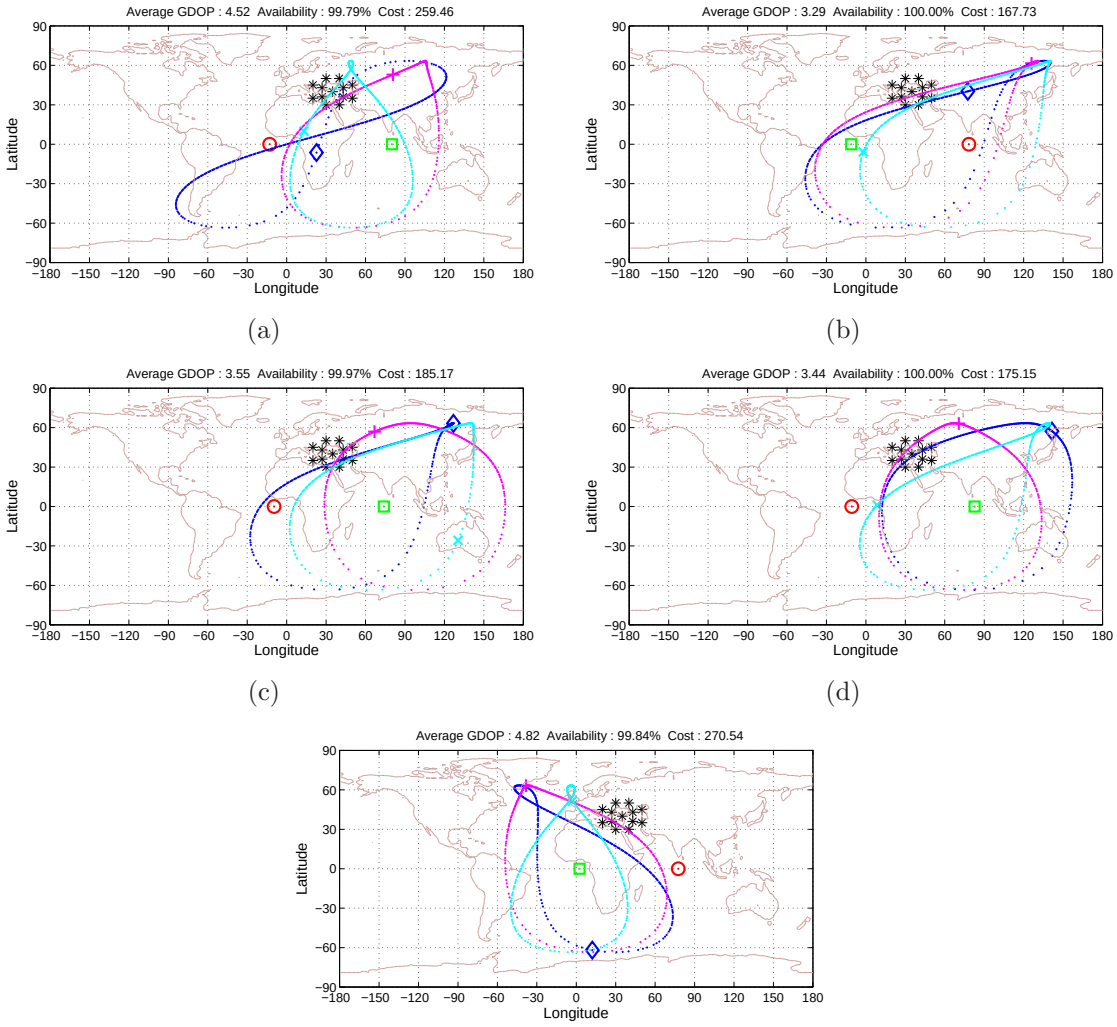

(a) (b) (c) (d) (e)

Figure A.14: a through e) Ground Tracks of the Generated Solutions for Case 14 (Seed 1 through 5, respectively)

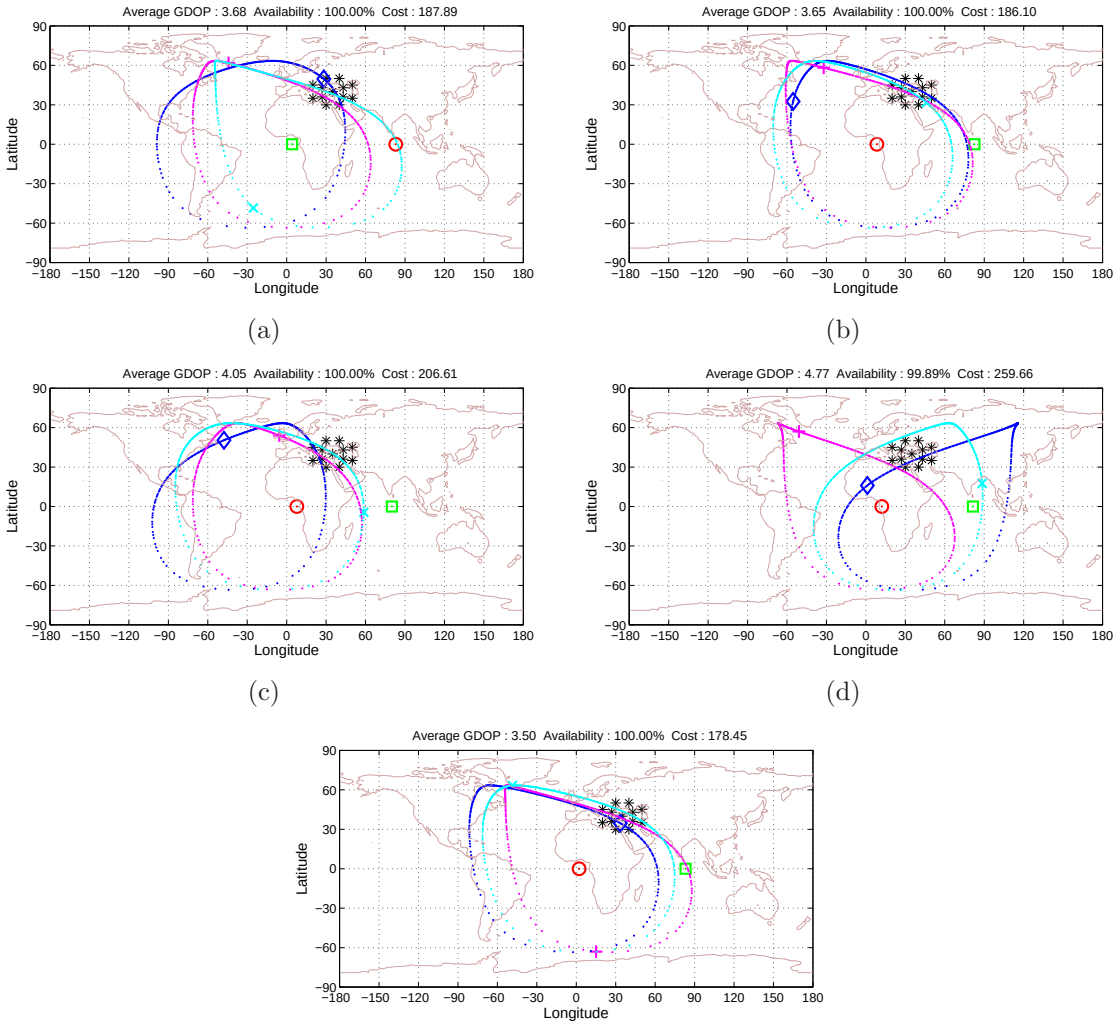

Figure A.15: a through e) Ground Tracks of the Generated Solutions for Case 15 (Seed 1 through 5, respectively)

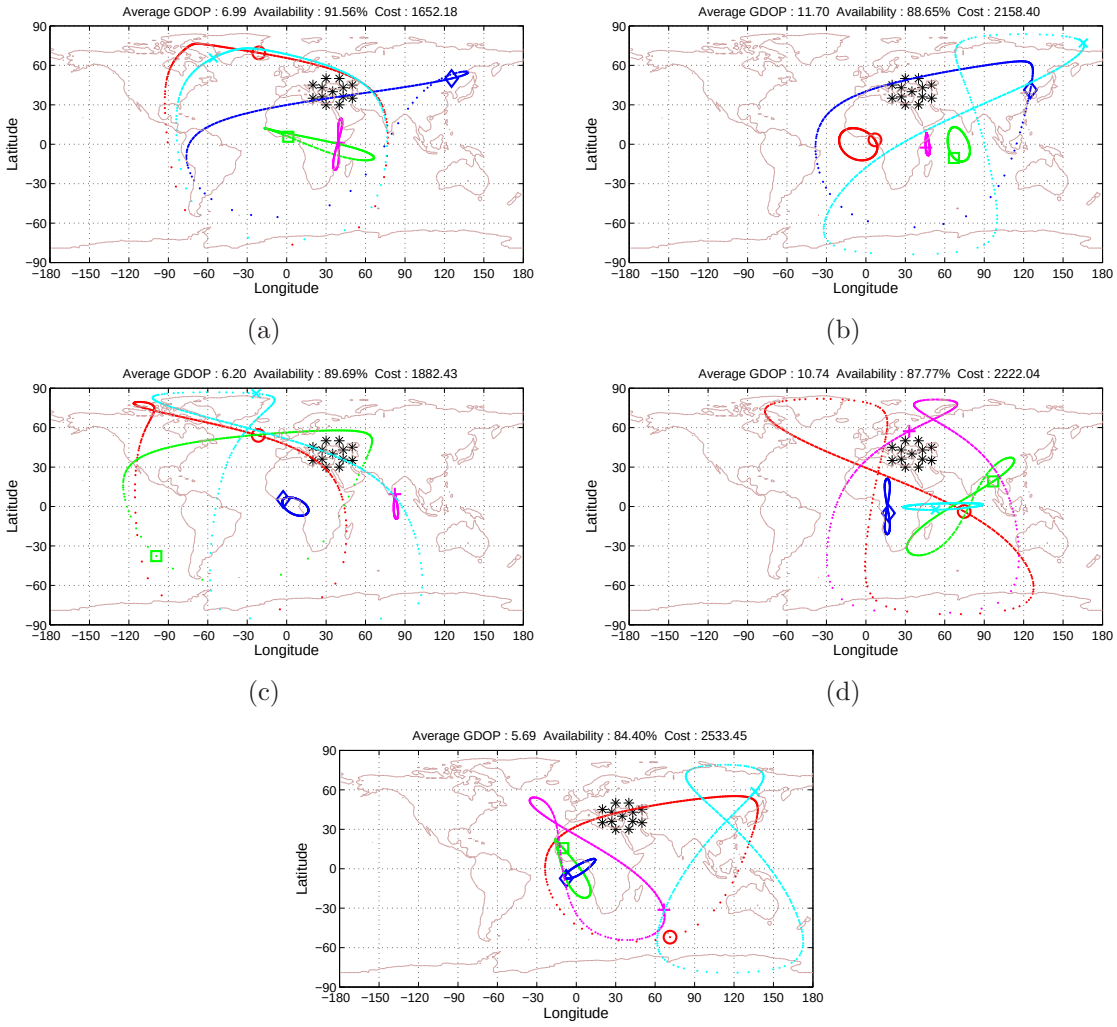

Figure A.16: a through e) Ground Tracks of the Generated Solutions for Case 16 (Seed 1 through 5, respectively)

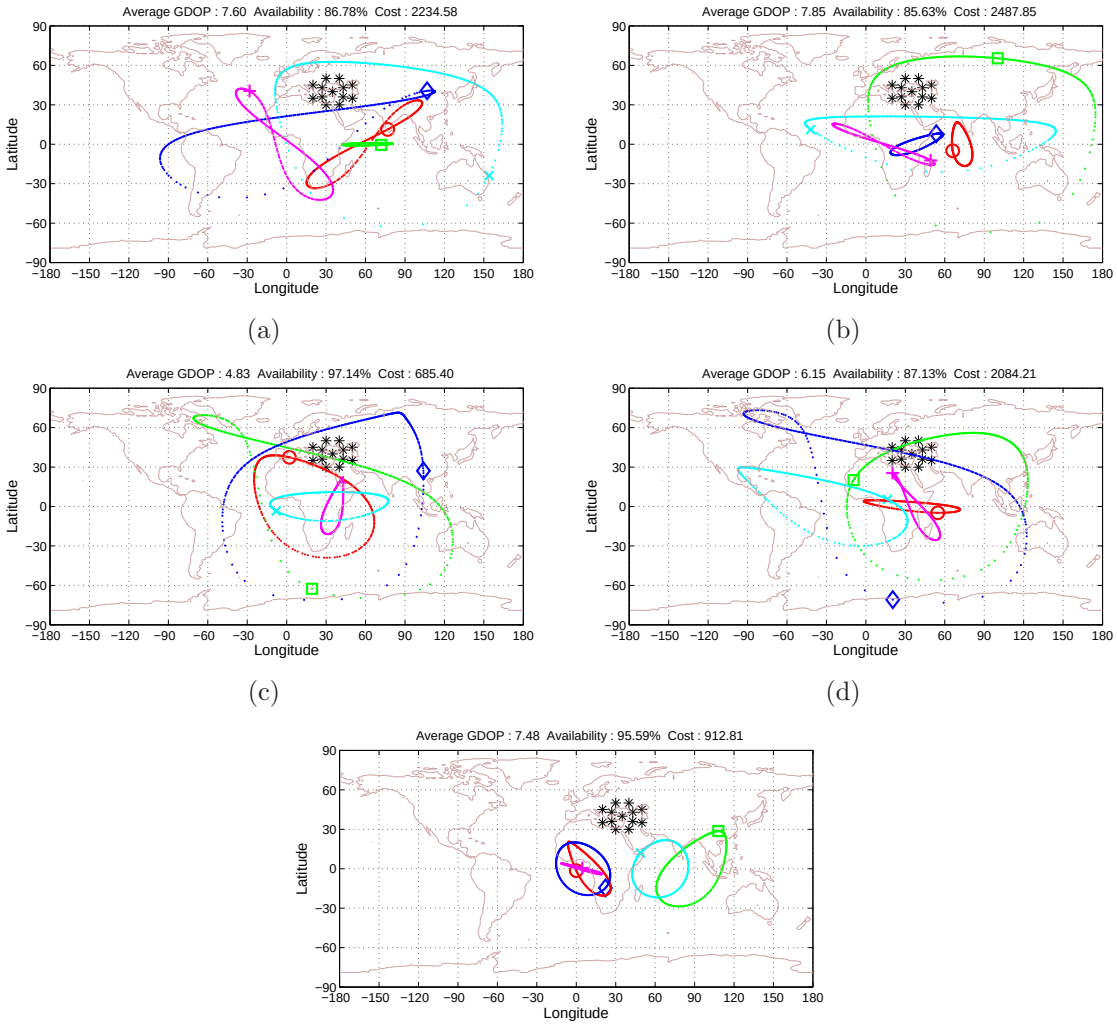

Figure A.17: a through e) Ground Tracks of the Generated Solutions for Case 17 (Seed 1 through 5, respectively)

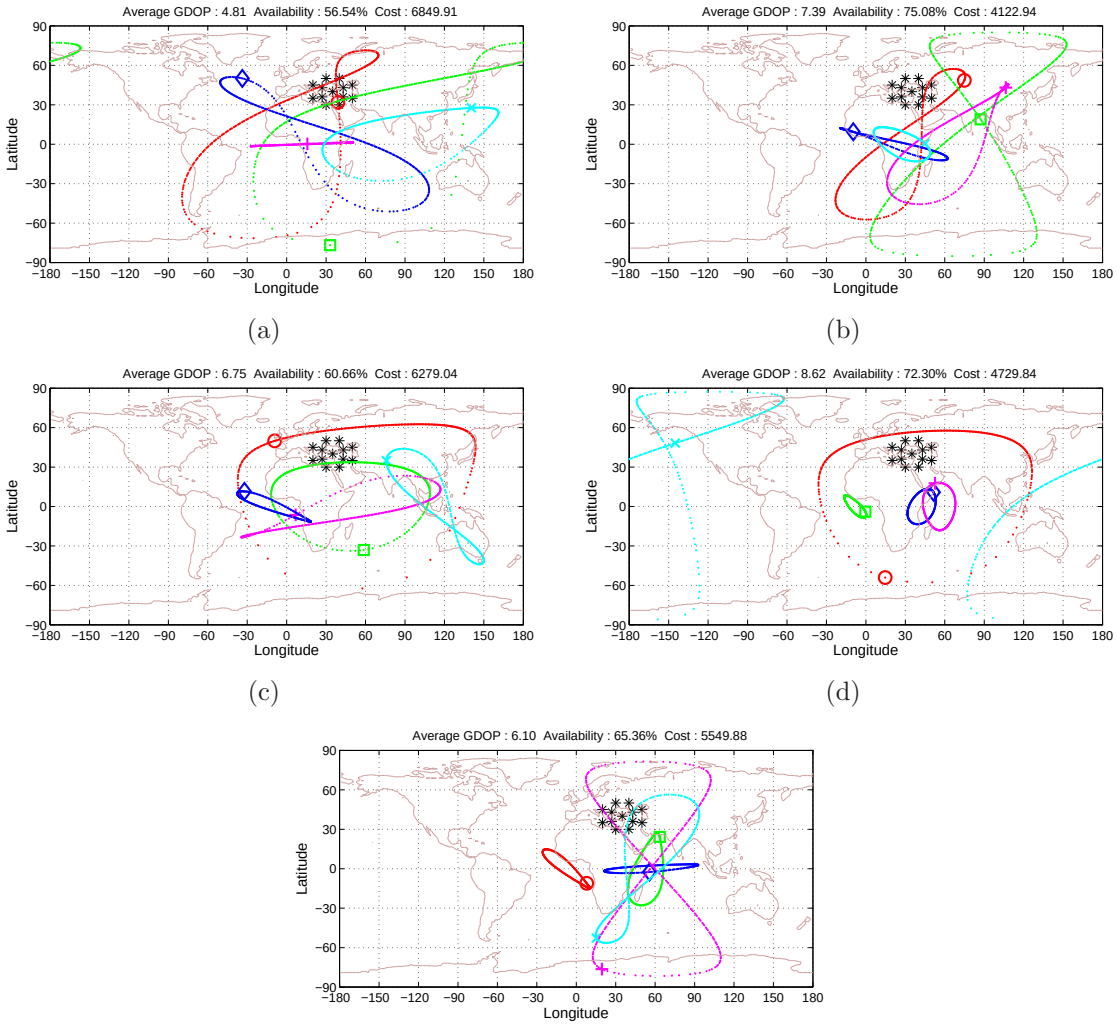

Figure A.18: a through e) Ground Tracks of the Generated Solutions for Case 18 (Seed 1 through 5, respectively)

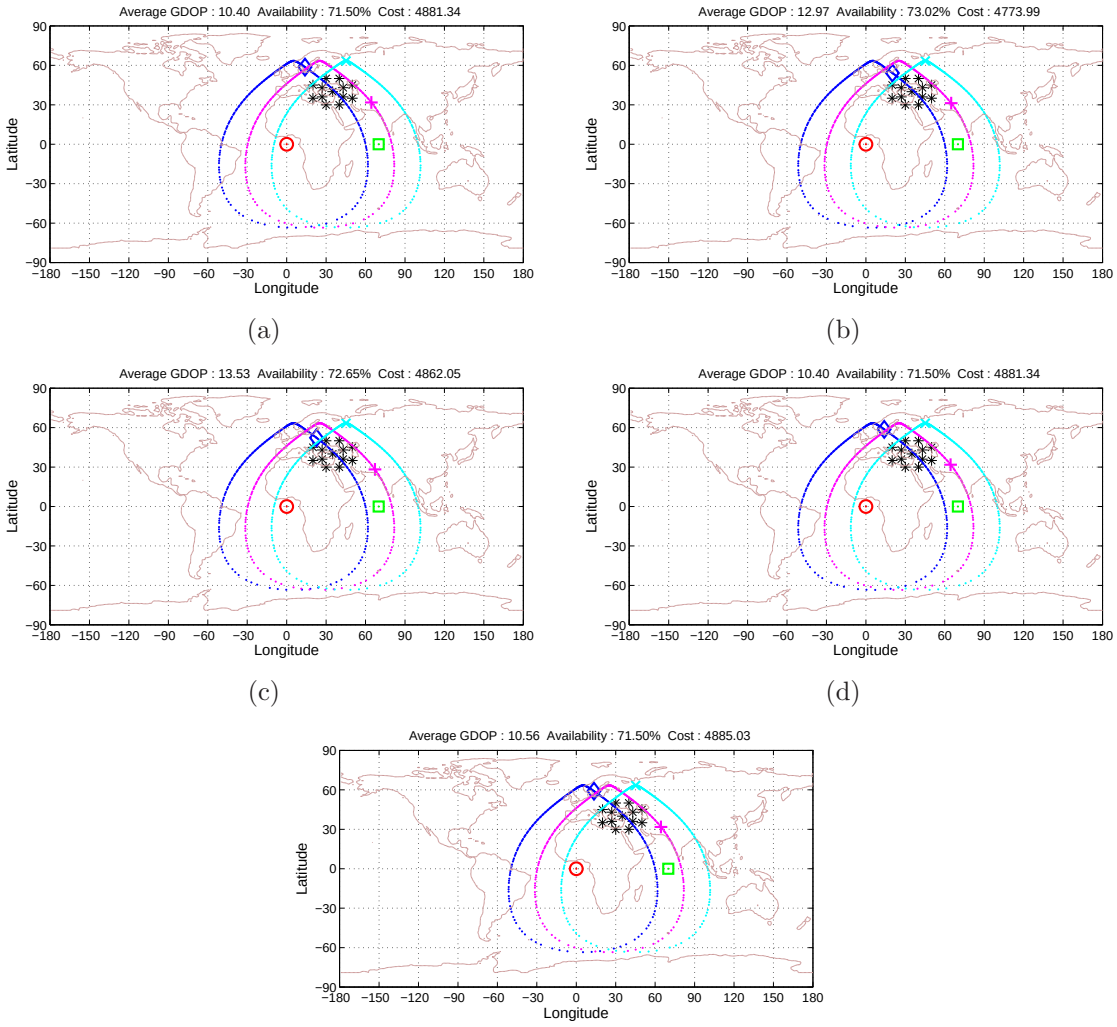

Figure A.19: a through e) Ground Tracks of the Generated Solutions for Case 19 (Seed 1 through 5, respectively)

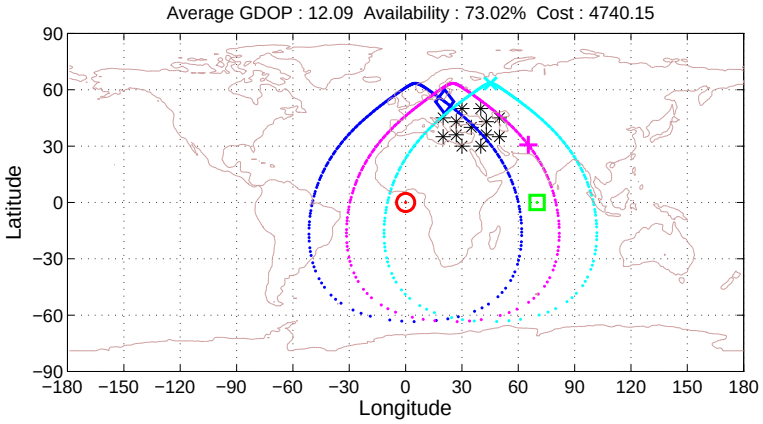

Figure A.20: Ground Tracks of the Generated Solutions for Case 20 (Benchmark)

Bibliography

1. "MATLAB®, The Language of Technical Computing", January 2007. Version 7.4.0.287 (R2007a). The Mathworks, Inc.

2. "Current GPS Constellation", January 2008. URL `http://tycho.usno.navy.mil/gpscurr.html`.

3. "GPS Primer", January 2008. URL `http://www.aero.org/education/primers/gps/GPS-Primer.pdf`.

4. "Orbital Elements", January 2008. URL `http://spaceflight.nasa.gov/realdata/elements/graphs.html`.

5. Beasley, David, David R. Bull, and Ralph R. Martin. "An Overview of Genetic Algorithms: Part 2, Research Topics". *University Computing*, 15(4):170–181, 1993. URL `citeseer.ist.psu.edu/article/beasley93overview.html`.

6. Busetti, Franco. "Genetic Algorithms Overview", August 2007. URL `http://www.geocities.com/francorbusetti/gaweb.pdf`.

7. Carnebianca, C. "Regional to Global Satellite Based Navigation Systems". *IEEE Position Location and Navigation Symposium*, 25–33. IEEE Press, New York, NY, 1998.

8. Cobo, M.M. Romay-Merino J.A. Pulido and E. Herraiz-Monseco. "Design of High Performance and Cost Efficient Constellations for a Future Global Navigation Satellite System". *Proceedings of the 11th International Meeting of the Satellite Division of the Institute of Navigation*, 1085–1095. Nashville, TN, September 1998.

9. Coley, David A. *An Introduction to Genetic Algorithms for Scientists and Engineers*. World Scientific Publishing Co. Pte. Ltd., Singapore, 1999.

10. Crossley, William A. "Optimization for Aerospace Conceptual Design through the Use of Genetic Algorithms". *Proceedings of the 1st NASA/DOD workshop on Evolvable Hardware*, 200–207. IEEE Computer Society, Washington DC, 1999.

11. Ferringer, Matthew P. and David B. Spencer. "Satellite Constellation Design Optimization Via Multiple-Objective Evolutionary Computation". *AIAA/AAS Astrodynamics Specialist Conference*. Lake Tahoe, August 2005. Paper No. AAS 05-280.

12. Frayssinhes, Eric. "Investigating New Satellite Constellation Geometries with Genetic Algorithms". *Proceedings of the the AAIA/AAS Specialist Conference*, 582–588. San Diego, CA, 1996.

13. Gen, Mitsuo and Runwei Cheng. *Genetic Algorithms and Engineering Design*. John Wiley and Sons, Inc., New York, NY, 1997.

14. Haupt, Randy L. and Sue Ellen Haupt. *Practical Genetic Algorithms*. John Wiley and Sons, Inc., Hoboken, New Jersey, 2nd edition, 2004.

15. Jayaraman, K.S. "India To Develop Regional Navigation System", May 2006. URL `http://www.space.com/spacenews/archive06/India-052206.html`.

16. Kaplan, Elliott D. and Christopher J. Hegarty (editors). *Understanding GPS: Principles and Applications*. Artech House, Norwood, MA, 2nd edition, 2006.

17. Kawase, S. "Regional Navigation Service Using Communication Satellites", August 2007. URL `http://www2.nict.go.jp/w/w122/control/people/kawase/03.pdf`.

18. Khan, Muhammad S. "Political and Economic Dimensions of Global Navigation Satellite System (GNSS)". *Aerospace Conference, 2001, IEEE Proceedings*, volume 3, 3/1271–3/1276. 2001.

19. Larson, Wiley J. and James R. Wertz (editors). *Space Mission Analysis and Design*. Microcosm Press and Springer, El Segundo, CA and New York, NY, 1999.

20. Micheau, P. and V. Thiebolt. "Satellite Constellation Design for Navigation Needs". *Proceedings of the International Workshop on Mission Design and Implementation of Satellite Constellations*, 169–177. Toulouse, France, 1997.

21. Miller, Brad L. and David E. Goldberg. "Genetic Algorithms, Tournament Selection, and the Effects of Noise". *Complex Systems*, 9:193–212, 1995. URL `citeseer.ist.psu.edu/article/miller95genetic.html`.

22. Mitchell, Melanie. *An Introduction to Genetic Algorithms*. The MIT Press, Cambridge, MA, 1999.

23. Parkinson, Bradford W. "Origins, Evolution, and Future of Satellite Navigation". *Journal of Guidance, Control, and Dynamics*, 20(1):11–25, January-February 1997.

24. Pratap Misra, Per Enge. *Global Positioning System: Signals, Measurements and Performance*. Ganga-Jamuna, Lincoln, Massachusetts, 2nd edition, 2006.

25. Reeves, Colin R. and Jonathan E. Rowe. *Genetic Algorithms-Principles and Perspectives: A Guide to GA Theory*. Kluwer Academic Publishers, Norwell, MA, 2003.

26. Renault, H. "Constellatin Studies for Future Navigation System". *Proceedings of the International Workshop on Mission Design and Implementation of Satellite Constellations*, 163–168. Toulouse, France, 1997.

27. Rizos, Chris. "The future of Global Satellite Navigation Systems". *Proceedings in IEICE Tech. Rept.*, volume 107.2, 25–30. Perth, Australia, April 2007.

28. Spaans, Jac. "The Munich Satellite Navigation Summit 2007". *European Journal of Navigation*, 5(2):47–51, May 2007.

29. Spears, William M. and Kenneth A. De Jong. "An Analysis of Multi-Point Crossover". G. J. E. Rawlins (editor), *Foundations of Gednetic Algorithms*, 301–315. Morgan Kaufmann, San Mateo, CA, 1991.

30. T.A. Ely, W.A. Crossley and E.A. Williams. "Satellite Constellation Design for Zonal Coverage Using Genetic Algorithms". *The Journal of the Astronautical Sciences*, 47, December 1999.

31. Tafazolli, M. Asvial R. and B.G. Evans. "Modified GSC for Hybrid Satellite Constellation". *Electronics Letters*, 38(20):1216–1217, September 2002.

32. Tafazolli, M. Asvial R. and B.G. Evans. "Satellite Constellation Design and Radio Resource Management Using Genetic Algorithm". *IEEE Proceedings in Communication*, 3, 204–209. IEEE Press, New York, NY, June 2004.

33. Vallado, David A. *Fundamentals of Astrodynamics and Applications*. Microcosm Press, El Segundo, CA, 2nd edition, 2001.

34. Zalzala, A. M. S. and P. J. Flemming (editors). *Genetic Algorithms in Engineering Systems*. Number 55 in Control Engineering Series. The Institution of Electrical Engineers, London, United Kingdom, 1997.

Vita

Özdemir Halil İbrahim was born and raised in Ankara in 1977. Upon graduating from Kuleli Military High School in 1994, Özdemir attended to the Turkish Air Force Academy in 1994. He graduated from the TUAFA with Electrical Engineering degree in 1998. His first assignment was at Çiğli/İzmir 2nd Air Training Base as a pilot trainee. He completed his pilot training as an F-16 pilot. In 2001 he was assigned to the 192^{th} Flight Squadron in Balıkesir. In September 2006, he entered the Graduate School of Engineering and Management, Air Force Institute of Technology. Upon graduation, he will be assigned to the 151^{th} Flight Squadron.

Devilbiss, Stewart 2241 Avonics Circle Area B Bldg 620 Wright Patterson, OH 45433 Bus: (937) 785-6127 x4274 E-mail: stewart.devilbiss@WPAFB.AF.MIL

REPORT DOCUMENTATION PAGE

Form Approved
OMB No. 0704–0188

1. REPORT DATE *(DD–MM–YYYY)*	2. REPORT TYPE	3. DATES COVERED *(From — To)*
27–03–2008	Master's Thesis	Sept 2006 — Mar 2008

4. TITLE AND SUBTITLE

Constellation Design Of Geosynchronous Navigation Satellites Which Maximizes Availability And Accuracy Over A Specified Region Of The Earth

5a. CONTRACT NUMBER

5b. GRANT NUMBER

5c. PROGRAM ELEMENT NUMBER

6. AUTHOR(S)

Halil Ibrahim Ozdemir, Capt, TUAF

5d. PROJECT NUMBER

5e. TASK NUMBER

5f. WORK UNIT NUMBER

7. PERFORMING ORGANIZATION NAME(S) AND ADDRESS(ES)

Air Force Institute of Technology
Graduate School of Engineering and Management (AFIT/EN)
2950 Hobson Way
WPAFB OH 45433-7765

8. PERFORMING ORGANIZATION REPORT NUMBER

AFIT/GSS/ENG/08-01

9. SPONSORING / MONITORING AGENCY NAME(S) AND ADDRESS(ES)

AFRL (Stewart Devilbiss)
2241 Avonics Circle, Area B Bldg 620
Wright Patterson, OH 45433
(937) 785-6127 x4274 stewart.devilbiss@WPAFB.AF.MIL

10. SPONSOR/MONITOR'S ACRONYM(S)

11. SPONSOR/MONITOR'S REPORT NUMBER(S)

12. DISTRIBUTION / AVAILABILITY STATEMENT

Approval for public release; distribution is unlimited.

13. SUPPLEMENTARY NOTES

14. ABSTRACT

Currently, there are four Global Navigation Satellite Systems (GNSS) either being developed or in existence-GPS, GLONASS, Compass, and Galileo. Additionally, there are several Regional Navigation Satellite Systems (RNSS) planned or in existence, as well as numerous augmentation systems (which require a GNSS for operation). It can be anticipated that there will be interest in developing additional independent regional navigation satellite systems to cover areas of interest to particular countries or regions, who want to have their own system.
In this paper, a genetic algorithm is used in an effort to determine near-optimal RNSS constellations. First, a cost function is setup, which involves a weighted combination of dilution of precision (DOP) values and percentage availability for any number of receiver locations on the ground (which themselves can be weighted). Effectively, using this approach it is easy to quantify the quality of coverage, in terms of measurement geometry, over a specific region of the earth. Next, a genetic algorithm is used in order to attempt to converge to the lowest-cost constellation possible.

15. SUBJECT TERMS

regional navigation satellite system, genetic algorithm, constellation optimization, J2 perturbation

16. SECURITY CLASSIFICATION OF:			17. LIMITATION OF ABSTRACT	18. NUMBER OF PAGES	19a. NAME OF RESPONSIBLE PERSON
a. REPORT	b. ABSTRACT	c. THIS PAGE			Dr.John Raquet
U	U	U	UU	149	19b. TELEPHONE NUMBER *(include area code)* (937) 255–3636, ext 4580; John.Raquet@afit.edu